NASA Tech Briefs

Official Publication of the
National Aeronautics and
Space Administration
July 1993 Vol.17 No. 7

Transferring Engineering
Technology to Over 200,000
Qualified Readers Throughout
Industry and Government

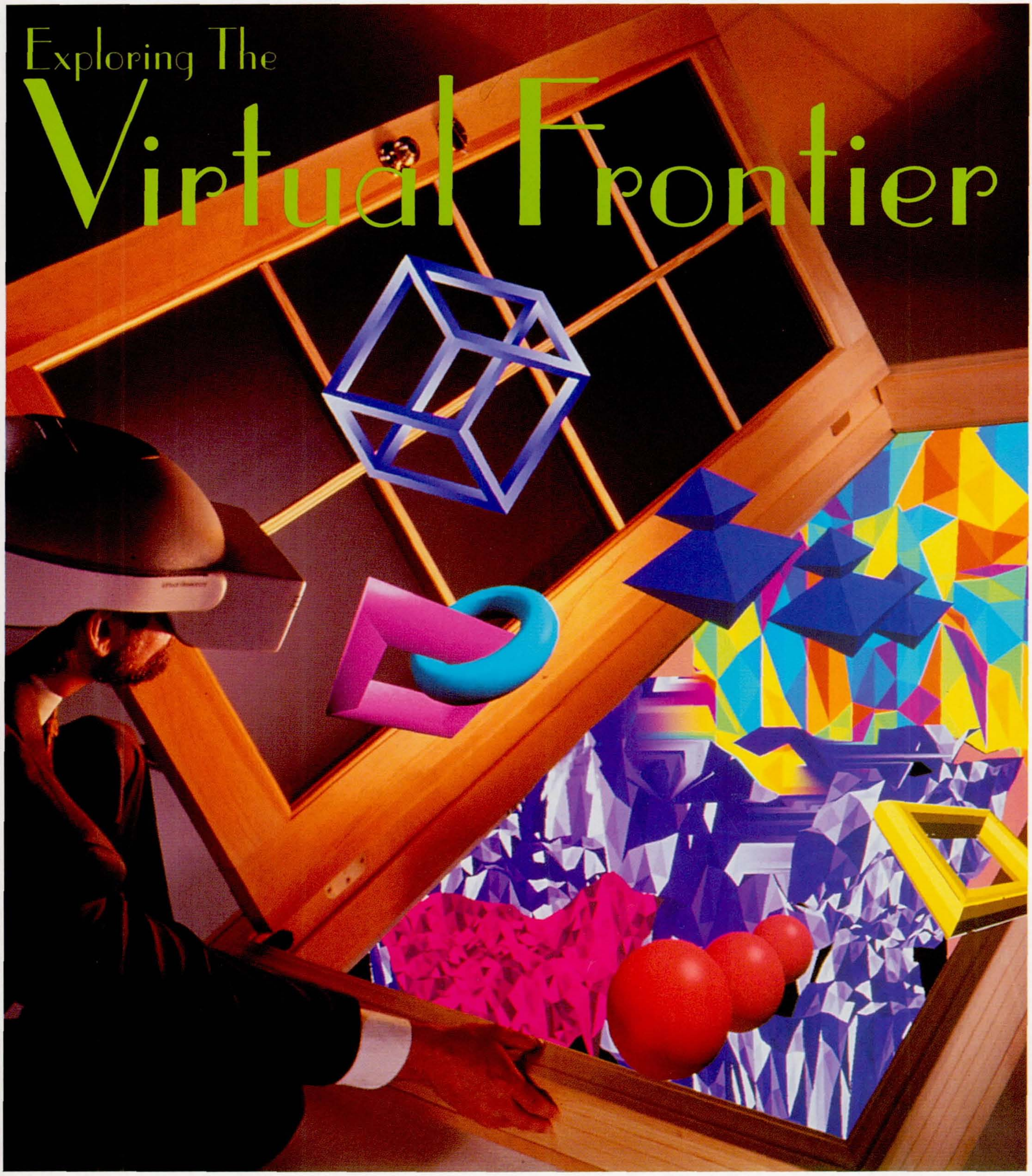

The right tool for the job.

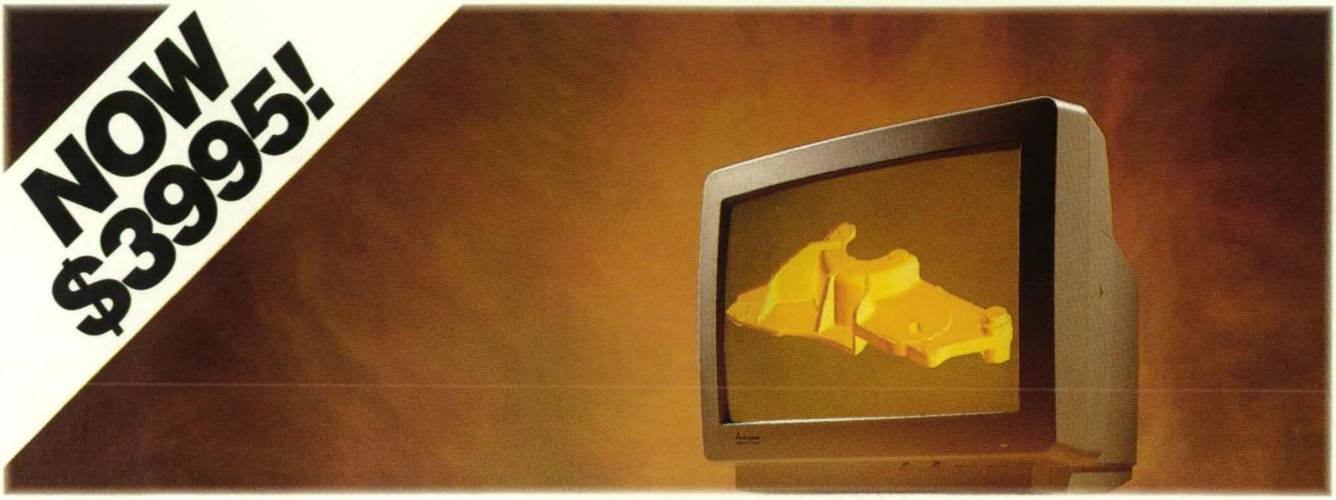

Having the right tool, like brake spring pliers or an oil filter wrench, can turn a potentially frustrating job . . . into one that is manageable and enjoyable. If your job is mechanical design, then the right tool for the job is Personal Designer® software. It provides the right combination of CAD capabilities including: ■ Comprehensive 2-D Drafting/Detailing ■ True 3-D Modeling ■ Hidden Line Removal ■ Bezier and NURB Surfaces ■ Faceted and Smooth Shaded Pictures.

With Personal Designer software, you're equipped to tackle challenging mechanical design problems. Build sizeable models (up to 64,000 entities) with complete associativity. Change the part, and all drawings, dimensions, crosshatching, and multiple views update automatically. Create drawings to ANSI, ISO, and JIS standards. Customize the user interface. And exchange data with other CAD packages via IGES or DXF.™

There's a lot more. You can fillet, sweep, and intersect complex surface geometry, and take advantage of software options for project management (PDex) and integrated 2½- and 3-axis NC programming (Personal Machinist®). To further expand your horizons, utilize the hundreds of available third party offerings. And draw on the expertise of Computervision's worldwide network of VARs.

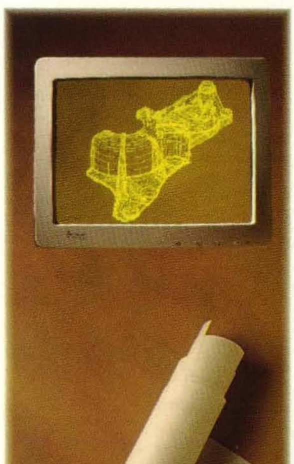

There's a direct translator available, too. So, should you ever need Computervision's top-of-the-line CADDS® software, you can take Personal Designer data bases with you.

The bottom line: Personal Designer software is a smart buy in today's crowded marketplace. It's available for 386/486 PCs as well as the SPARCstation® workstation. And prices for 2D start at $1,995.

Get the right tool for the job, from the company that pioneered CAD/CAM.

Computervision Corporation
Personal CAD/CAM Business Unit
100 Crosby Drive, Bedford, MA 01730
Telephone (800) 248-7728 (U.S. except MA)
(617) 275-1800, ext. 4594 FAX (617) 271-0015

COMPUTERVISION

PERSONAL CAD CAM PRODUCTS

For More Information Circle No. 554

Personal Designer® 5.0

Part database courtesy of American Tool and Mold, Inc., St. Joseph, MI.

THE MOST IMPORTANT ADDITION TO A NETWORK SINCE DAVID LETTERMAN.

Now you can set up tests from anywhere on the net. You can monitor data quality all during the test. And get the full set of data right at your work station immediately after the test. ■ All this convenience comes with the Precision DAServer, our new networked data acquisition and recording system. It manages the data acquisition, so your computer doesn't have to. It stores test data directly in RAM, on disk, disk array or tape. ■ You can have greater than 16-bit resolution with up to 10 MSPS throughput. For long duration recording, transient capture or a combination. As many channels as you wish. ■ DAServer connects to your network for access by all your computers. The graphical user interface uses the X Window system so you get point and click convenience. ■ A new approach by Precision. A systems approach that can also host all Precision transducer conditioning, filtering and switching in one integrated system. All on a turnkey basis. ■ To hear more, call 607-277-3550. Fax 607-277-4466. Or write Precision Filters, Inc., 240 Cherry Street, Ithaca NY 14850.

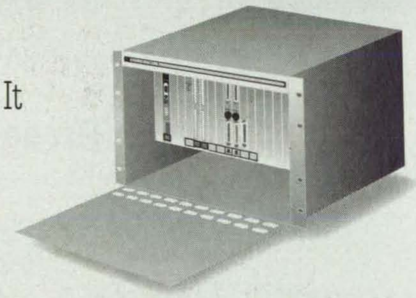

NEW DASERVER. IT CAPTURES YOUR TEST DATA FOR ACCESS OVER YOUR NETWORK.

PRECISION FILTERS, INC.
CONDITIONERS•SWITCHES•DATA ACQUISITION•SYSTEMS

For More Information Circle No. 636

HI JetPro®. A day's work in under an hour.

9:00 AM
A- to C-Size CAD Plots

No more waiting for pen plotter check plots. HI JetPro Series V100 and V50 plotters create HP-GL™/2, HP-GL and DM/PL™ CAD "review plots" at 360 dpi in under five minutes! No options needed. Includes real and protected mode ADI® drivers.

9:05 AM
FAX Output

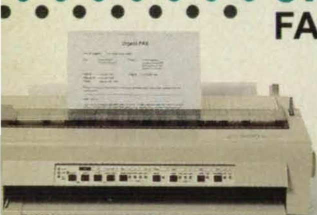

HI JetPro V100 outputs FAX/modem files directly for high-resolution A- to C-size plain paper copies. Optional sheet feeder for A- and B-size output.

9:10 AM
Spreadsheets

C-size and rollfeed capability allow you to create large, readable spreadsheets. Drivers are available for Windows™ 3.0 and 3.1 compatibility.

9:15 AM
Multiple Review Copies

For meetings create A-size review copies in one minute; high-quality, C-size review copies in under five minutes.

9:30 AM
Documents

HI JetPro Series emulates the IBM® Proprinter™ XL24 to create high quality reports and letters from a wide range of word processing packages.

9:35 AM
Scanner Output

HI JetPro V100 automatically reads and outputs high-resolution, scanned, raster images from hand-held (PCX), desktop (TIFF) and large-format scanners (RLC and CALS). At a fraction of the cost of electrostatic plotters.

9:40 AM
Project Schedules

The rollfeed accessory allows long project management charts to be plotted from rolls of opaque or translucent bond paper.

9:50 AM
Presentation Charts

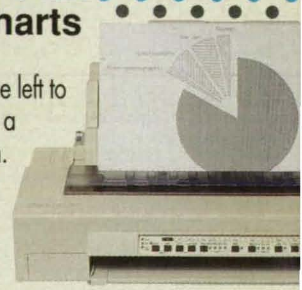

There's even time left to do large-scale charts for a 10:00 AM presentation. For information on HI JetPro Series plotters, or the name of your local dealer, call 1-800-444-3425.

New HI JetPro® Series Plotters.

HOUSTON INSTRUMENT®

Every decision should be this easy.™

For More Information Circle No. 550

Draw Your Complete Analysis Solution with LabVIEW® Graphical Programming

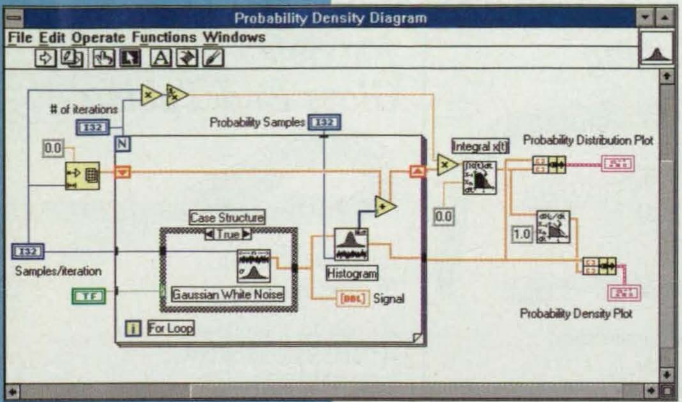

LabVIEW is a complete graphical programming language.

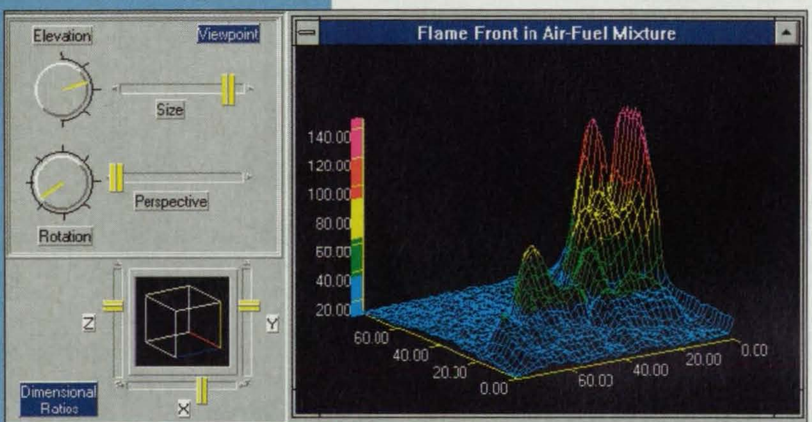

Surface plot of a flame front using LabVIEW and the SurfaceView toolkit.

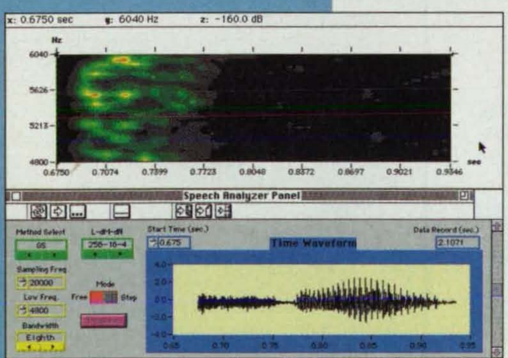

Data courtesy of NIH.

Gabor Spectrogram
National Instruments

The Gabor Spectrogram displays a portion of the sentence "I take two people out for breakfast," computed and displayed with LabVIEW.

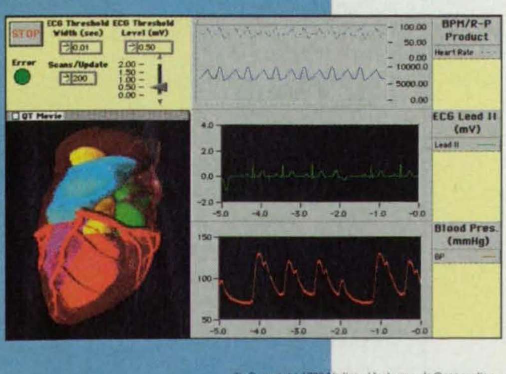

EKG signal and QuickTime heart video using LabVIEW.

Productive and Creative Methodology

Quickly develop programs for analysis, simulation, and algorithm development with the complete graphical programming language found in LabVIEW. It is more than a math calculator. LabVIEW has graphical constructs for While Loops, For Loops, and Case structures.

Advanced Visualization and Plotting

Rapidly create spectrograms, 2D plots, 3D plots, waterfall plots, strip charts, contours, and XY graphs with annotation, printing, and importing.

Powerful Mathematics

The award-winning LabVIEW Gabor Spectrogram algorithm for joint time-frequency analysis (JTFA) is an example of industry-leading innovation. In addition, LabVIEW has hundreds of analysis function blocks for signal processing, digital filters, statistics, and linear algebra. Add-on analysis toolkits include:

- image processing
- surface rendering
- PID control
- 3D plotting
- speech processing
- JTFA

Beyond Analysis

Acquire data from GPIB, VXI, and RS-232 instruments and plug-in data acquisition boards. Connect to other applications with DDE, Apple Events, QuickTime, or TCP/IP. With the open design of LabVIEW, you can easily call programs from C and other languages. In addition, LabVIEW executes at speeds comparable to compiled C code.

Graphical User Interface (GUI) Tools

Easily create virtual instruments and interactively control real-world processes using the GUI controls and indicators built into LabVIEW.

Call for your **FREE** LabVIEW demo and the application note, "Making Real-World Measurements with Fast Fourier Transforms and LabVIEW."

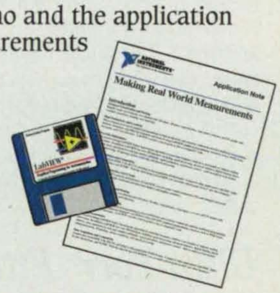

(800) 433-3488 (U.S. and Canada)

LabVIEW is now available on Windows, Sun, and Macintosh.

NATIONAL INSTRUMENTS®
The Software is the Instrument®

6504 Bridge Point Parkway
Austin, TX 78730-5039
Tel: (512) 794-0100
95 (800) 010 0793 (Mexico)
Fax: (512) 794-8411

Branch Offices
Australia 03 879 9422 • Belgium 02 757 00 20 • Canada 519 622 9310
Denmark 45 76 26 00 • Finland 90 527 2321 • France 1 48 65 33 70
Germany 089 7 14 50 93 • Italy 02 48301892 • Japan 03 3788 1921
Netherlands 01720 45761 • Norway 03 846866 • Spain 91 896 0675
Sweden 08 984970 • Switzerland 056 27 00 20 • U.K. 0635 523545

See us at Science Innovation

For More Information Circle No. 681

CAJON Products for Vacuum Service...

IMMEDIATE delivery from local stocks

VCR® Coupling

All metal gasket seal

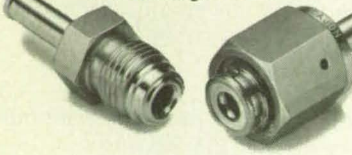

Patented

- Zero-clearance for disassembly
- Critical vacuum
- Choice of end connections from 1/16″ to 1″
- Connects to various weld, SWAGELOK Tube Fitting, NPT and straight thread components
- Variety of configurations
- Sold as individual components to minimize inventories
- 316L & 316 stainless steel
- Helium leak tested to 4.0×10^{-9} atm. cc/sec.
- Pressures — vacuum to 11,000 psi
- Temperatures to 1000°F (537°C)

VCO® Coupling

O-Ring face seal

Patented

- Zero-clearance for disassembly
- Variety of configurations
- Connects to various weld, SWAGELOK Tube Fitting, NPT and straight thread connections
- Sold as individual components to minimize inventories
- Brass & 316 stainless steel
- 1/8″ to 2″
- Helium leak tested to 4.0×10^{-9} atm. cc/sec.
- Pressures — vacuum to 10,000 psi
- Temperatures to 450°F (232°C)
- Fast make-up

Flexible Tubing

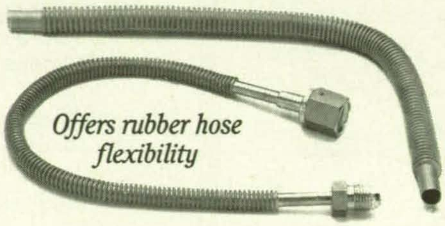

Offers rubber hose flexibility

- 321 stainless steel construction
- Compressible by 20%, extendable by 50%
- Absorbs vibration, relieves thermal expansion, compensates for misalignment
- 1/4″ to 1-1/2″ tube O.D.
- Nominal lengths 1″ to 36″

Flexible Glass End Tubing

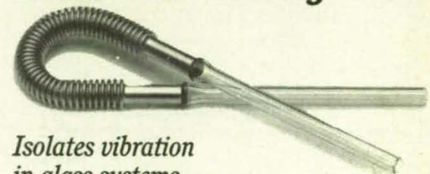

Isolates vibration in glass systems

- Relief for thermal expansion
- Compressible by 20%, extendable by 50%
- 1/4″ to 1″
- Nominal lengths 2″ & 3″
- 321SS fused to 7740 Pyrex glass
- Ultra-high vacuum to 25 PSI
- Single or double end glass

Glass/Metal Transition Tube

One step glass to metal transition eliminates graded seals

- Converts a glass system to a metal system
- Smooth internal surface for high conductance
- Non porous transition area to prevent absorption & outgassing
- Metal, 304SS — Glass, 7740 Pyrex
- Temperature to 960°F (515°C)
- Ultra-high vacuum to 25 PSI
- 100% Helium leak tested
- 1/4″, 3/8″ & 1/2″ sizes
- 6″ lengths

Hose Connectors

Positive gripping-easy to install

- Used on soft plastic or rubber tubing
- NPT & Tube Adapter ends
- Hose clamps for safety
- Reuseable
- 316SS and brass
- 1/8″ to 3/4″

Weld Fittings

For automatic or manual welding

- High conductance
- 316L & 316 stainless steel construction
- 1/4″ to 1″
- Pressures to 5100 psi
- Thin wall design for cleaner, lower profile appearance

Ultra-Torr® Fitting

Provides vacuum-tight seal on glass, metal or plastic

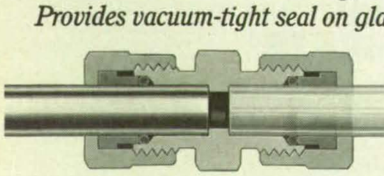

Patented

- Quick finger-tight assembly, reuseable
- Helium leak tested to 4.0×10^{-9} atm. cc/sec.
- 1/16″ to 1-1/2″
- Use with undersize tubing
- Variety of configurations
- Brass & 316 stainless steel
- Temperatures to 450°F (232°C)

Vac Goop®

Anti-gall lubricant for use on threads, O-Rings, gaskets, glass seals and metal parts

- Low vapor pressure minimizes outgassing problems
- Compatible with system materials
- Use on temperatures to 400°F (204°C)
- Impervious to moisture

SWAGELOK/VAC GOOP — TM Crawford Fitting Company
PYREX — TM Corning Glass
ULTRA-TORR/VCO/VCR — TM Cajon Company

CAJON
A SWAGELOK® COMPANY

CAJON COMPANY
9760 Shepard Rd.
Macedonia, OH 44056

For More Information Circle No. 380

July 1993
Volume 17 Number 7

Contents

NASA Tech Briefs

Transferring Engineering Technology to
Over 200,000 Qualified Readers
Throughout Industry and Government

(continued on page 8)

Contents *(continued)*

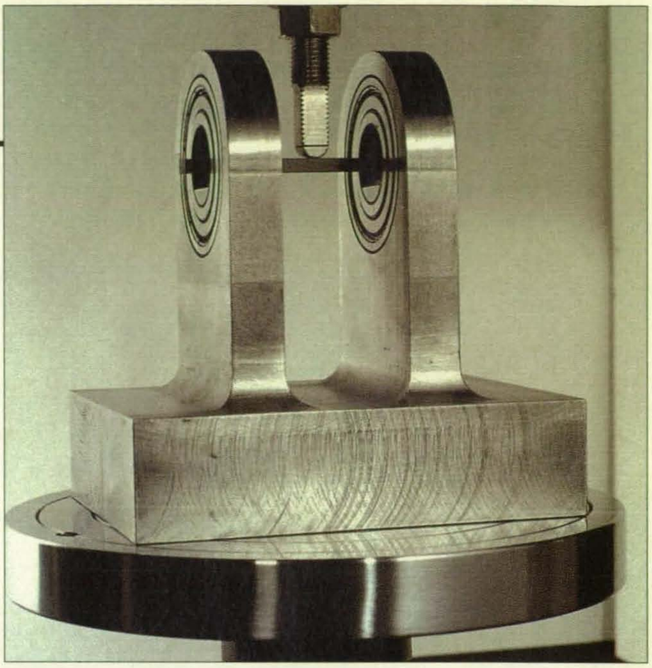

Photo courtesy Langley Research Center

A flexure test developed at Langley Research Center assesses the ply strength of off-axis unidirectional composites. Data on the effect of tensile stress perpendicular to the fibers combined with shear stress parallel to the fibers provides a basis to predict the onset of damage in composite structures. See the tech brief on page 65.

DEPARTMENTS

On the cover:

The WorldToolKit™ software package from Sense8 Corp. opens the door to virtual reality applications for mainstream users in such industries as finance, architecture, communications, medical imaging, and education. The hardware-independent development tool enables users to build real-time, interactive 3D graphics simulations quickly and easily. Turn to Mission Accomplished, page 16. Photo courtesy Sense8 Corporation

NASA Tech Briefs, ISSN 0145-319X, USPS 750-070, copyright © 1993 in U.S., is published monthly by Associated Business Publications Co., Ltd., 41 E. 42nd St., New York, NY 10017-5391. The copyrighted information does not include the (U. S. rights to) individual tech briefs which are supplied by NASA. Editorial, sales, production and circulation offices at 41 East 42nd Street, New York, NY 10017-5391. Subscription for non-qualified subscribers in the U.S. , Panama Canal Zone, and Puerto Rico, $75.00 for 1 year; $125.00 for 2 years; $200.00 for 3 years. Single copies $10.00. Foreign subscriptions one-year U.S. Funds $150.00. Remit by check, draft, postal, express orders or VISA, MasterCard, and American Express. Other remittances at sender's risk. Address all communications for subscriptions or circulation to NASA Tech Briefs, 41 East 42nd Street, New York, NY 10017-5391. Second-class postage paid at New York, NY and additional mailing offices.

POSTMASTER: please send address changes to NASA Tech Briefs, 41 E. 42nd Street, Suite 921, New York, NY 10017-5391.

SCIENCE/SCOPE®

NASA will use new and more durable batteries for two future spacecraft. These super nickel cadmium batteries are made by Hughes Aircraft Company. The batteries combine an improved cell separator material and improved electrodes, for a 15-year life at 80% depth of discharge in spacecraft applications. This outperforms other cells that have a 10-year life at only 50% depth of discharge. The improved batteries, which helped earn Hughes a 1990 Research & Development Award, will be used in NASA's X-Ray Time Explorer and the Total Rainforest Mapper Mission, both scheduled for launch in 1995 to explore the earth's environment.

More and more developing nations are now taking advantage of VSATs for their public and private satellite communications needs, because they are affordable and readily accessible. Hughes, the largest manufacturer of these very small aperture terminals, has supplied many VSATs to these countries, and is prepared to fill the ever increasing demand. It is predicted that this demand will be six times greater in 1996 than it was in 1990. When linked with today's high-powered satellites, VSATs are especially useful for transmitting data and voice communications to and from areas that do not have modern terrestrial telephone systems.

The problem of viewing instrument information in the bright sunlight of military aircraft cockpits can be eliminated with a new full-color display system being developed by Hughes. The Highbright™ display provides high brightness, high color contrast, sunlight rejection, high color saturation and high color stability; and it offers the widest range of colors currently available in an avionics display. It features Hughes' patented liquid crystal projection technology, which dramatically improves reading displays in sunlight over other display technologies. In addition to standard cockpit displays, liquid crystal projection technology can be used to create panoramic displays that will enhance situation awareness for pilots.

Hughes has joined forces with Russia's leading aircraft manufacturer, Mikoyan, and its leading organization for avionics integration, GosNIIAS, to jointly explore developing and producing advanced flight training systems for the Russian MiG 29 and MiG 31, two of the world's most advanced combat aircraft. These systems will cover everything from basic flight and maintenance procedures to full combat missions — especially in mission rehearsal — where they can provide a high level of integration between flight, weapons, and avionics systems. This joint Hughes-Russian venture will also extend into developing training systems for other military and civilian aircraft.

A new pay-per-view television service will soon bring entertainment programming to homes across the country via a high-power satellite. Hughes' Direct Broadcast Satellite (DBS) service, called DirecTv™, will give subscribers a variety of programming choices, including hit movies with multiple starting times. DirecTv will use 27 high power transponders on two satellites and utilize digital compression technology to deliver more than 100 channels of programming to low-cost 18-inch antennas. To implement this new service, Hughes is creating an entirely new infrastructure, which includes telemarketing, customer service, and retail outlet distribution for the satellite antennas. This organization will be in place by the time the first DirecTv satellite is launched in late 1993.

For more information write to: P.O. Box 80032, Los Angeles, CA 90080-0032

HUGHES

Subsidiary of GM Hughes Electronics

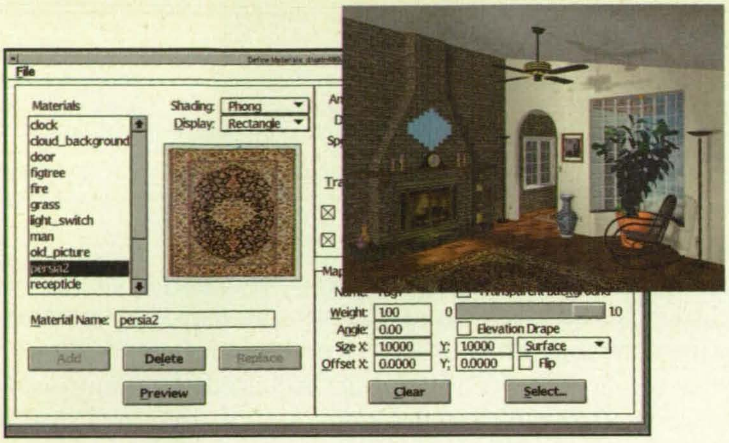

Rendering. *Visualization and flythroughs – at your fingertips! MicroStation offers photo-realistic rendering to every designer, right in the software. It's easy to make your image reflect your imagination.*

Windows. *It walks and talks Windows. Behind MicroStation lies the user-responsive programming you look for in good Window software. Version 5 gives you the ultimate in integration of CAD, engineering, and business applications.*

MORE POWER TO YOU.

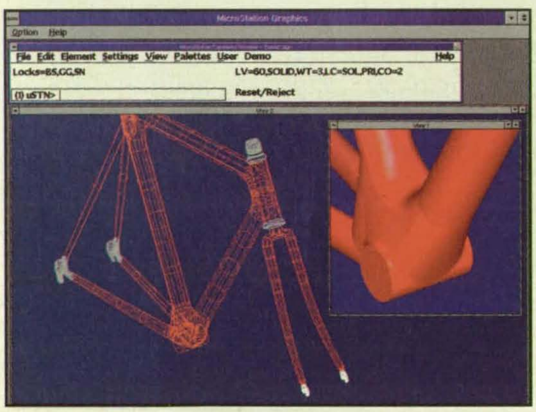

Modeling. *Model any surface you can imagine in MicroStation. NURBS surface modeling combined with 3D Boolean operations gives you astounding flexibility in creating and modifying freeform models.*

Read & write AutoCAD .dwg

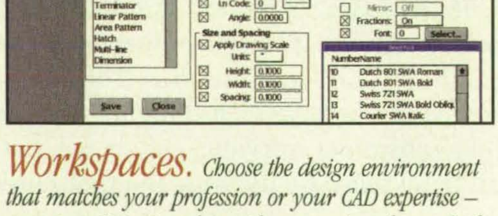

Workspaces. *Choose the design environment that matches your profession or your CAD expertise – even AutoCAD. Complete with custom interfaces, drafting styles, and design environment management. CAD has never been so streamlined!*

Drafting. *MicroStation gives you first-rate drafting pow – without the limitations of old technology. Enjoy the advantage of contemporary features like as ciative patterning/hatching, plot preview, standard text editing a fonts, and context-sensitive Hypertext help.*

O
mas
Mo
point.
for fut
parts.
can be
CIT and

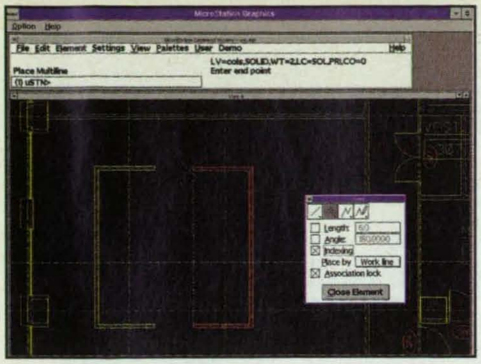

Usability. *What does computer-aided drafting have to do with the way you think? Everything. MicroStation software works for you. It understands the drafting process so well that it infers what you'll do next.*

Power. *Take your pick of popular environments: DOS, Mac, Windows, Windows NT, or UNIX. Have a look at MicroStation on Intergraph's Technical Desktop Series personal workstations.*

Graphical User Interface. MicroStation's easy-to-use interface includes pull-down menus, dialog boxes, tear-off tool palettes, and tool settings window. Choose your interface – Windows or Motif – on any platform. *Transparent Modeless Operation.* The software supports the way you naturally work, maintaining command execution while you fine tune: change element attributes or command parameters, manipulate views, change the dimensioning system, and more. *Powerful View Manipulation.* MicroStation supports up to eight active views that can be moved, sized, and overlapped to fit your design. Zoom and area at any scale. Move around your design fast with built-in dynamic panning. *Workspace Editor.* Tailor pull-down menus, dialog boxes, and tool palettes – even disable commands – with a graphically oriented toolset for customizing your chosen interface. *Text Capabilities.* A convenient text editor lets you easily edit single-line or paragraph text. Choose from TrueType, PostScript, AutoCAD SHX, and MicroStation fonts. ASCII text files can be imported and exported. *Multiple Undo/Redo Commands.* Undo mistakes and perform "what-if" designs in a flash with unlimited undo and redo. *Plotting.* Plot raster and vector information by view or defined areas, at any scale. Visually preview the plot before plotting, saving time and materials. *Online HELP.* MicroStation's HELP remains active, tracking the command you're currently using, so there's no searching through manuals for assistance. *Associative Patterning and Hatching.* Associate patterning with graphics. Change graphics and the patterning updates. Flood-fill hatching/patterning intelligently fills an area, detecting boundaries and holes with a single pick. *Associative Dimensioning.* Dimensions are associated with the geometry, not with a point in space, so that when you change the geometry, the dimensions automatically update. *Custom Line Styles.* Create space-saving custom line styles and place railroad tracks, trees, isobars – anything – just as you would place a line.
ulti-lines. Define line string elements comprising up to 16 parallel lines of varying symbology and store them in a style library for
ll. Architects can use multi-lines for fast and easy placement and intersection cleanup of walls and partitions. *2D Boolean*
ons. Quickly modify, measure, and hatch multiple 2D shapes with integrated Boolean operations. *Mass Properties.* Calculate area and
s of your model: surface area, volume, mass, centroid, moments and products of inertia, principal moments and directions, and radii of gyration.
. Define relationships among graphic entities with intuitive drawing modes such as tangent, parallel, perpendicular, midpoint, intersection, and end-
nsion-driven Symbols. Based on established relationships, you can assign variables to dimensioned graphics and save the graphics as cell
ic placement. Changes in dimensions automatically drive changes to graphics. Dimension-driven design saves valuable time in the design of families
Symbol Libraries. Designs and complex elements can be saved to a library to be recalled later via MicroStation's convenient Cell Browser. Ce
vidually or as shared cells. *Cell Library Browser.* View a cell before you place it with the Cell Browser dialog box. Raster Viewing. You can vi
formats as well as hybrid raster/vector formats and expedite the drafting process.

MicroStation Version 5 puts you in charge.

Call 800-345-4856 for a free brochure on MicroStation Version 5 and the name of an Intergraph representative in your area.

MicroStation

INTERGRAPH

Solutions for the Technical Desktop™

For More Information Circle No. 638

NASA Tech Briefs

Official Publication of National Aeronautics and Space Administration

ABP BPA

NASA Tech Briefs

Published by .... **Associated Business Publications**
Editor-in-Chief/Publisher .... **Bill Schnirring**
Associate Publisher/Editor .... **Joseph T. Pramberger**
Associate Editor .... **Sarah L. Gall**
Assistant Editor .... **Gregg McQueen**
Technical Advisor .... **Dr. Robert E. Waterman**
Director of Manufacturing .... **Gregg Weatherby**
Traffic Manager .... **James E. Cobb**
Contract Control Manager .... **Donna Jones**
Art Director .... **Pierre Granier**
Assistant Art Director .... **J. Kent Alexander**
Marketing Director .... **Wayne Pierce**
Advertising Coordinator .... **Nipa Joshi**
Telecommunications Specialist .... **Evelyn Mars**
Reader Service Manager .... **Scott Floman**
Circulation .... **Anita Gillespie**

Briefs & Supporting Literature:
Provided to National Aeronautics and Space Administration by
International Computers & Telecommunications, Inc., NY, NY
Technical/Managing Editor .... **Ted Selinsky**
Art Director .... **Ernest Gillespie, Jr.**
Administrator .... **Elizabeth Texeira**
Chief Copy Editor .... **Lorne Bullen**
Staff Writers/Editors .... **Dr. Larry Grunberger, Dr. Theron Cole, Jordan Randjelovich, George Watson, Oden Browne**
Graphics .... **Zinaida Gimpeleva, Pamela Baynham, Charles Sammartano**
Editorial & Production .... **Bill Little, Ivonne Valdes, Susan Kyu Oh, Frank Ponce**

NASA:
NASA Tech Briefs are provided by the National Aeronautics and Space Administration, Technology Transfer Division, Washington, DC:
Administrator .... **Daniel S. Goldin**
Deputy Assistant Administrator(Programs) .... **Frank E. Penaranda**
Deputy Director Technology Transfer Division (Publications Manager) .... **Leonard A. Ault**
Manager, Technology Transfer Office, NASA Center For AeroSpace Information .... **Walter M. Heiland**

Associated Business Publications
41 East 42nd Street, Suite 921, New York, NY 10017-5391
(212) 490-3999 FAX (212) 986-7864
President/Chief Executive Officer .... **Bill Schnirring**
Executive Vice President/Chief Operating Officer .... **Domenic A. Mucchetti**
Treasurer .... **Joseph T. Pramberger**
Controller .... **Athena Thomas**
Credit/Collection .... **Felecia Lahey**
Trade Show Director .... **Wendy S. Janiel**
Human Resources Manager .... **Lourdes Del Valle**
MIS Manager .... **Ted Morawski**
Accounting .... **Sylvia Valentin**
Mailroom Manager .... **Thomas C. Snyder**

Advertising:
New York Office: (212) 490-3999 FAX (212) 986-7864
Account Executives:
NY, NJ .... **Brian Clerkin** at (201) 366-2751
PA, DE, NJ (Area Code 609) .... **Tara Morie** at (215) 640-3118
VA, DC, MD, WV .... **John D. Floyd, CBC** at (215) 399-3265
Eastern MA, NH, ME, RI .... **Paul Gillespie** at (508) 429-8907; **Bill Doucette** at (508) 429-9861
Western MA, CT, VT .... **George Watts** at (413) 253-9881
Southeast, Southwest .... **Douglas Shaller** at (212) 490-3999
OH, MI, IN, KY .... **Scott Burrows** at (216) 688-6232
Northern IL, WI .... **Paul Lesher, CBC** at (312) 296-2040
Southern IL, MO, IA, MN, ND, SD, NE, KS .... **Melinda Mead** at (312) 296-2040
Northwest—WA, OR, ID, MT, WY .... **Bill Hague** at (206) 858-7575
West Coast—CA, AZ, NV, NM, UT .... **Stillman Group** at (310) 372-2744
for Area Codes 602/702/505/801/818/805: **Tom Stillman**
for 310/619/714: **Robert D'Alexander**
for 408/415/916/209/707: **Robert Hubbard**

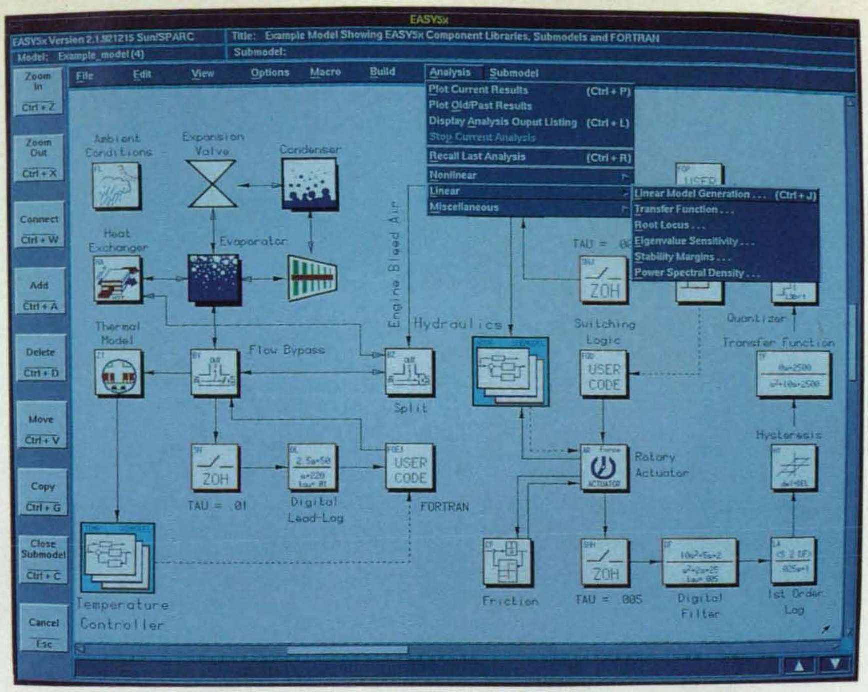

Modeling and analysis completed with a Motif®-based X Window™ interface.

Does it go bump in the night?

Is it stable? Can you control it? And, what happens when you turn it on?

If you design electrical, hydromechanical, chemical, and/or digital control systems, these are the kinds of questions you probably have.

You want to know how the system behaves, and if it can be controlled. But you can't afford to spend a lot of time and money in the process.

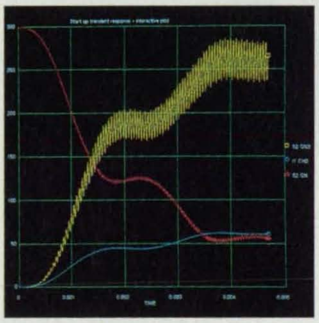

Non-linear simulation results viewed interactively or off-line.

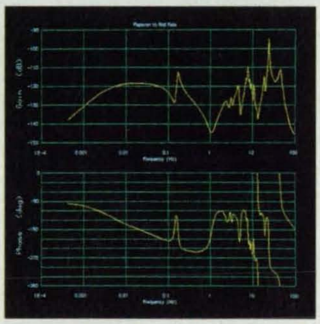

Frequency-response data displayed in Bode, Nichols, or Nyquist formats.

With EASY5x®, you'll get the answers you want. And you'll get them cost-effectively.

Proven software.

Developed, tested, and refined at Boeing, EASY5x has been used to model, simulate, and analyze complex and highly non-linear systems. Especially those containing microprocessor-based controllers.

And today, engineers worldwide are using EASY5x in a variety of industries. For example, EASY5x helps build the cars you drive, the airplanes you fly, and the power plants you depend on.

Unparalleled system modeling.

With EASY5x, modeling difficult system dynamics can be a routine exercise.

That's because EASY5x comes with hundreds of modeling blocks. Including discontinuous elements like friction, hysteresis, and hard limits.

Our libraries are also full of physical elements such as hydraulics, heat exchangers, and freon components.

You can even create your own modeling blocks and share them freely. EASY5x helps by maintaining tight configuration control for you.

Efficient analyses.

EASY5x provides simulation performance up to 100 times faster than other software on the market.

Even our control system analysis tools will save you time, particularly when you analyze multi-rate sampled-data systems.

And if you need world-class solutions to real-time simulation problems, EASY5x software now interfaces with hardware supplied by Applied Dynamics International.

Call for a free trial.

EASY5x is sophisticated enough to be simple to use. It's supported by a highly trained technical staff. And the software is mature enough to provide answers to really tough dynamics problems accurately and quickly.

You can get started with EASY5x on your Sun, Hewlett-Packard, Digital, Silicon Graphics, or IBM RS6000™ UNIX® workstation for $8,900. (U.S. and Canadian universities may join our University Program at no cost.)

All things considered, EASY5x is the best value on the market. And we'd like to prove it to you.

Call for a free, 30-day trial. Phone 1-800-426-1443 or FAX 206-865-2966. Or write to Boeing, P.O. Box 24346, M/S 7L-46, Seattle, WA 98124-0346, USA.

For More Information Circle No. 416

BOEING

Arabsat

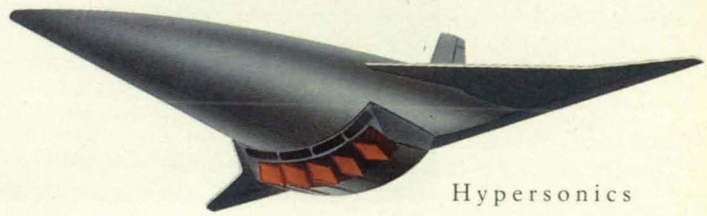

Hypersonics

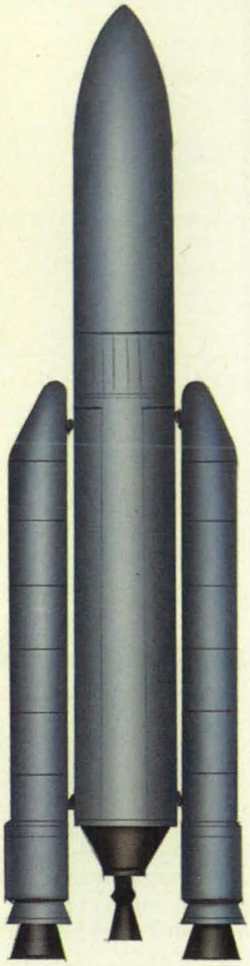

Ariane 5

Ariane 4

Meteosat

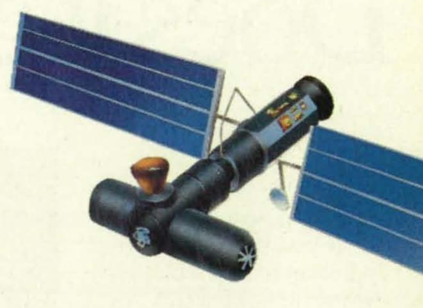

space station

We're capable

Highly diversified skills, and an unusually wide product range make Aerospatiale Espace & Défense the only company in the world with complete mastery in all fields of both civil and military space. Industrial architect for Ariane, Aerospatiale has already delivered more than 100 stages of this launch vehicle, and will build some 50 more Ariane 4's before the year 2000. Aerospatiale is also developing the new, and more powerful Ariane 5 launcher, and is leading the industrial team behind Hermes, the European spaceplane. As Europe's major satellite manufacturer, Aerospatiale has already contributed to more than 60 weather, telecommunications, direct TV broadcasting, Earth observation, and scientific satellites. In its capacity as industrial prime contractor for the missile systems of the French nuclear deterrent force, Aerospatiale is also the only European company to design, develop, and manufacture strategic ballistic missiles.

A C H I E V E M E N T   H A S   A   N A M E .

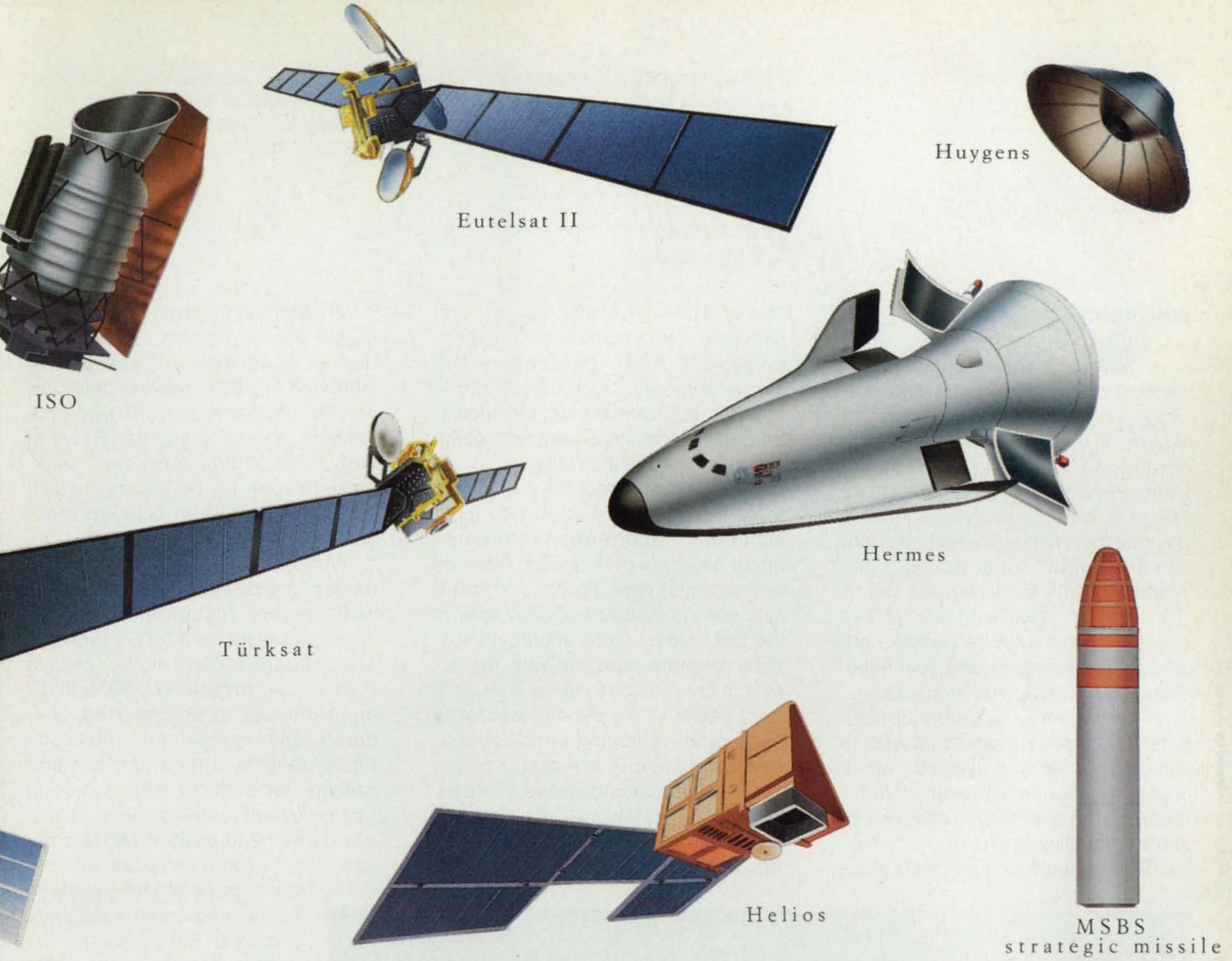

of anything.

AEROSPATIALE
ESPACE & DEFENSE

For More Information Circle No. 627

Mission Accomplished

Through the technology transfer process, many of the systems, methods, and products pioneered by NASA are reapplied in the private sector, obviating duplicate research and making a broad range of new products and services available to the public.

Virtual reality (VR) technology, once the exclusive province of large government and military laboratories, is rapidly becoming accessible to a wide circle of developers for use in applications ranging from architectural and molecular design to financial analysis and medical imaging. Helping to open the door into these new virtual worlds is the WorldToolKit™ from Sense8 Corp., Sausalito, CA. Developed with NASA's assistance, the software package enables users to rapidly and cost-effectively build 3D graphics simulations.

In virtual reality, an array of computer technologies are employed to immerse a user in a synthetic world, creating a sensory-based environment that interactively responds to and is controlled by the user's behavior. The more efficient and natural the flow of data—the sights, sounds, and sensations that mimic actual experience—the more persuasive the sense of reality. Such verisimilitude requires substantial computer power and, until recently, expenses prohibitive to independent developers.

Traditionally, real-time graphics tools were targeted mainly to flight simulation laboratories that could afford networks of dedicated graphics workstations, data gloves, and headsets costing upwards of $250,000. In the late 1980s, more affordable systems became possible with the arrival of lower-cost platforms with sufficient power in the main processor to perform 3D rendering in real time, a new generation of low-cost graphics accelerators, and advanced VR hardware, such as low-cost position sensors and headmounted stereoscopic video displays.

VR application developers, however, still had to program each application from scratch. WorldToolKit, launched in 1991, relieves this burden by encapsulating 3D real-time rendering in a simple-to-use library of C routines. A fully-functional "walk-through" can be built from just 20 lines, each of which calls up thousands of lines of C code.

WorldToolKit integrates a real-time rendering pipeline and 3D modelers with sensors, input and output devices, and graphics display hardware. The software permits models or data from a wide range of 2D, 3D, and 6D input devices to be imported, rendered, and manipulated intuitively. Input from head-mounted position sensors, for example, can be used to update WorldToolKit's stereoscopic display for head position and orientation. The hardware-independent software supports cross-platform development and extension. Priced at $3500 for the PC version, it is available on IBM PC-AT, Sun SPARCstation, and Silicon Graphics computers, from Indigo through the Reality Engine.

With NASA's help, according to company president Tom Coull, Sense8 doubled to 400 the number of function calls in version 2.0 of the software, released in May. "We've established a very tight feedback loop with Ames Research Center, which has served as a beta site," he said. "At their request, we improved such functions as terrain generation and rendering."

NASA's relationship with Sense8 began last July, when it licensed WorldToolKit for use in telerobotic planning and operation. "We were working to combine virtual reality with telepresence techniques to construct an operator interface," explained

WorldToolKit™, platform-independent software from Sense8 Corp., provides an environment for building interactive, real-time 3D graphics and virtual reality applications.

BACKUP 50 GB IN HALF THE TIME.

Two 8mm tape drives, each capable of storing up to 25 GB, can be combined in a single desktop cabinet. This dual configuration lets you take full advantage of our Advanced SCSI Processor.

Now, two drives can work together simultaneously to maximize backup speed and capacity with a variety of recording modes.

STRIPING MODE. In striping mode, you can write data to two tapes at once, in alternate blocks–doubling speed and capacity. In fact, you can back up 50 GB overnight this way.

MIRRORING MODE. In mirroring mode, you write the same data to two tapes at the same time. This is ideal for users who want to keep a backup off-site, for extra security, or for users who need to exchange data with other sites.

OFF-LINE COPY. An off-line copy function lets you copy the contents of one tape to another–without tying up the host. Off-line verify ensures that the tapes are identical.

CASCADE MODE. In cascade mode, data spills over to the second tape when the first tape is full.

FLEXIBILITY IS ONLY HALF THE STORY. Our data compression option is the fastest available. And it's switch-selectable, so you can still read and write standard 8mm tapes. Bright backlit status displays give you complete drive status information: recording mode, transfer rate, compression ratio,tape remaining and more.

Best of all, you get the advantages of 8mm helical scan technology–reliable, unattended operation and the best price-performance on the market.

Plug compatible with virtually every computer system, the drives are fully backed by our 12-month warranty that includes support from our in-house engineering staff.

For information, call today at

(804) 873-9000

CONTEMPORARY
CYBERNETICS

TRUE PLUG COMPATIBILITY

Alliant	Convergent	DEC Unibus	ICL	Novell	Plexus	Sun
Alpha Micro	Data General	Gould/Encore	Intergraph	OS/2	Prime	Texas
Altos	DEC 3100/5000	HP	Macintosh	PS/2	Pyramid	Instruments
Apollo	DEC BI-Bus	IBM AS/400	McDonnell	Parallel Port	Sequent	Unisys
Arix	DEC DSSI	IBM Mainframe	Douglas	PC 386/ix	Silicon	Wang
AT&T	DEC HSC	IBM RISC/6000	Motorola	PC MS-DOS	Graphics	*and more*
Basic-4	DEC Q-Bus	IBM RT	NCR	PC Xenix/Unix	STC	
Concurrent	DEC TU/TA81	IBM S/38	NeXT	Pertec	Stratus	

Rock Landing Corporate Center • 11846 Rock Landing • Newport News, Virginia 23606 • Fax (804)873-8836

For More Information Circle No. 422

Butler Hine, leader of the Intelligent Mechanisms Group at NASA Ames. "WorldToolKit enabled us to do rapid prototyping, which saves a lot of time."

Ames researchers used the software to create a virtual environment that simulates a robot arm to integrate into the teleoperator interface. The virtual arm enables operation, via Ethernet, of an actual robotic arm in another laboratory.

In December 1992, scientists in an Ames laboratory used the interface to control, via satellite video link, the camera on an underwater research vehicle in the Antarctic. And in May, Ames researchers used it to maneuver a Russian planetary rover in a Moscow laboratory. According to Hine, the long-term goal is to use stored plans from a virtual environment simulation to control a real robot on Mars. Such a system would compensate for lengthy transmission delays between Earth and other planets when using remote control.

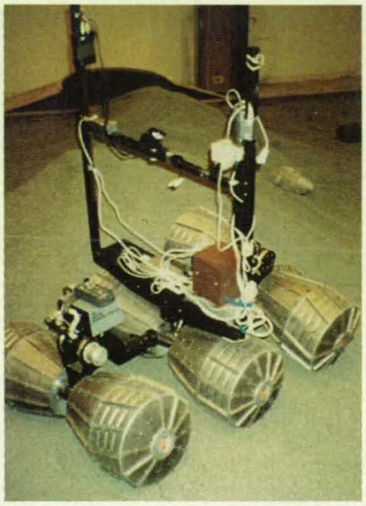

A teleoperator interface developed using WorldToolKit enabled researchers at Ames Research Center in California to remotely control a Russian planetary rover (above) in Moscow.

WorldToolKit already is addressing various problems here on Earth. The Hines Rehabilitation and R&D Center in Illinois applied it to create software that helps architects assess whether proposed designs provide accessibility to the disabled. A wheelchair user, for example, can navigate through a virtual kitchen to evaluate the design, spacing, and dimensions of cupboards and counters.

Maxus Systems International used WorldToolKit to produce Capri, a market analysis tool that enables inventors to visualize important industrial trends. Users can "fly" through the financial world, represented as a huge grid with each quadrant corresponding to a country and industry group. Individual stocks are represented as polygons that change in color and size according to current market activity. WorldToolKit also was used to create a PC-based virtual reality exhibit at the Computer Museum in Boston, MA.

Upcoming software products from Sense8 are designed to further extend the accessibility of VR technology. Mercury, a low-cost VR development toolkit based on WorldToolKit, targets hobbyists and home users. Scheduled for release in August and priced under $1000, the VGA-based software will contain much of WorldToolKit's functionality with the exception of some advanced features such as support for high-end graphics platforms. The company also is focusing on the nonprogrammer. Currently under development is Odyssey, a VR environment that will run on standard X86 machines and come with a number of ready-to-use, extensible VR applications. ❑

For more information about the technologies described in this article, contact Tom Coull, President, Sense8 Corporation, 1001 Bridgeway, #477, Sausalito, CA 94965, Tel: 415-331-6318.

New Product Ideas

New Product Ideas are just a few of the many innovations described in this issue of *NASA Tech Briefs* and having promising commercial applications. Each is discussed further on the referenced page in the appropriate section in this issue. If you are interested in developing a product from these or other NASA innovations, you can receive further technical information by requesting the TSP referenced at the end of the full-length article or by writing the Technology Utilization Office of the sponsoring NASA center (see page 24). NASA's patent-licensing program to encourage commercial development is described on page 24.

Microwave Pretreatment for Hydrolysis of Cellulose

Microwave pretreatment enhances the enzymatic hydrolysis of cellulosic wastes (e.g., paper, cornstalks, bagasse) into soluble saccharides that can be used as feedstocks for foods, fuels, and other products. The process can be a viable alternative to composting.
(See page 54.)

Portable Lifting Seat

A portable lifting machine assists a user in rising from a seated position to a standing position, or in sitting down. It is small and light enough to be easily carried like a briefcase.
(See page 75.)

Electronic Edge Finder

A new edge finder would help in measuring the dimensions of machined parts to within 0.0001 in. (2.5 μm). Such accuracy is not attainable with ordinary touch-type indicators.
(See page 76.)

System Applies Polymer Powder to Filament Tow

This powder-coating system applies dry polymer powder to a continuous fiber tow. The unique filament-spreading technique, combined with precise control of tension on the fibers, ensures uniform application of polymer powder to the web of spread filaments.
(See page 77.)

Recessed-Contact Cleaner

A tool cleans receptacles for electronic-circuit-card connectors. It is shaped somewhat like a circuit card and holds a lint-free cloth around one of its edges.
(See page 79.)

Kinetic Tetrazolium Microtiter Assay

A new assay continuously measures metabolism and thereby makes it possible to determine the rate of action of an antimicrobial agent in real time. Quick assays are extremely important in treatment of water, treatment of waste, and disinfection of hospital rooms, and in the pharmaceutical, agricultural, and food-processing industries.
(See page 86.)

High-Performance Water-Iodinating Cartridge

This cartridge iodinates water to near saturation in a single pass. The cartridge can be reused several times before a refill with fresh iodine crystals.
(See page 86.)

CAN YOU

McDonnell Douglas did. The faint outline of a new space station drifting across the night sky. Finding it took a remarkable group of engineers. And an equally remarkable computer. The Apple® Macintosh.® Why did they choose Macintosh? Maybe they wanted computers with the power to work quickly, efficiently and, above all, intuitively. Perhaps it was because our systems run critical engineering applications, like Alias Sketch!, Microstation and Presenter Pro. Or because ours are the only computers able to read from

SEE IT?

and write to Macintosh, DOS, OS/2 and Windows floppy disks, offering compatibility with most existing systems.* It could have been our built-in networking and file sharing, which let everyone tap into the same information, turning the idea of concurrent engineering into a reality. Or maybe, just maybe, McDonnell Douglas chose Macintosh for the same reasons everyone else does. For the power to explore new ideas. The power to chase dreams. The power to be your best.® Macintosh for Engineers.

HOW YOU CAN BENEFIT FROM NASA's TECHNOLOGY UTILIZATION SERVICES

If you're a regular reader of TECH BRIEFS, then you're already making use of one of the low-and no-cost services provided by NASA's Technology Transfer Program. But a TECH BRIEFS subscription represents only a fraction of the technical information and applications/engineering services offered by this Program. In fact, when all of the components of NASA's Technology Transfer Network are considered, TECH BRIEFS represents the proverbial tip of the iceberg.

We've outlined below NASA's Technology Transfer Network—named the participants, described their services, and listed the individuals you can contact for more information relating to your specific needs. We encourage you to make use of the information, access, and applications services offered.

How You Can Access Technology Transfer Services At NASA Field Centers:

Technology Utilization Officers & Patent Counsels—Each NASA Field Center has a Technology Utilization Officer (TUO) and a Patent Counsel to facilitate technology transfer between NASA and the private sector.

If you need further information about new technologies presented in *NASA Tech Briefs*, request the Technical Support Package (TSP). If a TSP is not available, you can contact the Technology Utilization Officer at the NASA Field Center that sponsored the research. He can arrange for assistance in applying the technology by putting you in touch with the people who developed it. If you want information about the patent status of a technology or are interested in licensing a NASA invention, contact the Patent Counsel at the NASA Field Center that sponsored the research. Refer to the NASA reference number at the end of the Tech Brief.

Ames Research Ctr.
Technology Utilization
Officer:Geoffrey S. Lee
Mail Code 223-3
Moffett Field, CA 94035
(415) 604-4044
Patent Counsel:
Darrell G. Brekke
Mail Code 200-11
Moffett Field, CA 94035
(415) 604-5104

Lewis Research Center
Technology Utilization
Officer: Anthony F.
Ratajczak
Mail Stop 7-3
21000 Brookpark Road
Cleveland, OH 44135
(216) 433-5568
Patent Counsel:
Gene E. Shook
Mail Code LE-LAW
21000 Brookpark Road
Cleveland, OH 44135
(216) 433-5753

John C. Stennis Space Center
Acting Technology
Utilization Officer:
Richard A. Galle
Code HA-30
Stennis Space Center,
MS 39529
(601) 688-1929

John F. Kennedy Space Center
Technology Utilization
Officer: James A.
Aliberti
Mail Stop DE-PAT
Kennedy Space
Center, FL 32899
(407) 867-3017
Patent Counsel:
Bill Sheehan
Mail Code DE-PAT
Kennedy Space
Center, FL 32899
(407) 867-2544

Langley Research Ctr.
Technology Utilization
Officer: Joseph J.
Mathis, Jr.
Head, TU & AO Office
Mail Stop 200
Hampton, VA 23681-0001
(804) 864-2484
Patent Counsel:
Dr. George F. Helfrich
Mail Stop 143
Hampton, VA 23681-0001
(804) 864-3221

Goddard Space Flight Center
Technology Utilization
Officer: Dr. George Alcorn
Mail Code 702
Greenbelt, MD 20771
(301) 286-5810
Patent Counsel:
R. Dennis Marchant
Mail Code 204
Greenbelt, MD 20771
(301) 286-7351

Jet Propulsion Lab.
NASA Resident Office
Technology Utilization
Officer: Arif Husain
Mail Stop 180-801D
4800 Oak Grove Drive
Pasadena, CA 91109
(818) 354-4862
Patent Counsel:
Thomas H. Jones
Mail Code 180-801G
4800 Oak Grove Drive
Pasadena, CA 91109
(818) 354-5179

Technology Utilization
Mgr. for JPL:
Wayne Schober
Mail Stop 122-116
4800 Oak Grove Drive
Pasadena, CA 91109
(818) 354-2240

George C. Marshall Space Flight Center
Technology Utilization
Officer: Ismail Akbay
Code AT01
Marshall Space Flight
Center,
AL 35812
(205) 544-2223
Patent Counsel:
Robert L. Broad, Jr.
Mail Code CC01
Marshall Space Flight
Center,
AL 35812
(205) 544-0021

Lyndon B. Johnson Space Center
Technology Utilization
Officer: Richard B.
Ramsell
Mail Code IC-4
Building 4 South
Houston, TX 77058
(713) 483-3809
Patent Counsel:
Edward K. Fein
Mail Code AL3
Houston, TX 77058
(713) 483-4871

NASA Headquarters
Technology Utilization
Officer: Leonard A. Ault
Code CU
Washington, DC 20546
(202) 358-0721
Associate General
Counsel for Intellectual
Property: Jack Mannix
Code GP
Washington, DC 20546
(202) 453-2424

How You Can Utilize **NASA's Regional Technology Transfer Centers (RTTCs)**— A nationwide network offering a broad range of technology transfer and commercialization services.

You can contact NASA's network of RTTCs for assistance in solving a specific technical problem or locating technology or markets that match your interests. The RTTCs are experienced in working with industry to define technology needs and acquire and commercialize applicable technology. User fees are charged for most services. **For more information, call 1-800-472-6785** and you will be connected to the RTTC in your geographical region (or you may call or write directly to the RTTC in your region).

REGIONAL TECHNOLOGY TRANSFER CENTERS (RTTCs)

RTTC Directors

NORTHEAST
Dr. William Gasko
Center tor Technology
Commercialization
Massachusetts Technology Park
100 North Drive
Westborough, MA 01581
(508) 870-0042

MID-ATLANTIC
Ms. Lani S. Hummel
University of Pittsburgh
823 William Pitt Union
Pittsburgh, PA 15260
(412) 648-7000
(800) 257-2725 (toll-free US)

SOUTHEAST
Mr. J. Ronald Thornton
Southern Technology Application
Center
University of Florida
College of Eng.
Box 24
One Progress Boulevard
Alachua, FL 32615
(904) 462-3913
(800) 225-0308 (outside FL)

MID-CONTINENT
Mr. Gary Sera
Texas Engineering Experiment Station
Texas A&M University System
237 WERC Collge Station,
Texas 77843-3401
409-845-8762

MID-WEST
Dr. Joseph W. Ray
Great Lakes Industrial Technology Center
25000 Great Northern Corporate Center
Suite 450
Cleveland, OH 44070-5310
(216) 734-0094

FAR-WEST
Mr. Robert Stark
Technology Transfer Center
University of Southern California
3716 South Hope Street,
Suite 200
Los Angeles, CA 90007-4344
(213) 743-6132
(800) 642-2872 (CA only)
(800) 872-7477 (toll-free US)

If you are interested in information, applications, research, training, and services relating to satellite and aerial data for Earth resources, contact NASA's transfer point for earth observing technology: **Technology Application Center, University of New Mexico, 2500 Yale Blvd. S.E., Suite 100, Albuquerque, NM 87131-6031; Dr. Stan Morain, Director (505) 277-3622.**

If you represent a public sector organization with a particular need, you can contact NASA's Application Team for technology matching and problem solving assistance. Staffed by professional engineers from a variety of disciplines, the Application Team works with public sector organizations to identify and solve critical problems with existing NASA technology. **Technology Application Team, Research Triangle Institute, P.O. Box 12194, Research Triangle Park, NC 27709; *Dr. Doris Rouse, Director,* (919) 541-6980**

A Shortcut To Software: **COSMIC®**—For software developed with NASA funding, contact COSMIC, NASA's Computer Software Management and Information Center. New and updated programs are announced in the Computer Programs section. COSMIC publishes an annual software catalog. For more information call or write: **COSMIC®**, 382 East Broad Street, Athens, GA 30602 *John A. Gibson, Director,* (706) 542-3265; FAX (706) 542-4807.

If You Have a Question..**NASA Center For AeroSpace Information** can answer questions about NASA's Technology Transfer Network and its services and documents. The CASI staff supplies documents and provides referrals. Call, write or use the feedback card in this issue to contact: **NASA Center For AeroSpace Information,** Technology Transfer Office, 800 Elkridge Rd, Linthnicum Heights, MD 21090-2934. *Walter M. Heiland, Manager,* (410) 859-5300, Ext. 245.

Fred Molinari, President

No Data Acquisition Application Is Beyond Our Grasp.

Whether you're making scientific measurements to 24-bit accuracy, performing FFTs in real time, or looking for a robust yet low cost solution, Data Translation has the right data acquisition solution for you. With more than 300 products, you can easily find exactly what you need.

Using our Windows-compatible software, you'll get your project up and running faster than ever. For immediate application gratification, choose one of our icon or menu-driven packages and you'll be acquiring data within minutes. Develop your applications using one of our DT-Open Layers™ compliant software tools, and rest assured that your code will run any supported board with little or no reprogramming.

SOFTWARE
- Windows and DOS applications
- Extensive C and Visual Basic software tools for programmers

HARDWARE
- 8–24 bits
- Up to 1 MHz throughput
- Up to 224 inputs
- Optional anti-aliasing filters
- Simultaneous sampling
- Onboard DSP

Whatever your needs, call Data Translation first. We have it all: the right hardware, easy-to-use software, and exceptional pre- and post-sales customer support.

And that's quite a handful.

FOR MORE INFORMATION, CALL 1-800-525-8528, EXT. 363

DATA TRANSLATION®

UK Headquarters: (0734) 793838, Germany Headquarters: (07142) 95 31-0, France Headquarters: 50.45.95.83, Italy Headquarters: (39) 30242-5696. Sales Offices: Australia 2699-8300; Austria: (222) 36-7660; Belgium (02) 466.81.99; Brazil 11564-6024; Canada (416) 625-1907 or (800) 268-0427; Denmark (45) 4227-4511; Finland (358) 0351-1800; Greece (30) 1361-4300; Hong Kong (852) 515-0018; India (91) 2223-1040; Israel (972) 954-5685; Japan (81) 33502-5550 or (81) 335379-1971; Korea (82) 2718-9521; Malaysia (60) 3248-6786; Mexico (52) 5575-6091, (52) 5575-6098; Netherlands (31) 70399-6360; New Zealand (64) 9415-8362; Norway (47) 22434150; Poland 4822 580701;Portugal (351) 1793-4834, (351) 1793-4934; Singapore (65) 336-4767; South Africa (27) 12803-7680/93; Spain (34) 1555-8112; Sweden (46) 8765-0208; Switzerland (41) 1386-8686; Taiwan (88) 62303-9836; Turkey (90-1) 288-6213 (90-1) 288-6215

For More Information Circle No. 662

Biological Information Signal Processor

A new class of DNA-sequence-alignment coprocessors is being developed.

NASA's Jet Propulsion Laboratory, Pasadena, California

The Biological Information Signal Processor (BISP), which is in the early stages of development, is a computing system that will analyze data on deoxyribonucleic acid (DNA) sequences for molecular genetic analyses. Many of these data are being generated in the effort to list and map the DNA sequences of the human genome. As the number of these data grows at exponentially increasing rates, the analyses consume increasing amounts of time on present computing systems.

The BISP will include coprocessors — specialized microprocessors that will complement present and future computers by performing rapidly the most-time-consuming DNA-sequence-analyzing functions, establishing relationships (alignments) between both global sequences and defining patterns in multiple sequences. The BISP will also include state-of-the-art software and data-base systems on both conventional and parallel computer systems to augment the analytical abilities of the developmental coprocessors.

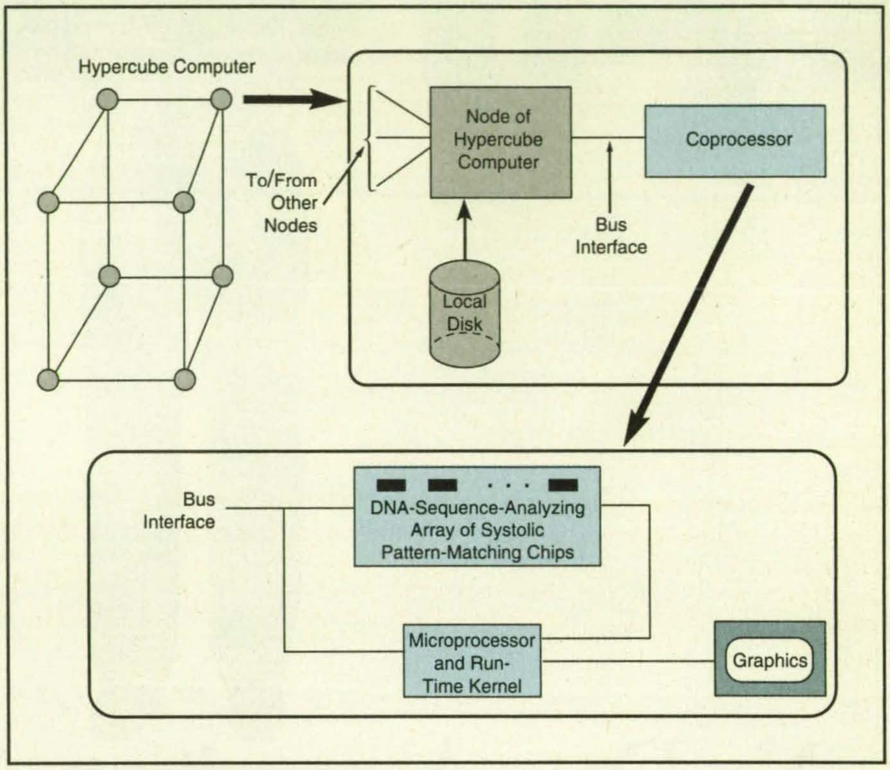

A **DNA-Sequence-Analyzing Coprocessor** could be incorporated into each node of a hypercube computer.

The development of an alignment coprocessor will be an incremental, evolutionary process, probably entailing a series of hybrid coprocessors incorporating more and more of the needed functionalities in custom-made integrated-circuit chips. Because of the formidable difficulties in achieving full functionality initially on a single chip, at least the initial coprocessors will be hybrid systems on printed-circuit (PC) boards. The PC assembly will include an array of systolic pattern-matching chips tightly coupled with a dedicated microprocessor. This microprocessor will run a stripped-down, run-time kernel and will regulate the flow of data to and from the systolic array and the central processing unit of the host computer (host CPU). Disk input/output will be direct to the systolic array, also controlled by the microprocessor. This will allow the maximum data stream to pass through the array. Information on alignment and on scoring (numerical indications of the degree of partial alignment of sequences) from the array will be analyzed by machine-level procedures in the microprocessor, which will be responsible for communicating results to the host CPU or directly to output or memory devices The PC board will communicate with the host through standard interface systems.

The two most probable "bottlenecks" will be the disk input/output speed and the performance of the microprocessor. The question of local memory or cache must also be considered. With appropriate filters, most sequence comparisons will be recognized as insignificant before alignment information is passed to the processor chip. This may mean that the results that stream to the processor will have bursts rather than a steady flow. Caching between the systolic array and the processor may avoid most delays when the flow of results exceeds the throughput rate of the microprocessor. Likewise, caching of alignment results could eliminate most input/output bottlenecks. Recent commercial availability of megabit memory chips affords the possibility of substantial buffering capabilities.

The alignment algorithm(s) of the earliest BISP systems must be more directly aimed at identifying regions of local similarities. The system must be able to return a biologically realistic similarity score, and, hence, a more flexible and complex scheme for weighting gaps must be implemented. This means that scoring parameters must be programmable, rather than hard-wired into the chips. This will take some level of processing at the chip level and will probably require local random-access memory. Information about the actual alignment of the two sequences must be returned by the process. The chips will not do the alignments. This will be a function of the dedicated processor, using path-scoring information from the chips.

A significant feature for biologists will be the addition of models, defined by users, of conservative relationships between residues, bases, codons, and the like. These models require the definition of similarity tables. Only one copy of such a table is needed in software.

As the data bases grow larger, it will eventually become necessary to consider computing architectures that provide for economical concurrency of multiple

processors. For example, each node of a hypercube computer could incorporate an alignment-coprocessor system (see figure). Each node would have extensive local memory and direct control of a dedicated disk. Each node would be responsible for only a portion of the search of the data bases, increasing throughpout by a factor equal to the number of nodes. Multiple processor boards, each with its own disk drive, could also be run on one workstation-class system.

This work was done by Edward T. Chow, John C. Peterson, and Michael M. Yoo of Caltech for **NASA's Jet Propulsion Laboratory**. *For further information, Circle 75 on the TSP Request Card.*

In accordance with Public Law 96-517, the contractor has elected to retain title to this invention. Inquiries concerning rights for its commercial use should be addressed to

William T. Callaghan, Manager
Technology Commercialization
Jet Propulsion Laboratory
(M/S 301-350)
4800 Oak Grove Drive
Pasadena, CA 91109

Refer to NPO-18044, volume and number of this NASA Tech Briefs *issue, and the page number.*

Programmable Multiple-Ramped-Voltage Power Supply

Ramp waveforms can range up to 2,000 V.

NASA's Jet Propulsion Laboratory, Pasadena, California

A laboratory high-voltage power-supply system puts out a variety of stable voltages that can be programmed to remain fixed with respect to ground or to float with respect to a ramp waveform. The system also measures the voltages it produces with high resolution; automatically calibrates, zeroes, and configures itself; and produces a variety of input/output signals for use with other instruments.

The system was developed for use with an ultraviolet spectrometer. The concept of the system is applicable, however, to the control of electron guns in general and to the operation of such diverse equipment as that used in measuring scattering cross sections of subatomic particles and in industrial electron-beam welders.

The heart of the system is a high-voltage ramp generator, which produces a rapidly rising voltage, controlled either automatically by data-acquisition-and-control logic or manually (see figure). During operation under automatic control, the ramp waveform is synchronized with the channel-advance signal of a multichannel scaler. The offset, range, and gain of the ramp waveform can be programmed independently of each other: this is very convenient in experimental physics. For example, the maximum ramp voltage can be set at 50, 400, or 2,000 V, depending on the needs of the experiment. The ramp voltage and current are displayed on panel meters.

The ramp generator also produces voltages and programming for a retarding-potential analyzer. This circuit, in turn, produces stable, programmable potentials of 300 V and less for use in a Faraday-cup circuit.

The system includes a high-voltage-lens-control unit that contains four ±300-V programmable voltage supplies and a programmable constant-current filament power supply (6 V at 5 A) for an electron gun. All these supplies float on the ramp voltage, which can range up to 2,000 V.

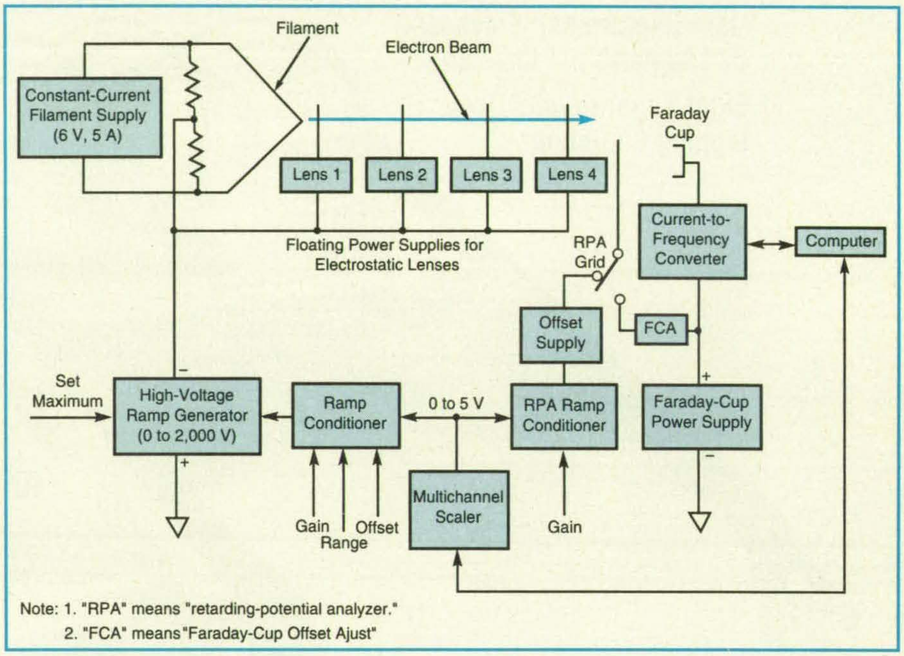

Lens and Filament Voltages float on a programmable ramp voltage. Other voltages provided by the system include low and high voltages for the Faraday cup. A personal computer controls the voltages and the acquisition of data.

A high-voltage measurement unit is essential for configuring the system for experiments and acquiring data from them. It includes a series of isolated switches that are used to measure any ground-referenced or floating voltage produced by the system.

The interface between the ramp generator and the multichannel scaler is a programmable current-to-frequency converter. This unit issues the channel-advance pulses to both the ramp generator and the multichannel scaler once it has measured a specified Faraday-cup current. It is programmed by high-level software from a remote personal computer, which displays diagnostic, configuration, and user information. The current-to-frequency converter provides autocalibration, autoconfiguration, and autozero functions and generates the input/output interface signals for external instruments.

The system is housed in four units. It is partitioned into modular circuit boards to facilitate maintenance, repair, and modification.

This work was done by Joseph M. Ajello and S. K. Howell of Caltech for **NASA's Jet Propulsion Laboratory**. *For further information, Circle 68 on the TSP Request Card.* *NPO-18669*

Improved Real-Time Monitoring Using Multiple Expert Systems

Functions include real-time monitoring and analysis.

NASA's Jet Propulsion Laboratory, Pasadena, California

The Monitor/Analyzer of Real-Time Voyager Engineering Link (MARVEL) computer program implements a combination of techniques of both conventional automation and artificial intelligence to improve the monitoring of a complicated engineering system. MARVEL is designed to support ground-based operations of the Voyager spacecraft but could also be adapted to other systems. MARVEL enables more-accurate monitoring and analysis of telemetry, enhances the productivity of monitoring personnel, reduces the required number of such personnel by performing routine monitoring tasks, and helps ensure consistency in the face of turnover of personnel.

The figure illustrates aspects of the functions of current and anticipated near-future versions of the MARVEL system architecture. MARVEL provides simultaneous real-time monitoring of data from multiple subsystems aboard the spacecraft, real-time analysis of anomalous conditions, and both real-time and non-real-time user-interface functions. MARVEL implements a data-management process and, at present, three subsystem processes. Each subsystem process has its own real-time monitor, productivity-enhancement functions, input/output capabilities, and knowledge-based analysis process.

The data-management process routes data to the appropriate subsystem monitor, which displays data, and through which the data can be obtained, manipulated, and stored in archival files. Anomalous data are sent to an appropriate reasoning module for diagnostics and corrective recommendations. Additional subsystem monitors from the same or other missions can be added.

The MARVEL system currently resides on a Sun-4 workstation and consists of approximately 20,000 lines of code, not including object code from commercial software packages. It differs from other programs of this type in two distinct ways. First, it is programmed in the C language and includes a commercial expert-system software shell that is also written in C. This enables better real-time performance than do LISP-based application programs. Secondly, the reasoning is distributed rather than centralized, for independent analysis of spatially distributed anomalies. Both of these features are considered crucial for real-time monitoring of complex systems. However, the architecture can be improved with regard to real-time performance for applications with substantially higher data rates, distributed user interfaces, and distributed data bases.

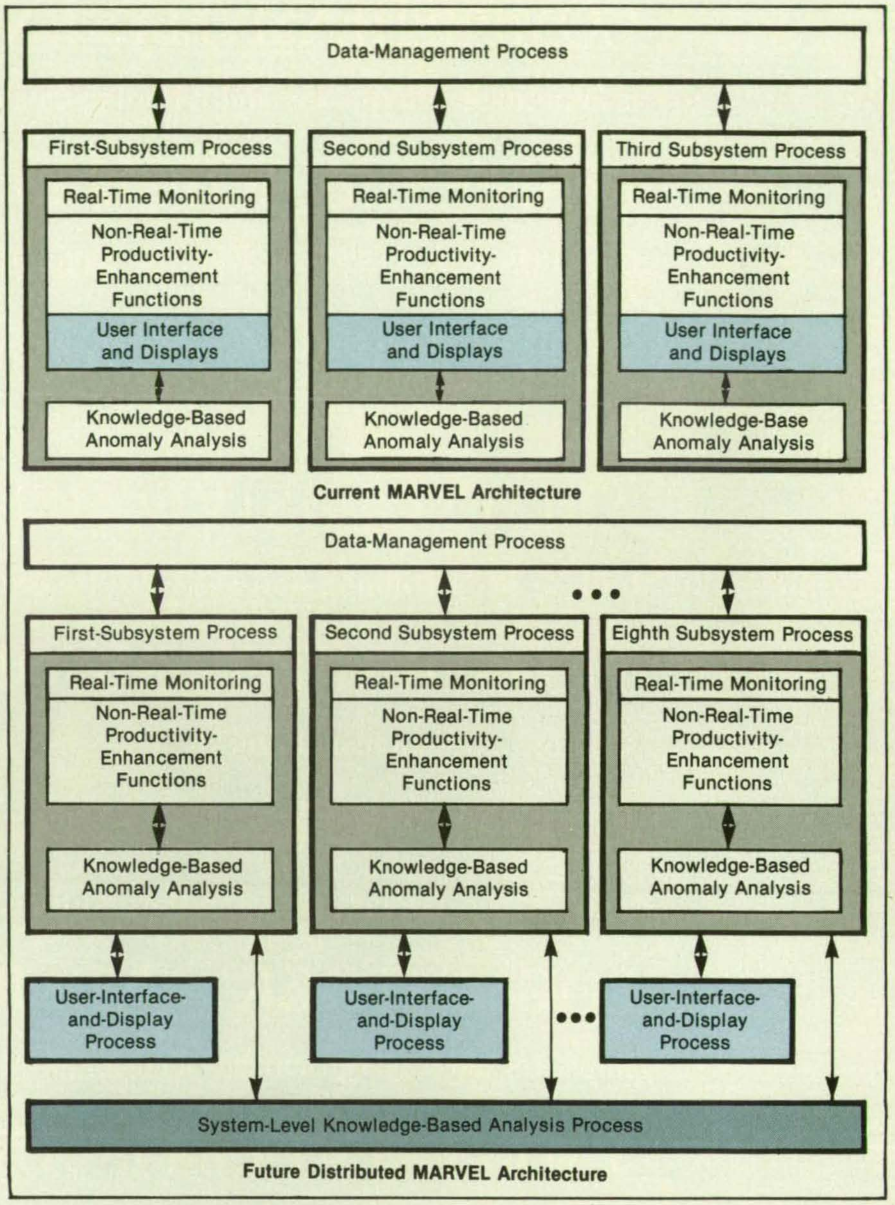

The **MARVEL System Architectures** combine data-management and subsystem processes. The future distributed version will provide system-level analysis of data to identify anomalies.

Each MARVEL subsystem monitor is designed to function independently from the others in the following ways. Each subsystem monitor features a full screen display that has been customized to meet the unique monitoring requirements of that subsystem. Each subsystem monitor receives a continuous stream of telemetry data from the monitored subsystem; the data are allocated to the appropriate subsystem by the top-level process. Each monitor provides mouse and menu selections pertaining to the user interface needed for that subsystem. Each monitor also has access to its own set of archival data files.

Each subsystem monitor features password access to all critical user-interface functions. It provides on-line help, it monitors incoming data by comparing them to predictions, and it is equipped with an embedded expert system that analyzes anomalies. Each subsystem monitor writes alarm messages that describe anomalies on one common window display that pops up over all other window displays. A central window display for posting alarm messages enables the analysts to monitor all three subsystems from two spacecraft while displaying and/or actively working with only one subsystem from a single spacecraft. This is possible because the central post-

ing of alarm messages ensures that no alarms from any subsystem (or spacecraft) can be overlooked, regardless of what else is being displayed on the monitor.

A distributed version of the MARVEL system that is being developed will accommodate eight processes distributed among multiple workstations. By use of network-based windowing, each subsystem monitor can be allocated to its own workstation, while maintaining access to data and displays from the other subsystems. This change is being accommodated by separating the user-interface and display functions from the subsystem monitors into their own processes. The primary functional advantage of this approach is that changes and entries made by analysts at any one workstation will affect the displays and data of all the workstations, enabling analysts at different workstations to monitor each others' subsystems.

In addition, the MARVEL expert systems will exchange information to solve system-level analysis problems cooperatively. These are problems that affect or are manifested in more than one spacecraft subsystem and therefore cannot be solved by any one subsystem monitor alone. Toward this end, a higher-level expert system that is being developed will coordinate the activity of the subsystem experts. This system-level expert will respond to input from the subsystem experts in the same data-driven way in which the subsystem experts respond to the subsvstem monitors: anomaly information that could have system-level impact will be passed from the subsystem experts to the system-level expert. The system-level expert will then request additional information as needed from the other subsystem experts and subsystem monitors. Without distributing this computational load across multiple workstations, such analysis could not be achieved in real time without access to significantly faster computers.

This work was done by Ursula M. Schwuttke, Robert Angelino, Alan G. Quan, John Veregge, and Cynthia Childs of Caltech for **NASA's Jet Propulsion Laboratory**. *For further information, Circle 8 on the TSP Request Card.*
NPO-18594

Computing Bandwidths of PCM/PSK/PM Signals

Approximate closed-form equations are simple.

NASA's Jet Propulsion Laboratory, Pasadena, California

An analysis of the spectral properties of a class of pulse-code-modulated, phase-shift-keyed (PSK) radio signals shows that one can obtain approximate, simple, closed-form equations for the widths of the frequency bands occupied by such signals. These equations can reduce the amount of computation and time needed to determine allocations of frequency and power among competing radio-communication systems or to determine whether two different radio-communication systems are compatible.

The analysis applies to a signal of a type often used in telemetry: the total signal includes a residual carrier signal, and a binary data signal is phase-shift-keyed onto a sinusoidal or square-wave subcarrier signal that is, in turn, phase-modulated onto the carrier signal. The overall signal is given by

$$S(t) = \sqrt{2}A\sin[\omega_c t + md(t)P(t)]$$

where t is time, A is the rms voltage, ω_c is the angular carrier frequency, m is the modulation index, $d(t)$ is a non-return-to-zero, binary-valued data sequence, and $P(t)$ is the subcarrier waveform.

The approximate closed-form equation that is sought in this analysis is one that expresses the width (BW) of the frequency band occupied by a given fraction of the signal power as a function of the ratio (n), between the subcarrier frequency and the bit rate (R_S) of the data signal, with the modulation index (m) as a parameter. The information sought is contained implicitly in the applicable infinite-series expression for the normalized power spectral density of the signal in the sine-wave-subcarrier or square-wave-subcarrier case (see Figure 1). The integral of this expression over a given bandwidth for a given n and m is the fraction of total signal power contained within that bandwidth, and this integral can be computed iteratively to obtain that bandwidth (called the "occupied bandwidth") that contains 99 percent or another specified fraction of the total power.

The foregoing computations can be repeated for other values of n and m. The results can be displayed conveniently as a plot of normalized occupied bandwidth (BW/R_S versus n, with m as a parameter. As shown in Figure 2, each such plot turns out to be nearly linear. Thus, by use of a simple curve-fitting technique, one can extract the desired approximate equation, which is of the form

$$BW/R_S = an + b$$

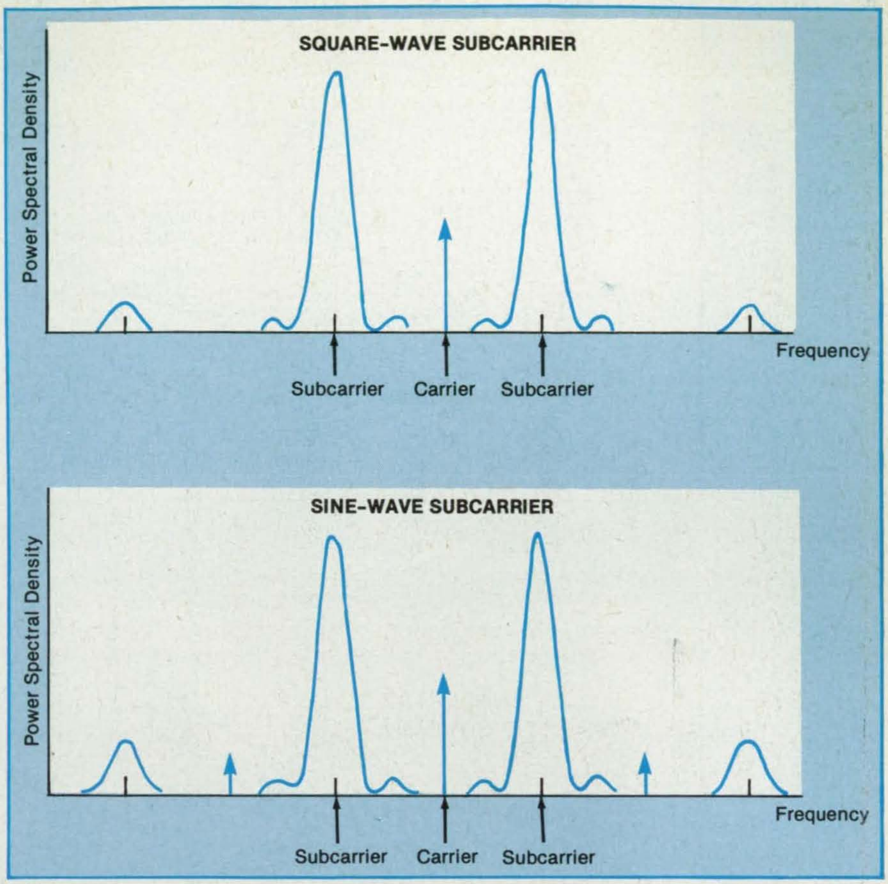

Figure 1. The **Power Spectral Densities** of phase-shift-keyed signals like those described in the text can be computed exactly.

where a and b depend on m and on whether the subcarrier waveform is square or sinusoidal. Computations with typical numerical values show that at low modulation indices, the occupied bandwidths of signals with square-wave subcarriers are 10 to 15 times those of the corresponding signals with sine-wave subscarriers.

This work was done by Tien M. Nguyen of Caltech for **NASA's Jet Propulsion Laboratory**. *For further information, Circle 52 on the TSP Request Card.*
NPO-18576

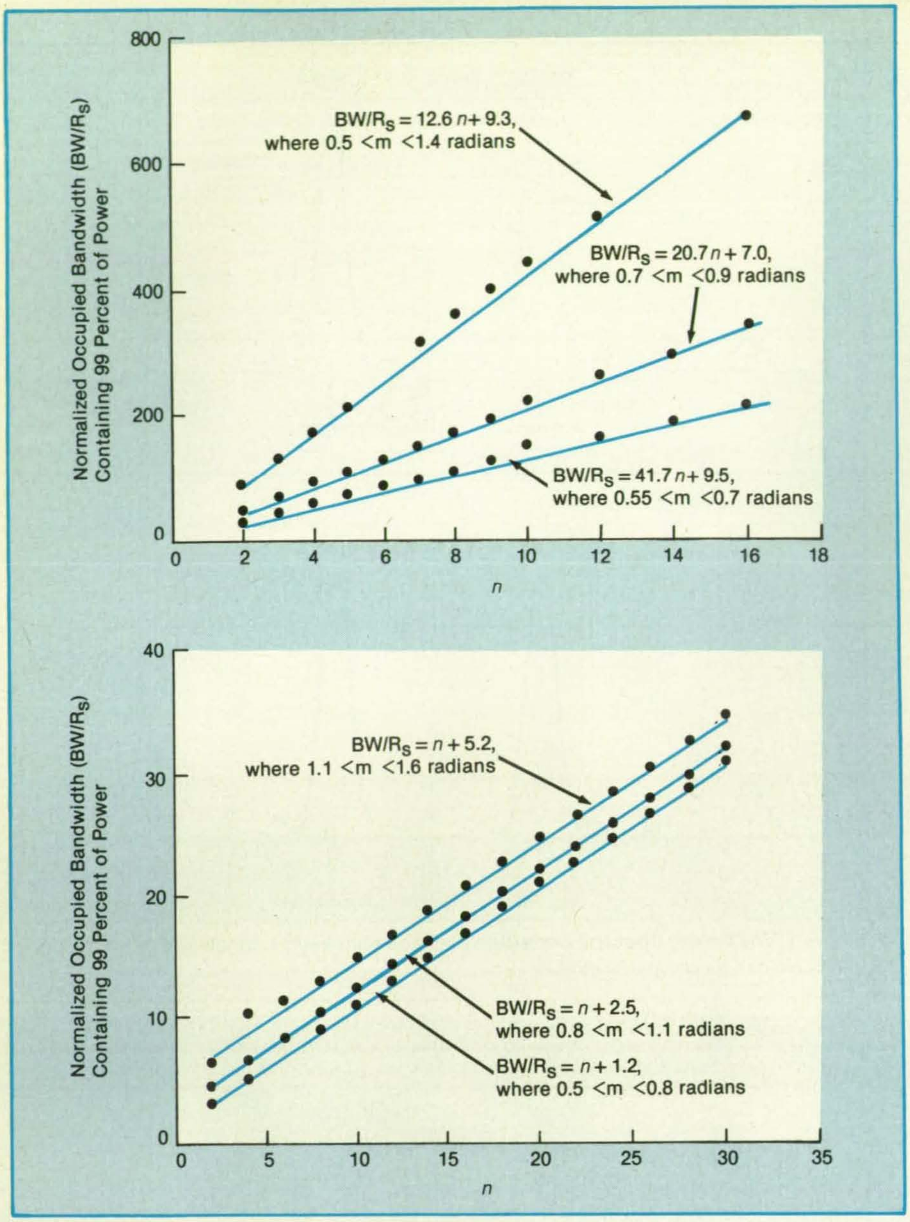

Figure 2. **Straight-Line Approximations** can be fitted to these data, which are computed from the equations for the power spectral densities.

Interactive Image-Analysis Program

BLOBTOOL prepares image data for further analysis.

Digital images are frequently analyzed to obtain various quantitative measurements of objects or structures present in the images. The BLOBTOOL computer program can be used to prepare an image for analysis and to generate such measurements. Also included are basic input/output capabilities, an option to display built-in color tables, and access to on-line help.

The generation of geometric properties of digital images requires segmentation of the image through the application of a thresholding technique. This separates the image into two classes — foreground and background. BLOBTOOL provides this capability by enabling the user either to specify a threshold value or allow automatic selection of a threshold value. The user can choose a method of automatic selection best suited to the digital image from among different thresholding methods (Otsu's, entropy analysis, moment preservation, or minimum error).

After the image has been segmented, an object-detection algorithm can be used to determine the existence of any objects in the image. This application program does not recognize objects as specific identifiable items but rather as anomalies on the background. Once objects have been detected, the geometric properties (e.g., area and perimeter) can be generated and saved to a permanent disk file or sent on to a line printer.

BLOBTOOL is written in C Language for Sun-series computers that have color-display capabilities and that run Sunview or OpenWindows under SunOS. No binaries are included with this distribution. This program requires 213K of random-access memory for execution. The standard distribution medium is a 0.25-in. (6.35-mm) streaming-magnetic-tape cartridge in UNIX tar format. BLOBTOOL was developed in 1991.

Sun, Sunview, OpenWindows, and SunOS are trademarks of Sun Microsystems, Inc. UNIX is a registered trademark of AT&T Bell Laboratories.

This program was written by Desiree M. Leonard of Computer Sciences Corp. and Mary-Anne K. Posenau of **Langley Research Center**. *For further information, Circle 98 on the TSP Request Card.*
LAR-14767

Probabilistic Scale-Space Filtering Program

PSF helps to construct sparse representations of complicated signals.

Scale-space filtering is used to construct sparse, qualitative representations of signals that produce complex curves. The Probabilistic Scale-Space Filtering (PSF) computer program implements the scale-space technique to describe input signals as collections of nested hills and valleys organized in a treelike structure. In many applications (e.g., differential thermal analysis), such signals are the results of collections of physical processes that may potentially overlap.

PSF attempts to analyze the input signals to isolate and describe the effects of each individual physical process on the signals. Each physical process is assumed to produce a single hill, valley, or trend in a signal. These are considered to be features of the signal. Because a signal is sometimes too complex to determine with certainty whether some of its features are real or artificial, PSF calculates probabilities, with the extracted features corresponding to physical processes.

Because the probabilities associated with the features are derived from domain-specific statistics, it is most likely necessary to modify about 50 statements in the program that describe these statistics to make the statistics correspond to those of the user's particular domain. PSF also provides a standard scale-space filtering algorithm for use when the desired features can be identified with certainty or when it is not practical to get the domain-specific statistics.

The PSF algorithm is based on Witkin's scale-space filtering theory. The PSF program detects variations in a signal by finding the points of inflection in the input signal. A single physical process (corresponding to a feature of the input signal) corresponds to a pair of inflection points. The number and positions of these points depend upon the scale of the derivative operators used to detect them. For example, if a signal were smoothed with a large Gaussian operator, all small features from the signal would vanish, and only the larger features would still be present in the smoothed signal. Therefore, instead of assuming any single scale to be correct, PSF identifies points of inflection in a large number of different scales. It then describes the curve according to the groups of points of inflection, across all scales, caused by the same physical process. This unification of features of a signal across scales enables the program to separate a complex feature of a signal into its components.

PSF provides an output table that gives the following information: the abscissa of the first inflection of the peak, the type of peak, the distance between the first and second inflection points, the abscissa of the peak, and the probability that the feature corresponds to a physical process. The program also lists points that represent a graphical image of the signal and detected peaks. These data can be used with a standard plotting program (not included) to display the signal and its features graphically.

PSF is written in C language (49 percent) and Common Lisp (51 percent) for use on a Sun SPARC workstation running the UNIX operating system. PSF requires 4 Mb of random-access memory. The standard distribution medium for this program is a 0.25-in. (6.35-mm) streaming-magnetic-tape cartridge in UNIX tar format. It is also available on a 3.5-in. (8.89-cm) diskette in UNIX tar format. PSF was developed in 1991.

Sun and SPARC are trademarks of Sun Microsystems, Inc. UNIX is a registered trademark of AT&T Bell Laboratories.

This program was written by Deepak Kulkarni of **Ames Research Center** *and Kiriakos Kutulakos of the University of Wisconsin. For further information, Circle 107 on the TSP Request Card. ARC-13198*

For More Information Circle No. 640

SRAM as an Array of Energetic-Ion Detectors

Potential uses include gas densimetry, position sensing, and measurement of the cosmic-ray spectrum.

NASA's Jet Propulsion Laboratory, Pasadena, California

A static random-access memory (SRAM) has been designed for use as an array of energetic-ion (e.g., cosmic-ray) detectors. The design exploits the well-known tendency of incident energetic ions to cause bit flips (also known as "single-event upsets") in the cells of electronic memories: obviously, vulnerability to single-event upsets is a disadvantage in a memory but an advantage in a detector array. The design of the ion-detector SRAM involves modifications of standard SRAM design to increase the sensitivity to ions. The device can be fabricated by use of conventional complementary metal oxide/semiconductor (CMOS) processes.

Each cell of the ion-detector SRAM consists mostly of a conventional six-transistor memory cell that can be viewed as containing two inverters, self-explanatorily called the "detector inverter" and the "feedback inverter," connected back-to-back in a feedback loop (see Figure 1). The memory cells are arranged in columns, and data are written to or read from them by turning on electronic switches via word lines that connect the inverters to bit lines.

The detector inverter differs from a conventional SRAM inverter in two ways: (1) One of the metal oxide/semiconductor field-effect transistors (MOSFET's), called the "off" MOSFET, in this inverter includes a drain that has been enlarged into a detector diode to increase its sensitivity to ions. (2) An offset bias voltage, V_{off}, is supplied from additional circuitry to the detector diode circuitry through another of the MOSFET's (called the "on" MOSFET) in this inverter.

At the beginning of an operating cycle, the SRAM is set up by writing identical bits into all the cells. The cells are biased into the sensitive state by turning the switches "on," forcing the cells to assume a state as dictated by the bias on the bit lines. During this writing interval, V_{off} is set to ground. Next, the switches are turned "off," and V_{off} is set to a value at which the cells are vulnerable to single-event upsets.

The cells are maintained in this sensitive condition during a "stare" time. At the end of the stare time, V_{off} is set to ground;

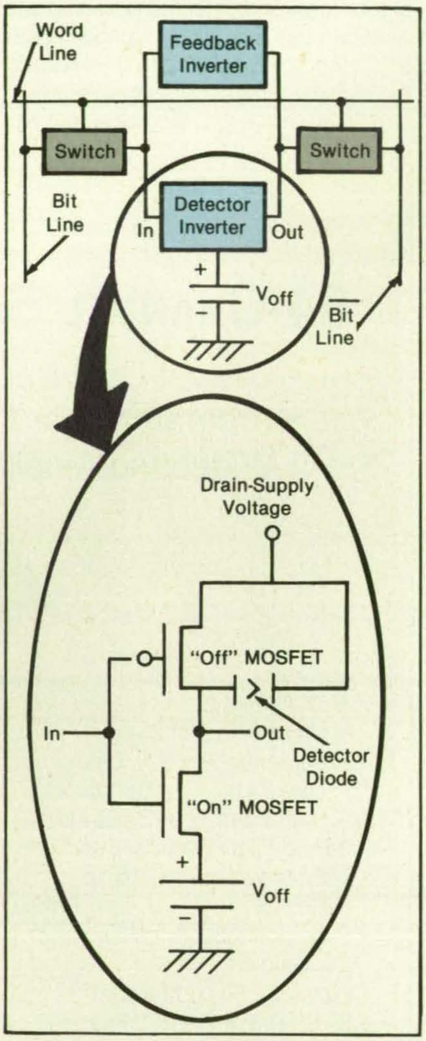

Figure 1. **Each Cell of the Ion-Detector SRAM** resembles that of a conventional SRAM except that one of its inverters has been modified to increase and take advantage of its sensitivity to energetic ions.

then the states of the cells are read by again turning the switches on to set the biases on the bit lines. The bias on each bit line is then read via a sensing amplifier.

Figure 2 illustrates one potential application, in which the device would be used to measure the density of a gas or other medium between it and a source of ionizing radiation. The ion-detector SRAM could also be used to determine the position (via the bit-flip pattern) of a mask that shields part of it from the source. In yet another potential application, the device could be used to study the spectrum of cosmic rays by varying V_{off} to discriminate among ions of different stopping powers.

This work was done by Martin G. Buehler, Brent R. Blaes, Udo Lieneweg, and Robert H. Nixon of Caltech for **NASA's Jet Propulsion Laboratory**. *For further information, Circle 21 on the TSP Request Card.*

In accordance with Public Law 96-517, the contractor has elected to retain title to this invention. Inquiries concerning rights for its commercial use should be addressed to

Edward Ansell
Director of Patents and Licensing
Mail Stop 305-6
California Institute of Technology
1201 East California Boulevard
Pasadena, CA 91125

Refer to NPO-18322, volume and number of this NASA Tech Briefs *issue, and the page number.*

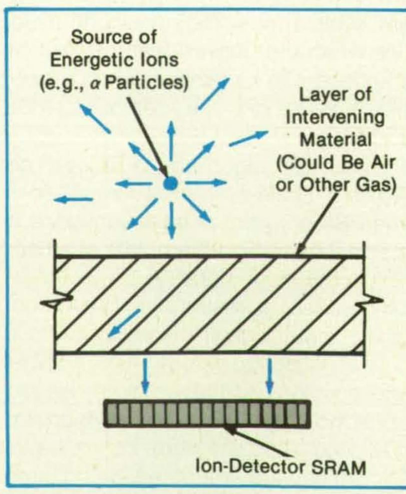

Figure 2. The **Ion-Detector SRAM** can be used to measure the density of the gas or other medium between itself and the source. The concept has been verified in air with a source of α particles.

Fast Differential Adder

Fewer components are used, with consequent decrease in power consumed and in signal-propagation delay.

Lewis Research Center, Cleveland, Ohio

The circuit illustrates a fast differential adding circuit (or, equivalently, a subtracting circuit) suitable for use in a high-frequency-switching, high power-regulating circuit. The phase of the current-feed-back signal in such a regulator must be shifted to prevent instability, and the fast differential adder implements a phase-shifted to prevent instability, and the fast differential adder implements a phase-shifting technique in which a compensating signal is added to the current-feedback signal. The current-feedback signal is a train of pulses of varying duration, while the compensating signal is a train of pulses of fixed duration.

In a basic active adding circuit of a type used heretofore to implement this phase-shifting technique, two or more signals are added, but the output of this circuit is inverted and must be inverted once more: this requires an additional inverting amplifier, with consequent waste of power and additional signal-propagation delay. In the new circuit, the addition is performed with only one differential amplifier.

In the new circuit, the signal fed to the inverting input of the sole differential amplifier is proportional to - e_1, where e_1 is the current-feedback signal voltage. The inversion of e_1 is obtained by reversing the polarity of rectifiers from that used in the basic circuit. a signal proportional to the compensating signal, e_2, is fed to the noninverting input of the differential amplifier is given by $v_0=ae_1 +be_2$ where a and b are positive constants of proportionality that depend upon the values of the resistors.

This work was done by Mort A. Arditti and Rosemary Silva of Rockwell International corp. For ***Lewis Research Center****. No further documentation is available. LEW-15127*

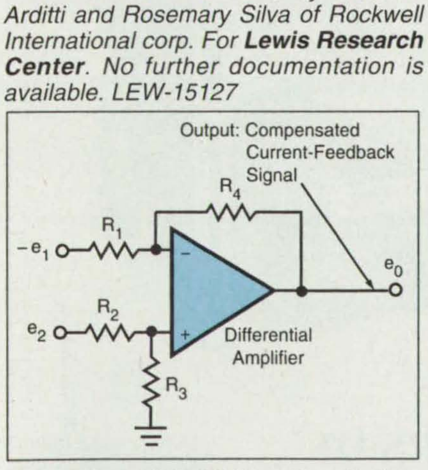

This **Differential Adding Circuit** (or, equivalently, subtracting circuit) is faster and consumes less power because it contains only one differential amplifier, whereas the prior version contained two.

Gauge Measures Hot Erosion of Insulation

Temperatures and increments of erosion are measured by use of embedded thermocouples and resistors.

Marshall Space Flight Center, Alabama

Compact ladder networks that contain thermocouples and resistors serve as gauges to measure the erosion of insulating materials by hot, flowing gases. Several gauges of this type have been designed for use in blast tubes during tests of rocket motors. The general design concept is readily specialized to other applications in which insulation is subject to erosion — for example, ducts that contain hot, erosive industrial process streams.

The gauge shown in Figure 1 includes six thermocouples, each (except the lowermost) in series with two metal-film resistors. The resistances in series with succeeding thermocouples increase as multiples of 10. The series thermocouple-and-resistor combinations are embedded in the insulating material at equal increments of depth [0.1 in. (2.54 mm) in the original application] and are connected electrically in parallel. A resistor connected in parallel at the top helps to linearize the output when only the uppermost thermocouple remains.

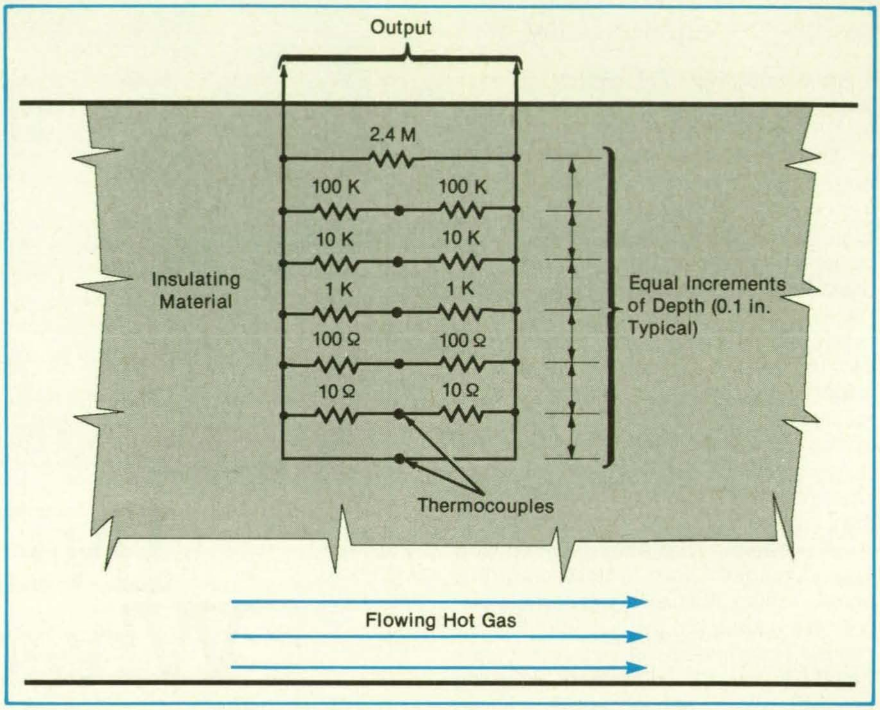

Figure 1. **Thermocouples and Resistors** in a ladder network are burned away in sequence as the bottom surface of the insulating material is eroded by the hot, flowing gas.

The lowermost (in the figure) thermocouple is embedded closest to the eroding

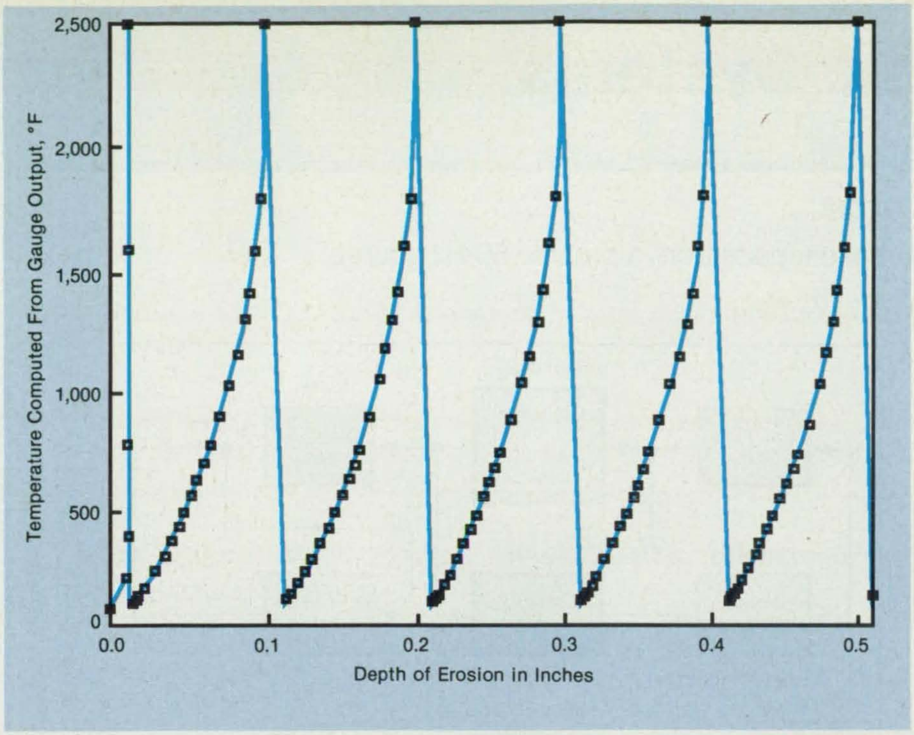

Figure 2. **The Peaks in These Simulated Data** indicate the passage of the erosion front by the successive thermocouples in a gauge like that in Figure 1.

surface of the insulating material. As the surface wears away toward this thermocouple, a measurable amount of heat begins to penetrate the thermocouple, and the thermocouple puts out a voltage indicative of the temperature at its location. Because of the parallel decade-resistor configuration, the voltage from this thermocouple predominates, at the output terminals, over the voltages from the other thermocouples. The output voltage thus indicates, predominantly, the temperature at the lowermost thermocouple. The output of the thermocouple reaches a maximum when the erosion exposes it directly to the hot gas. Then its output suddenly drops to zero as it burns away.

As the erosion continues toward the next thermocouple, it begins to indicate an increase in temperature. Because this thermocouple is now the one in series with the lowest resistance in the decade configuration, its output now predominates. Eventually, the output voltage rises to a peak, then suddenly falls as it did before. This cycle repeats, providing a series of sharp peaks that indicate the passage of the erosion front through the corresponding thermocouples (see Figure 2).

The decade-resistor configuration is not the only one that could be used. For example, the resistor values could all be the same or could increase in sequence as multiples other than 10. Of course, any change in the resistor configuration entails changes in the readout circuitry and in the interpretation of the output signal. For example, if the resistors all have the same value, it might be best to connect the gauge into a voltage-divider circuit and to interpret the output voltage as a sequence of divided thermocouple peaks superimposed on the divided supply voltage, which increases as the thermocouples and resistors are burned away.

This work was done by Reginald J. Gould of **Marshall Space Flight Center**.

For further information, Circle 2 on the TSP Request Card.

Inquiries concerning rights for the commercial use of this invention should be addressed to the Patent Counsel, Marshall Space Flight Center [see page 24]. Refer to MFS-28651.

Electronic Systems

Sidereal-Rate Generator

An innovative circuit derives sidereal seconds from a precise 60-Hz source.

Langley Research Center, Hampton, Virginia

Normal time, as indicated on common clocks, is based on the apparent position of the Sun. There are approximately 365.25 solar days in a year. A sidereal day is the average time between apparent meridian crossings by a star. There are approximately 366.25 sidereal days in a year. There is one more sidereal day than there are solar days in a year because the Earth revolves once around the Sun during the course of a year, canceling out one apparent rotation. Therefore, a solar day is longer than a sidereal day by a ratio of 1.00273790934 to 1 according to the Naval Observatory. A good approximation is 366.25/365.25 days or a ratio of 1,465/1,461. This ratio yields 1.00273785079, which is accurate to the seventh decimal place. The ratio of 1,465/1,461 has an error of only −0.00506 second per day or −1.846 seconds per year.

Heretofore, methods to convert from solar to sidereal time references have centered around the injection of pulses. These techniques resulted in timing pulses that were either nonuniform or not synchronized with solar references. Now, however, an instrument that generates sidereal equivalent seconds to the accuracy described above has been designed, fabricated, and tested at NASA Langley Research Center. This instrument, known as the sidereal-rate generator, derives sidereal seconds from an existing precise 60-Hz source. A phase-locked frequency multiplier is used to multiply the 60 Hz by 1,465 to obtain 87,900 Hz. Then, a divide-by-*N* circuit is used to divide this frequency by 1,461. The result is 60.164261 Hz, which is divided by 60 to arrive at 1.00273972603 Hz, or 1.000000 sidereal Hz. The output consists of uniformly timed pulses that are synchronized to the 60-Hz reference.

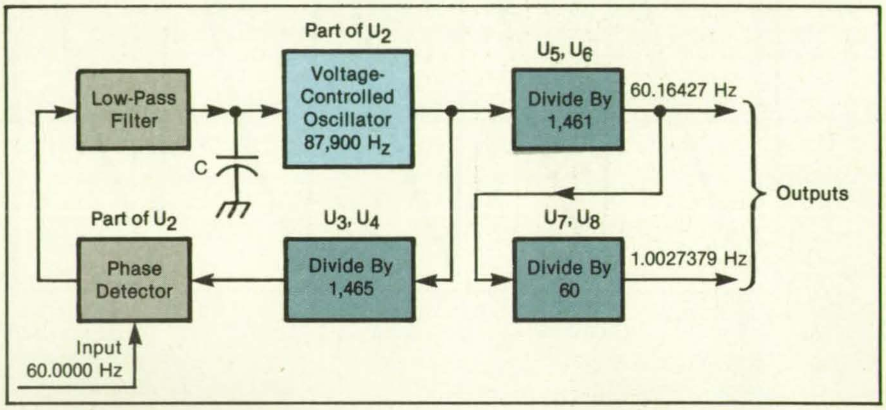

The **Sidereal-Rate Generator** puts out sidereal clock signals with an error of only about 1.8 seconds per year.

In the figure, U_4 denotes a multistage binary counter. U_3 decodes the output of U_4. When the count in U_4 reaches the binary equivalent of 1,465, U_3 resets U_4 to zero. U_4 counts the output pulses from the voltage-controlled oscillator in U_2. U_2 also compares the 60-Hz reference with the divided output from U_3. If the output from U_3 is below 60 Hz, the output from the phase detector goes high (+5 V), and the voltage across C increases slowly, increasing the frequency of pulses from the voltage-controlled oscillator. If the output from U_3 is above the 60-Hz reference, the output from the phase detector goes low (0 V), and the voltage on C decreases, lowering the output frequency of the voltage-controlled oscillator. Once locked, the frequency of the output of U_2 is exactly 1,465 times the 60-Hz reference frequency and is coherent in phase with the reference.

U_6 and U_5 divide the frequency of the output of U_2 by 1,461. U_8 and U_7 divide the resultant 60.164271 Hz by 60 to arrive finally at 1.0027379 Hz. An inverter is used to buffer the output. Another inverter is used to drive a light-emitting diode as a confidence light. This circuit, including the crystal oscillator/divider, was built on a 4-in. (10-cm) square circuit board, using point-to-point wiring.

While this approach may include more components than would a special frequency oscillator/divider circuit, it uses a standard reference frequency. The output pulse periods are uniform, solar and sidereal outputs are available from a single source, the circuit is compatible with normal digital clocks, and the circuit is driven by a readily available reference frequency. The sidereal rate generator has applications in stellar tracking, celestial navigation, and celestial photography.

This work was done by John M. Franke and Bradley D. Leighty of **Langley Research Center**. *No further documentation is available.*

Inquiries concerning rights for the commercial use of this invention should be addressed to the Patent Counsel, Langley Research Center [see page 24]. Refer to LAR-14350.

Slew Timer for Symbol Display Generator

The timer provides an end-of-slew signal related to the extent of the slew.

Ames Research Center, Moffett Field, California

A slew-length timer generates a delay and, at the end of the delay, a signal that indicates the end of one of the slews of the electron beam in a cathode-ray-tube display driven by a symbol generator. The end-of-slew signal constitutes "permission" for the symbol generator to begin drawing the next symbol segment. A slew is a blanked jump in position from the end of one visible segment to the beginning of the next, disconnected segment accomplished by stepping the deflection input to the new position and waiting for the deflection system to reach that position. If the display and symbol generator are not in the same

• AEROSPACE SIMULATION • GEOPHYSICAL EXPLORATION • POWER PLANT SIMULATION • ADA DEVELOPMENT •

Nothing Escapes The Night Hawk.

An ominous blip appears on the radar screen of a fighter during patrol. The temperature begins to rise within the core of a nuclear power generator. A hacker bent on espionage leans over his keyboard, sending password sequences.

Whether they're real-world situations or training simulations, crucial circumstances like these require critical computer performance. The most vital data can be lost in an instant, if your system gives you a delayed reaction instead of real-time response. But when microseconds count, Night Hawk flies.

Night Hawk is a complete family of real-time, open-architecture, multiprocessing computer systems using 88open™-compliant RISC technology, UNIX® and VME. Systems that are already proven in demanding real-time applications of all kinds, all over the world. Systems built by Harris, a $3 billion corporation with more than 20 years of continued leadership in advanced computing.

Night Hawk's modular design allows it to be easily upgraded in the field, protecting your investment and reducing your long-term cost of ownership. And it offers a multilevel secure environment for your sensitive applications.

When the capture of data is essential, you need a system that lets nothing escape. You need the Night Hawk.

For further information, write Marketing Communications, Harris Computer Systems, 2101 West Cypress Creek Road, Ft. Lauderdale, Florida 33309. Call 1-800-4HARRIS, ext. 4009, from inside the U.S. Or 1-407-727-9207, ext. 4009, from outside the U.S. FAX 407-724-3334.

HARRIS

The Price/Performance Leader

UNIX is a registered trademark of AT&T.
88open is a trademark of the 88open Consortium.

• SUPERVISORY CONTROL & DATA ACQUISITION (SCADA) • MULTILEVEL SECURITY • RADAR PROCESSING •

INDUSTRIAL AUTOMATION • SECURE NETWORKING • DATA ACQUISITION • POWER PLANT MONITORING AND CONTROL • TELEMETRY •

SIGNAL PROCESSING • ENERGY MANAGEMENT SYSTEMS (EMS) • PROCESS CONTROL • SECURE PROCESSING • ARTIFICIAL INTELLIGENCE

For More Information Circle No. 668

unit, or multiple displays are driven by one symbol generator, the obvious solution of monitoring the deflection amplifiers and generating an end-of-slew signal has undesirable test or failure mode charateristics. This slew-length timer overcomes the disadvantages of the closed-loop methods without wasting large amounts of writing time by providing end-of-slew signals related to the actual distance of movement of the writing electron beam.

As shown in the figure, the slew-length timer operates in conjunction with the symbol (or vector) generator, which puts out a sequence of digital signals representative of the desired Cartesian coordinates (*X*,*Y*) of the electron beam. These digital signals are entered into the *X* and *Y* registers, then coupled via buses to a digital-to-analog converter, which generates the analog beam-deflection signals. These signals are then sent to the display, amplified, and applied to the cathode-ray tube.

For the purpose of computing the slew lengths (time), the axes are divided into segments (typically 16 each). The maximum slew time for each possible combination of start and end segments for each axis is calculated, and a code for the slew time is entered in the appropriate place in the *X* and *Y* length memories. To save space in the following memory, several distinct but similar times are represented by one (typically 5-bit) code value. The segment number (upper bits of the position data) from the symbol generator immediately prior to the slew are latched into the start registers and are applied with the segment number for the stop position to the length memories to select the length codes for each axis. These codes then address the elapsed time/comparator memory, which contains a count representing the maximum time represented by the *X* and *Y* codes. This count is used by the variable delay generator to generate a delay equal to or slightly longer than the time required by the deflection system to perform the slew. At the conclusion of the delay, the counter sends the end-of-slew signal to the symbol generator, thereby allowing it to proceed with the next symbol segment.

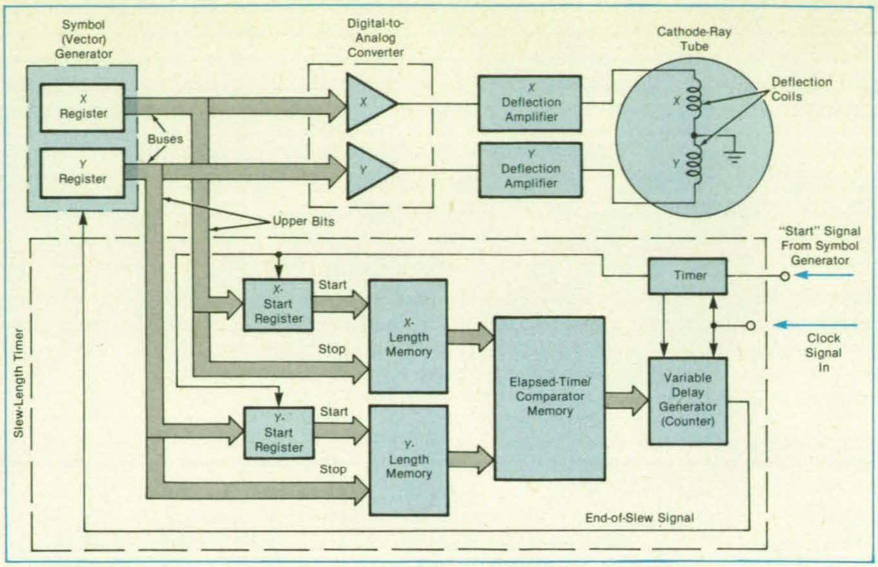

This **Slew-Length Timer** generates a delay equal to the time required to slew the the beginning of a segment of a symbol. At the end of the delay, it sends an end-of-slew signal to the symbol generator, thereby allowing the symbol generator to begin the segment.

This work was done by Paul A. Fisher of Honeywell Inc. for **Ames Research Center**. *For further information, Circle 29 on the TSP Request Card.*

Title to this invention, covered by U.S. Patent No. 4,532,504, has been waived under the provisions of the National Aeronautics and Space Act [42 U.S.C 2457(f)]. Inquires concerning licenses for its commercial development should be addressed to

Dale Jepsen, Associate Corporate Patent Attorney
Honeywell Inc.
21111 North 19th Ave.
Phoenix, AZ 85027

Refer to to ARC-11998, volume and number of this NASA Tech Briefs *issue, and the page number.*

Robotic Vision With Enhanced Detection of Edges

Blurring and background noise are reduced to avoid false detection of a moving target.

John F. Kennedy Space Center, Florida

A robotic vision subsystem provides enhanced detection of edges as it preprocesses the image of a target that moves in six degrees of freedom. The substystem was designed to filter out high (spatial) frequency components in an image, with the frequency response tuned to the size of object to be detected. The objects to be detected were subtargets on a target. In effect, this technology smooths the image data to remove background noise and blurring to avoid false detection of a moving target. The image produced is then used by another vision subsystem that guides a robot to mate with the target. Also, in comparison with older robotic image-preprocessing subsystems, this one produces less noise and operates more reliably.

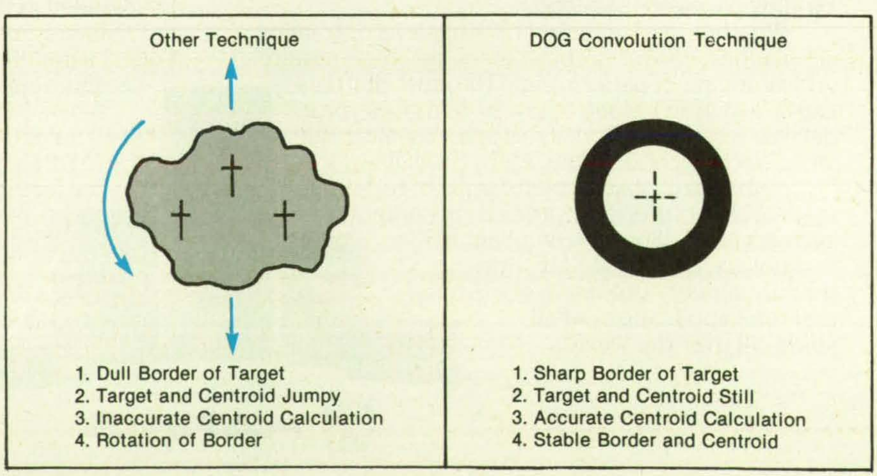

Image Improvement shown graphically here for clarity illustrates the relative advantages of the DOG convolution techniques.

This image-preprocessing subsystem implements an algorithm that precisely defines the edges of the moving target and provides a larger (in comparison with earlier algorithms) area for calculating the centroid of the target. First, a camera acquires an image of the target. As each image frame is acquired, it is processed through a pipeline processor. After the pipeline processing, the image is analyzed and then processed with information from previous images for tracking purposes.

Each image frame is directly processed with an approximation to a difference-of-Gaussian (DOG) operator. The resultant image is then thresholded, and the connected regions are found and their centroids and areas are computed for subsequent processing. In comparison with other techniques that might have been used to enhance the detection of edges in this application, the difference-of-Gaussian convolution filters to a higher degree and thus aids in reducing background noise and blurring to avoid false detection of a moving target. The figure graphically compares image improvement in sharpness.

This image-preprocessing sub-system includes commercially available pipeline image-processing circuit boards and a commercially available vision-system computer. However, the way the subsystem was packaged (hardware/software/noise and blurring reduction) was also "new technology" and allowed this subsystem to provide for the tracking of a target in all six degrees of freedom at a frame rate of 30 Hz. Other vision systems, even though they were shortly afterwards, could only track in two or three degrees of freedom at frame rates of only ½ to 4 Hz.

This work was done by V. L. Davis and L. Shawaga of **Kennedy Space Center**, *and P. Walsh and K. Kambies of Adaptive Automation, Inc. For further information, Circle 56 on the TSP Request Card. KSC-11505*

Light-Flash Wind-Direction Indicator

The timing of flashes would indicate the direction of the wind.

John F. Kennedy Space Center, Florida

A proposed wind-direction indicator could be read easily by distant observers. The indicator would emit bright flashes of light separated by an interval of time proportional to the angle between true north and the direction from which the wind is blowing.

The flashes, from high-intensity stroboscopic lights like those on radio towers and aircraft, could be seen by any number of viewers at distances up to 5 miles (8 kilometers) or even more. A windsock or weathervane, in contrast, cannot be seen beyond a few thousand feet (about 1 kilometer). The stroboscopic indicator could also be seen more easily through rain and fog. In addition, it would not be subject to the ambiguity that occurs when a weathervane or windsock is viewed head on, signifying that the wind could be blowing either directly toward or directly away from the observer.

The indicator would flash once at the beginning of the time interval and twice at the end of the interval. The time between the single start flash and the double end flash would be proportional to the angle between the wind and the true north, at a rate of 30° per second. For example, a 3-second interval would correspond to wind at 90° (from the 3 o'clock position, or due east). A 6-second interval would indicate wind at 180° (at the 6 o'clock position, or from the south). Wind exactly from the north (that is, at 12 o'clock or 0°) would produce a double flash only, because the single beginning flash would coincide with the first of the two end flashes.

An observer could estimate the direction of the wind by counting "one thousand one, one thousand two," and the like,after the beginning flash. For greater accuracy, a stopwatch measurement of elapsed time would give the direction within about 1°. In most applications, greater precision would be neither practical nor meaningful.

The wind-direction indicator would be self-contained. It would require no connections to other equipment. Its modest power demand could be satisfied by a battery or solar power or both. It could be set up quickly to provide local surface-wind data for aircraft pilots during landing or hovering, for safety officers establishing hazard zones and safety corridors during handling of toxic materials, for foresters and firefighters conducting controlled burns, and for real-time wind observations during any of a variety of wind-sensitive operations.

This work was done by Jan A. Zysko of **Kennedy Space Center**. *No further documentation is available.*

Inquiries concerning rights for the commercial use of this invention should be addressed to the Patent Counsel, Kennedy Space Center [see page 24]. Refer to KSC-11590.

Maximum-Likelihood Detection of Noncoherent CPM

Detectors analogous to those of coherent CPM could be used.

NASA's Jet Propulsion Laboratory, Pasadena, California

Simplified detectors have been proposed for use in maximum-likelihood-sequence detection of symbols in an alphabet of size *M* transmitted by uncoded, full-response continuous phase modulation over a radio channel with additive white Gaussian noise. The proposals were developed in a theoretical and computational study that began with maximum-likelihood-sequence detection metrics for an observation interval *N* symbol periods long, during which the phase of the carrier signal is constant but unknown. The bit-error-probability performances of the associated detection algorithms were analyzed. The special and popular case of minimum-shift keying (MSK)

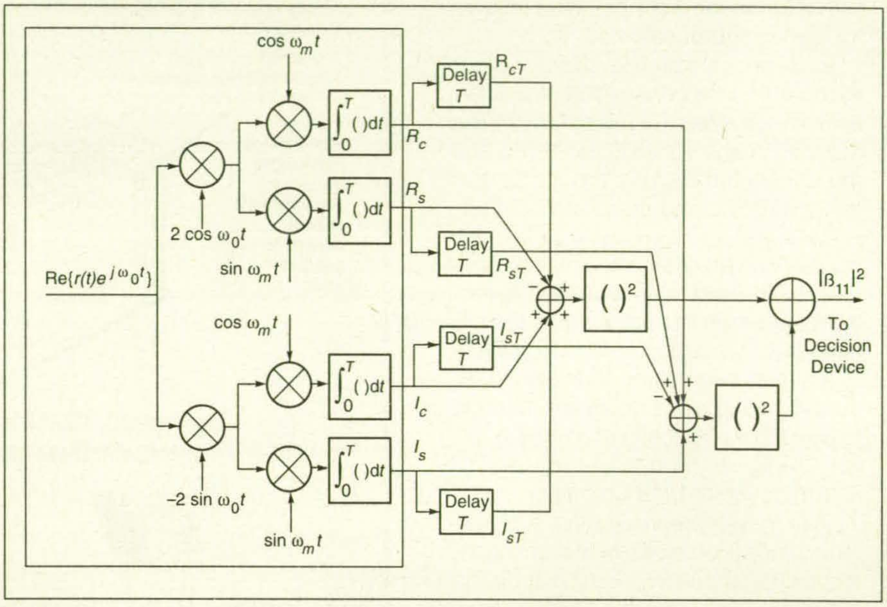

This **Simplified Receiver** structure would implement MLSE detection algorithms for MSK.

with a modulation index of ½, $M = 2$, and a rectangular frequency pulse was treated separately.

An important aspect of the study was emphasis on the simplification of structures of maximum-likelihood-sequence estimation (MLSE) receivers, which would implement the detection algorithms. The proposed simplified structures (see the figure for a particcular example corresponding to MSK) of the receivers are derived from a particular interpretation of the maximum-likelihood metrics. These receivers would include front ends, the structures of which would depend only on M, analogous to those in receivers of coherent CPM. The parts of these receivers that follow the front ends would have structures, the complexity of which would depend on N.

Because the proposed simplified receivers are derived from the maximum-likelihood principle, their performances could, intuitively, be expected to improve with increasing N. In preparation for a more rigorous theoretical demonstration that this should be so, an exact equation for the pairwise sequence error probability of a proposed MLSE receiver was derived. This equation was used, in turn, to derive upper bounds on the bit-error probabilities of several MLSE receivers of practical interest. By suitably approximating the pairwise sequence error probability at large signal-to-noise ratio, it was shown that in the limit as $N \rightarrow \infty$, the bit-error probability of an MLSE noncoherent receiver approaches that of an equivalent coherent receiver.

From the combined theoretical and computational results, it was concluded that significant gain can be achieved by making decisions over a full sequence of N symbols rather than by making a decision on each symbol individually in a sequence of the same length. Finally, it was shown that there is an optimum (in the sense of minimum error probability) modulation index, and that it is a function of the signal-to-noise ratio and of the length of the detected sequence. The values of optimum modulation indices were found to be quite close to those reported previously for symbol-by-symbol detection.

This work was done by Dariush Divsalar and Marvin K. Simon of Caltech for **NASA's Jet Propulsion Laboratory**. *For further information, Circle 12 on the TSP Request Card.*
NPO-18522

Pulse-Modulation Scheme for Voice and Telemetry

Information is conveyed via the frequencies and durations of pulses.

John F. Kennedy Space Center, Florida

A pulse-modulation scheme provides for the transmission of 1 channel of voice information along with 16 channels of serially multiplexed analog biotelemetric information, all on a single radio-frequency carrier signal. In this scheme, the biotelemetric information is conveyed by pulse-interval modulation (PIM), in which the interval between the leading edges of two given successive pulses is made proportional to the sampled biotelemetric quantity in a given channel. The voice information is conveyed by pulse-width modulation (PWM), in which the duration of each pulse is made proportional to the instantaneous amplitude of the voice signal. This combination of PIM and PWM encoding is called "pulse modulated data" or PMD.

The principal advantage of this scheme is simplicity: The comodulation of the voice along with the biotelemetry involves minimal additional circuitry in the transmitter. In the receiver, the biotelemetric data are extracted by ordinary PIM-decoding circuitry, which is not affected by the voice PWM; and a simple PWM decoder can be added to the receiver to recover the voice.

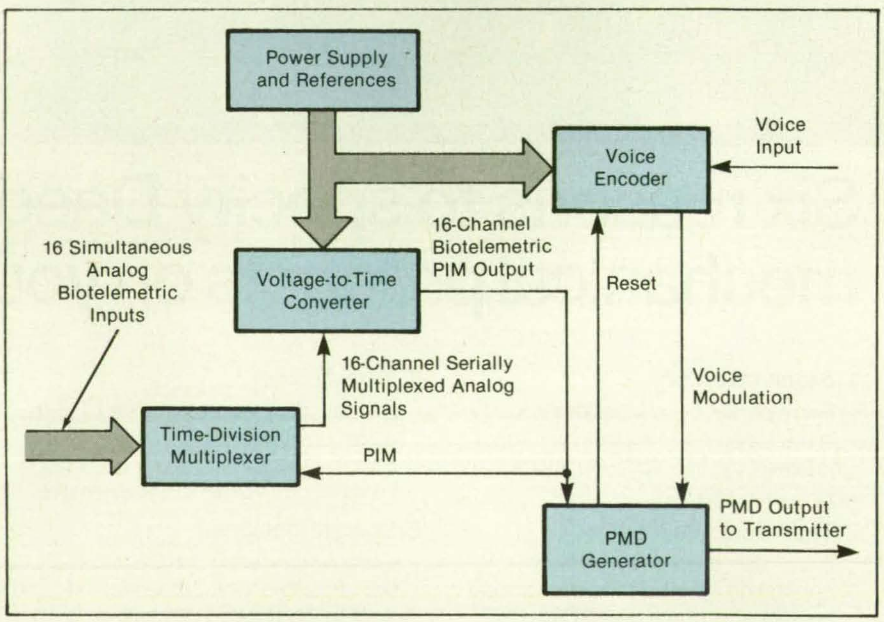

This **Encoder/Multiplexer Combination** effects the PMD scheme, in which biotelemetry is encoded in time-division multiplex PIM, while voice is encoded in PWM.

The pulse-modulation circuitry (see figure) includes a multiplexer and voltage-to-time converter, which act together to generate the pulses that mark the beginnings and ends of successive pulse intervals of varying duration. The circuitry also includes the voice encoder and the PMD generator. The voice encoder includes a voltage-to-time converter, which is held in "reset" mode until the PMD generator signals the end of each PIM interval, at which time the voice encoder is released from "reset" and starts to generate a pulse, the duration of which is proportional to its voice-voltage input. At the end of this pulse, the voice encoder returns to "reset" mode to await the end of the current PIM interval, and so the cycle repeats. The PMD generator mixes the PIM end/start event with the end-pulse event from the voice encoder.

This work was done by William J. Mills of Konigsberg Instruments, Inc., for **Kennedy Space Center**. *For further information, Circle 100 on the TSP Request Card.*

Inquiries concerning rights for the commercial use of this invention should be addressed to the Patent Counsel, Kennedy Space Center [see page 24]. Refer to KSC-11581.

Micromachined Dust Traps

Tiny traps capture particles for analysis.

NASA's Jet Propulsion Laboratory, Pasadena, California

Micromachined traps have been devised to capture dust particles for analysis without contaminating them. The operation of the traps is based on micromachined structures that retain particles, rather than on adhesives or greases that would interfere with scanning-electron-microscope analysis or x-ray imaging. Furthermore, unlike maze traps and traps that enmesh particles in steel wool or similar materials, the micromachined traps do not obscure the trapped particles.

A typical micromachined trap is made by etching a silicon wafer. A wafer 2 in. (5.1 cm) in diameter yields about 10 traps with openings of 300 by 800 μm. The wafer is divided into chips 0.4- by 0.4-in. (1 by 1-cm) square, each containing a single trap.

Particles that enter a trap collide repeatedly with the walls of the trap, losing energy as they do, and they come to rest at the inner end. Any of a variety of internal geometries (see figure) can be selected to retain particles of a given size that impinge upon a trap at a given velocity. Pits of various geometries have been demonstrated to capture dust particles with sizes ranging from 2 to 15 μm and speeds ranging from 50 to 200 m/s.

This work was done by Gregory H. Bearman and James G. Bradley of Caltech for **NASA's Jet Propulsion Laboratory**. *For further information, Circle 108 on the TSP Request Card.*
NPO-18276

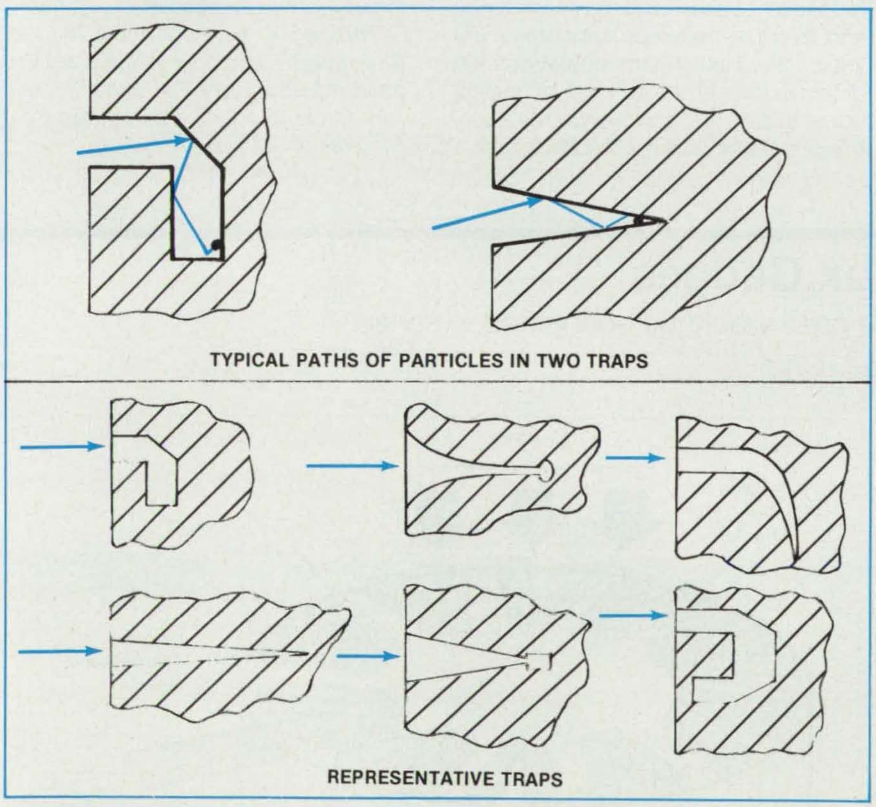

Internal Geometries of traps range from simple cones to U-shapes, all formed by etching silicon.

Canceling Torque Caused by Boiloff of Cryogen

One of two opposing exit streams is heated to increase its speed.

NASA's Jet Propulsion Laboratory, Pasadena, California

A proposed technique for the cancellation of the small torques caused by venting of cryogens from tanks in spacecraft might be adaptable to use in making small corrections in the orientations of terrestrial scientific instruments. The concept could be particularly useful in situations in which (1) conventional electromagnetic actuators might not be suitable because of constraints related to temperature, radiation, or vibration and (2) equipment is required to be robust, simple, reliable, light in weight, and without moving parts.

Whenever heat from any source is transferred to a mostly liquid cryogen, some of the cryogen is vaporized and must be vented. This venting creates a torque. A simple way to reduce this torque is to vent the vapor through a "T" from two nozzles that point in opposite directions. If the exit velocities from the two nozzles are exactly opposite and if the mass-flow rates are exactly equal, then the torques produced by the two streams cancel and the net torque is zero. However, in practice, manufacturing tolerances result in imperfect cancellation; that is, there is a small net torque.

The net torque can be reduced to approximately zero by heating whichever of the two streams is producing less torque: heating the stream increases its exit speed and, therefore, the torque that it exerts. The choice of which stream to heat and the determination of the amount of heating power to apply to it can be made by a control circuit that receives feedback from a torque or attitude sensor.

This work was done by Pradeep Bhandari of Caltech for **NASA's Jet Propulsion Laboratory**. *For further information, Circle 76 on the TSP Request Card.* *NPO-18474*

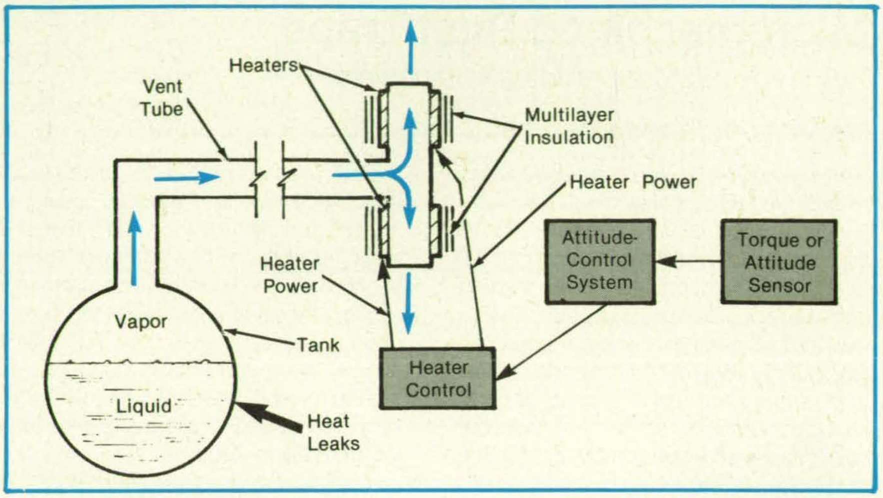

Torque Caused by the Venting of the Cryogen could be nearly eliminated by directing the exhaust gas through a "T" vent. To cancel the remaining small torque, that side of the "T" from which the exhaust produced the smaller thrust would be heated just enough to equalize the opposing thrusts.

High-Output Heat-Flux Gauges

Multiple differential thermocouple pairs would be connected in series.

Lewis Research Center, Cleveland, Ohio

Heat-flux gauges of a proposed type would put out relatively large signal voltages. The new gauges would be useful in such applications as engine instrumentation and radiation-measuring equipment.

Heretofore, a typical heat-flux gauge has included a single temperature sensor (thermocouple or resistance thermometer) on the top surface of an insulating layer and another single temperature sensor of the same kind on the bottom surface. The output of such a sensor is approximately proportional to the difference between the temperatures of the two surfaces which, in turn, is approximately proportional to the thickness of the insulating layer and to the flux of heat through it. Often, the output is too small to yield accurate and useful measurements unless the sensor is thick, the heat flux is large, or both.

The principle that underlies the new gauge concept is simple: fabricate a sensor with N top-surface/bottom-sur-

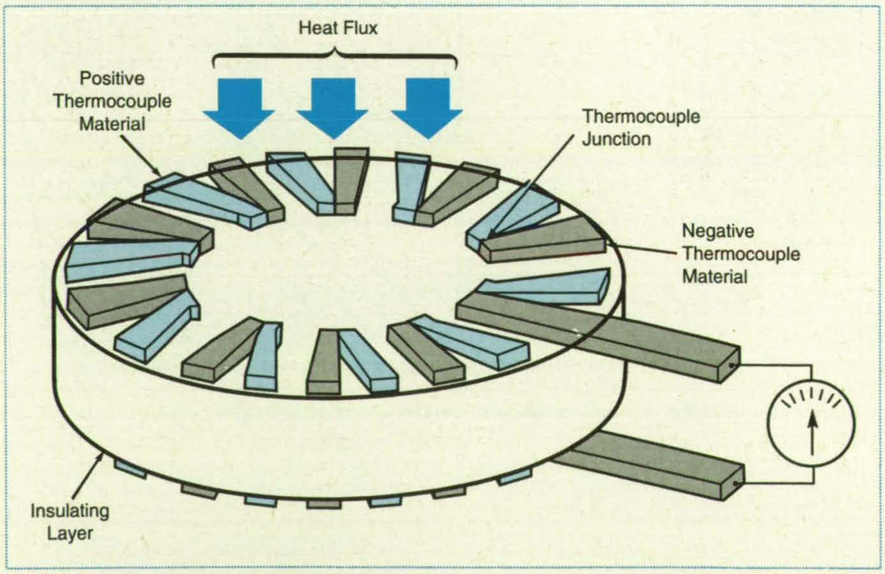

Thermocouples in *N* Top-Surface/Bottom-Surface Pairs connected in series would put out N times the voltage of a conventional (N = 1) pair on an insulating layer of the same thickness at the same heat flux.

face pairs of thermocouples, and with the N pairs connected in series to multiply the output voltage by N (see figure). This would make it possible to measure smaller heat fluxes accurately with a sensor of given thickness, or to make a thinner sensor to measure heat fluxes in a given range.

The multiple (N = 10 to 10,000) thermocouples would be arranged in circles or other convenient patterns on the top and bottom surfaces of the insulator. The wires that connect the top and bottom-surface thermocouples would be plated through holes in the insulator. These holes would be arranged in larger concentric circles or corresponding patterns to minimize the effect of the connecting wires on the flow of heat in the vicinity of the thermocouple junctions. Each through-hole connecting wire would be made of the same thermocouple alloy as that of the thermocouple legs it connects, so as not to set up spurious thermocouple junctions at positions other than in the designated thermocouple patterns.

The thermocouple alloys could be deposited on the top and bottom surfaces by such well-known techniques as sputtering, thermal evaporation, and plating. The alloys could be patterned by use of photoresist masks and chemical etching.

This work was done by Herbert A. Will of **Lewis Research Center**. *For further information, Circle 38 on the TSP Request Card.*
LEW-14730

Test Would Quantify Combustion Oxygen From Different Sources

Isotope tracers would be detected by mass spectroscopy.

Lyndon B. Johnson Space Center, Houston, Texas

A proposed isotope-enrichment scheme would enable the determination of the contributions of dual sources of oxygen for combustion. For example, it could be used to determine the contributions of natural oxygen in air and liquid oxygen supplied in a separate stream that may be mixed with air or sent directly into a combustion chamber.

The liquid oxygen or other artificial stream would be enriched with ^{18}O to about 1 percent by weight. (Natural oxygen consists of about 0.2 weight percent ^{18}O, most of the rest being ^{16}O.) The combustion products would be analyzed by a mass spectrometer to measure the relative abundances of $H_2{}^{18}O$ and $H_2{}^{16}O$. From the relative abundances of water products measured in this experiment, the natural relative abundances, and the relative (enriched) abundance of oxygen in the artificial stream, one can compute the relative contribution of oxygen extracted from the stream compared to the other source of oxygen in the combustion process.

This work was done by Ralph M. Tapphorn of Lockheed Engineering & Sciences Co. for **Johnson Space Center**. *For further information, Circle 1 on the TSP Request Card.* *MSC-21824*

Magnetic Compensation for Gravitational Pressure Gradient

A magnetic-field gradient produces a force that counteracts the gravitational force.

NASA's Jet Propulsion Laboratory, Pasadena, California

In a technique for the partial simulation of low gravitation in a diamagnetic or paramagnetic liquid, a magnetic field that has a suitable gradient produces a force that counteracts the gravitational force. This technique makes it possible to perform low-gravity experiments on the ground, at considerably less expense than in outer space. Many liquids are either diamagnetic (e.g., helium) or paramagnetic (e.g., oxygen).

The magnetic field needed to cancel the gravitational pressure gradient in a liquid is given by

$$B^2(z) = \frac{2gz\mu_0}{\frac{d\chi}{d\rho}}$$

where B is the magnetic field in Teslas, z is the vertical position in meters, g is the acceleration of gravity in m/s^2, μ_0 is the magnetic permeability of the vacuum, χ is the magnetic susceptibility of the liquid, and ρ is the density of the liquid in kg/m^3. For helium at 2 K, this becomes $B = 7.96 \sqrt{-z}$. This equation can be manipulated to show that the magnetic-field gradient needed to cancel the gravitational pressure gradient is smaller at greater intensities of the magnetic field.

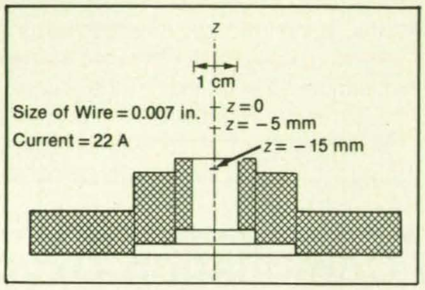

This **Three-Cylindrical-Coil Electromagnet** produces a magnetic field that counteracts the gravitational pressure gradient in liquid helium to within about 1 percent, in a region along the axis from $z = -5$ mm to $z = -15$ mm.

In practice, imperfections in the applied magnetic field prevent the perfect cancellation of gravitational effects, but reduction of gravitationally induced inhomogeneities in liquids to less than 1 percent of the original values appears practical. This would make it possible, for example, to make the condition in an experimental liquid approach a critical point more closely, thereby providing a better test of the applicable theory of fluctuations in the critical region. The reduction of the effects of gravitation would also enable the observation of effects that have finite sizes, in well-characterized geometries.

The three-coil electromagnet shown in the figure was designed to provide cancellation of the gravitational gradient of pressure along its axis, to demonstrate basic feasibility. By use of available computer programs, one could also design magnets that would optimize the gradient of the magnetic field at off-axis as well as at on-axis points. The needed magnetic-flux densities appear to be well within the capabilities of available superconducting magnets.

This work was done by Ulf E. Israelsson, Henry W. Jackson, and Donald M. Strayer of Caltech for **NASA's Jet Propulsion Laboratory**. *For further information, Circle 46 on the TSP Request Card.*
NPO-18599

Measuring Microwave Conductivities of Superconducting Films

Complex conductivities are computed from microwave-power-transmission data.

Lewis Research Center, Cleveland, Ohio

Microwave conductivities of thin films of high-temperature superconductors like $YBa_3Cu_3O_{7-\delta}$ can be measured by the noninvasive, nondestructive microwave-power-transmission method. These measurements yield useful information on the superconducting and normal states of the films and contribute to the evaluation of the films for use in microwave devices.

A film to be characterized by this method is supported by a dielectric substrate. The film and the substrate are clamped between two flanges in a test section of waveguide so that the film obstructs the waveguide. The flanges are cooled to a specified temperature (e.g., the superconducting-transition temperature of the film). The ends of the test section of waveguide are connected by other waveguides to microwave network analyzer, which measures the transmission coefficient, T (the ratio between the microwave power transmitted through the film, and the microwave power incident upon the film) and the phase shift, ϕ, in the transmitted wave.

The real and the imaginary parts of the microwave conductivity of the film are computed from T, ϕ, the wave number of the normally incident transverse electric wave propagating in the waveguide, the thickness of the film, and the thickness and the dielectric constant of the substrate (see Figure 1). Then the real and the imaginary parts of the microwave conductivity can be used to compute the magnetic penetration depth and the surface resistance.

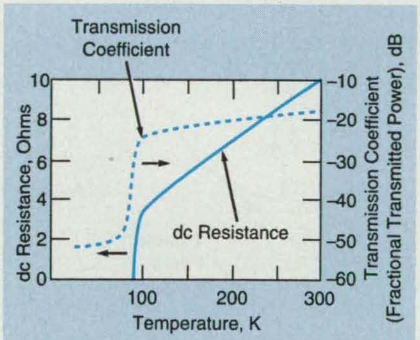

Figure 1. The **Transmission Coefficient** of a 2,655-Å-thick $YBa_2Cu_3O_{7-\delta}$ film on an $LaAlO_3$ substrate at a frequency of 35 GHz decreases with decreasing temperature as the film becomes increasingly conductive and, therefore, a more nearly perfect reflector. The real and the imaginary parts of the conductivity are computed from the transmission coefficient and other quantities.

In a test, the surface resistance of a film determined by the microwave-power-transmission method was compared with the surface resistance deduced from the change in the Q of a microwave resonant cavity when a copper wall of the cavity was replaced by the film (see Figure 2). Discrepancies between the values at temperatures near T_c are tentatively attributed to (1) normally conducting inclusions, which can affect the microwave-power-transmission measurements by allowing significant leakage through the film; and (2) the fact that the cavity measurements are influenced less by the inclusions and more by the surface properties of the film.

This work was done by K. B. Bhasin and J. D. Warner of **Lewis Research Center**, *F. A. Miranda and W. L. Gordon of Case Western Reserve University, and H. S. Newman of the Naval Research Laboratory. Further information may be found in NASA TM-103616 [N91-0780], "Determination of the Surface Resistance and Magnetic Penetration Depth of Superconducting $YBa_2Cu_3O_{7-\delta}$ Thin Films by Microwave Power Transmission Measurements."*

Copies may be purchased [prepayment required] from the National Technical Information Service, Springfield, Virginia 22161, Telephone No. (703) 487-4650. Rush orders may be placed for an extra fee by calling (800) 336-4700.

LEW-15394.

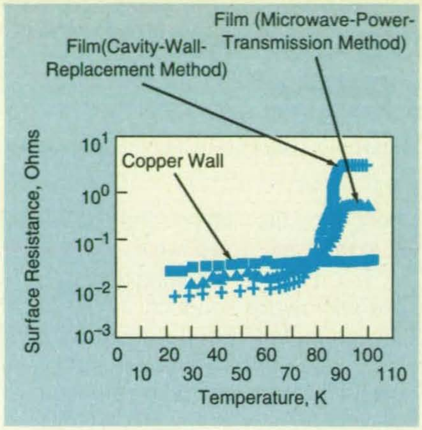

Figure 2. **Surface Resistances** of the film were determined at a frequency of 36 GHz by two different methods. Also shown for reference is the surface resistance of the replaced copper wall used in the cavity-wall-replacement method.

Generation of O_2 From CO_2 by Glow Discharge and Permeation

Carbon dioxide is converted to a useful and breathable oxygen supply.

Langley Research Center, Hampton, Virginia

A technique for generating a supply of highly pure O_2 from CO_2 has been developed. First, atomic oxygen at a useful partial pressure is generated by glow-discharge dissociation of the CO_2. The atomic oxygen is formed in the vicinity of a hot silver membrane and permeates through the membrane to a downstream region, where it thermally recombines into O_2 and is pumped away to a storage tank. The pure oxygen thus stored is suitable for human consumption and other uses.

The figure illustrates the technique schematically. CO_2 enters the chamber at a rate that maintains the pressure somewhere between 0.5 and 2 torr (about 0.07 to 0.3 kPa). A potential of 380 Vdc is applied at the electrode, creating a glow discharge in which impacts of electrons on the CO_2 molecules cause the molecules to dissociate as follows:

$$CO_2 + e^- \longrightarrow CO + O + e^-$$

The atomic oxygen can recombine to form CO_2 or O_2, but it can also be adsorbed and dissolved in the hot silver membrane, ultimately permeating to the downstream side where it recombines to form O_2. The O_2 is desorbed from the downstream surface and is pumped into the storage tank, thus maintaining the low pressure on the downstream side and the concomitant gradient of concentration across the membrane.

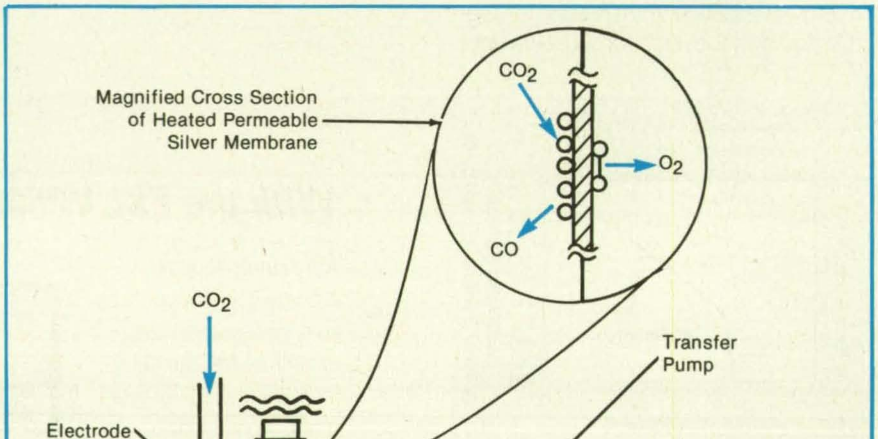

The **Atomic Oxygen** generated in the glow discharge passes through the permeable membrane and recombines into O_2 on the other side. The permeable membrane is a thin film of silver supported by a porous plug or by a silver mesh.

In an experiment in which a dc electric field was used to create the glow discharge, a mass spectrometer detected an increase in the concentration of O_2 by several orders of magnitude until a steady-state level was reached. The glow discharge can also be created by radio-frequency and microwave energy with an appropriate electrode geometry to provide optimum kinetics for the flux of atomic oxygen incident on the membrane.

This technique for generating oxygen was originally developed to convert the

Martian atmosphere of CO_2 to O_2 for astronaut consumption. Other potential applications include the purification of the atmospheres in the Space Shuttle and the Space Station *Freedom*. The byproduct CO must be handled by other techniques.

This work was done by R. A. Outlaw of **Langley Research Center**. *For further information, Circle 16 on the TSP Request Card.*

This invention is owned by NASA, and a patent application has been filed. Inquiries concerning nonexclusive or exclusive license for its commercial development should be addressed to the Patent Counsel, Langley Research Center [see page 24]. Refer to LAR-14398.

Counteracting Gravitation in Dielectric Liquids

Electric fields with suitable gradients produce vertical forces that oppose gravitation.

NASA's Jet Propulsion Laboratory, Pasadena, California

The force of gravity in a variety of dielectric liquids (for example, helium, neon, oxygen, argon, and xenon) can be counteracted by imposing suitably contoured electric fields. This technique could make it possible to perform, on Earth, a variety of experiments that previously could be performed only in outer space and, therefore, at great cost. The technique could also be used similarly in outer space to generate a sort of artificial gravitation.

The technique is based on the following equation for the change in the pressure of a dielectric liquid to which an electric field is applied:

$$\Delta p = \frac{1}{2}\rho\frac{d\varepsilon}{d\rho}E^2$$

where ρ is the density, ε is the dielectric constant, and E is the electric field. This equation is valid as long as the only fundamental thermodynamic property on which the dielectric constant depends is the density; this is expected to be the case for helium, neon, oxygen, nitrogen, argon, and xenon at the temperatures at which they are liquids.

By equating the change in pressure shown above to the gravitationally induced change in pressure with depth in a liquid, one obtains the following equation for the electric field necessary to counteract gravitation:

$$E^2(z) = \frac{2gz}{\frac{d\varepsilon}{d\rho}}$$

where g is the gravitational acceleration and z is the height or depth coordinate. The gradient in E, dE/dz, should be directed so that $|E|$ increases with height. Using the value of $d\varepsilon/d\rho$ of liquid helium at 2 K, the equation becomes $E = 7.55\times10^7\sqrt{z}$ V/m, where z is in meters. This equation is plotted in Figure 1. It has already been demonstrated that electric fields at least as large as 13 MV/m can be applied to liquid helium without causing electrical breakdown. For other liquids, $d\varepsilon/d\rho$ is larger, so that electric fields smaller than those for helium would be required.

Figure 2 shows two designs of cells that can be built to implement this technique. In one design, the horizontal distance between two curved electrodes is varied to yield the required vertical gradient of the horizontal electric field. In the other design, different voltages are applied to parallel electrodes arranged vertically. The voltages, which result in an electric field with approximately the required electric-field gradient, can be generated from a single high-voltage supply by use of a voltage-dividing resistor network.

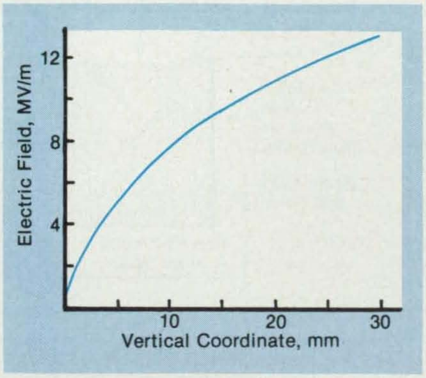

Figure 1. The **Horizontal Electric Field** required to counteract gravitation in helium at 2 K has a vertical gradient.

If the applied voltage is 20 kV, curved electrodes are used, and maximum available field in the design is restricted to about 10 MV/m in the case of ^{4}He at 2 K, then the required horizontal distance between electrodes varies from 1.9 mm at the top to 2.7 mm at a depth of 10 mm. If the applied voltage is 40 kV, the required width varies from 3.7 mm at the top to 5.3 mm at a depth of 10 mm.

Perfect cancellation of gravitation across the entire width of such a cell is possible only if the electric field is horizontal across the entire width. In reality, such an alignment of electric-field lines is not possible when a gradient in the field is required. In the 20-kV and 40-kV cells described above, the maximum error resulting from the deviation of the field lines from horizontal alignment is estimated to be 0.0044 g and 0.0176 g, respectively. If larger electric fields could be used without incurring breakdown or heating, the resulting errors would be smaller: doubling the field would reduce the error by a factor of 8.

This work was done by Ulf E. Israelsson, Henry W. Jackson, and Donald M. Strayer of Caltech for **NASA's Jet Propulsion Laboratory**. *For further information, Circle 11 on the TSP Request Card.* NPO-18597

Figure 2. **Either of These Cells** can be used to generate an electric field with a gradient like that of Figure 1.

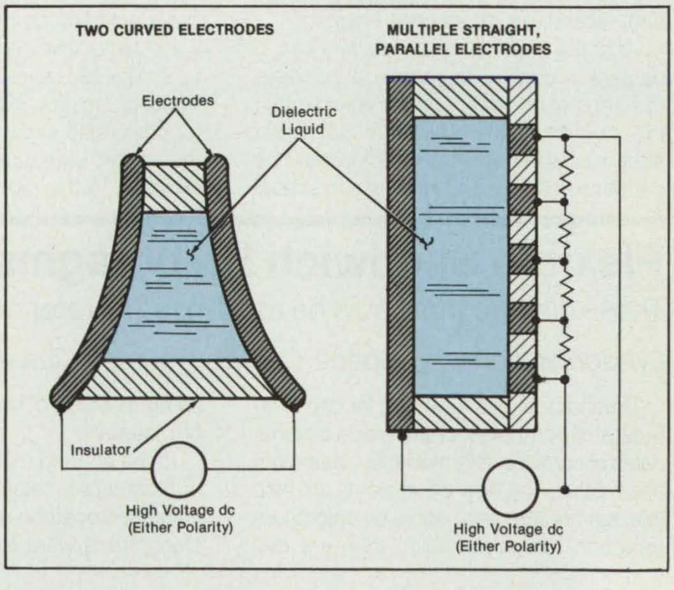

Microwave Pretreatment for Hydrolysis of Cellulose

Microwave pretreatment greatly increases the efficiency of enzymatic hydrolysis of cellulosic feed mixtures.

Lyndon B. Johnson Space Center, Houston, Texas

Microwave pretreatment enhances the enzymatic hydrolysis of cellulosic wastes (e.g., paper, cornstalks, bagasse) into soluble saccharides that can be used as feedstocks for foods, fuels, and other products. The low consumption of energy, high yield, and low risk of a proposed hydrolysis process that incorporates the microwave pretreatment could make the process a viable alternative to composting.

The figure is a schematic diagram of a proposed apparatus that would implement the process. The cellulosic feed material would be mixed with an aqueous acid stream — typically 3 to 7 parts (by mass) of acetic acid (other acids can be used) and about 3 to 7 parts of water per part of cellulosic material. The resulting slurry would be irradiated with microwaves in a pressure vessel. During irradiation, the mixture would be agitated, and a pressure controller would adjust the microwave power to maintain the equilibrium pressure, preferably in a range from about 4 atm (0.4 MPa) to about 10 atm (1 MPa). The temperature in the vessel would generally correspond to the saturation temperature. Typically, this pretreatment would be carried out for 5 to 60 min. Experimental pretreatments have demonstrated the viability of the concept. It has been theorized that the treatment disrupts the crystallinity of cellulose-based polymers, thereby enhancing their affinity for enzymes, and that the acid is sorbed at sites in the polymers, enhancing the impact of the radiation by preferentially absorbing microwave energy.

After the pretreatment, the slurry would be sent through a depressurization valve to a separation vessel, which would retain the treated solids while the gas/liquid stream of water and acetic acid would be condensed and recycled for use in subsequent pretreatment. The pretreated solids would be flushed with water or otherwise transferred from the separation vessel to a bioreactor. There, the solids would be mixed with a liquid reaction medium containing suitable enzyme(s) — for example cellulase, which is available commercially and can be produced from a culture of the mold *Trichoderma viride* and the fungus *Aspergillus niger*. The preferred reaction medium would be an aqueous acetic acid buffered to a pH between 4.5 and 5.5 and maintained at a temperature between 35 °C and 45 °C. In experiments, nearly complete conversion of available polysaccharides has been accomplished in 72 hours of such enzymatic digestion.

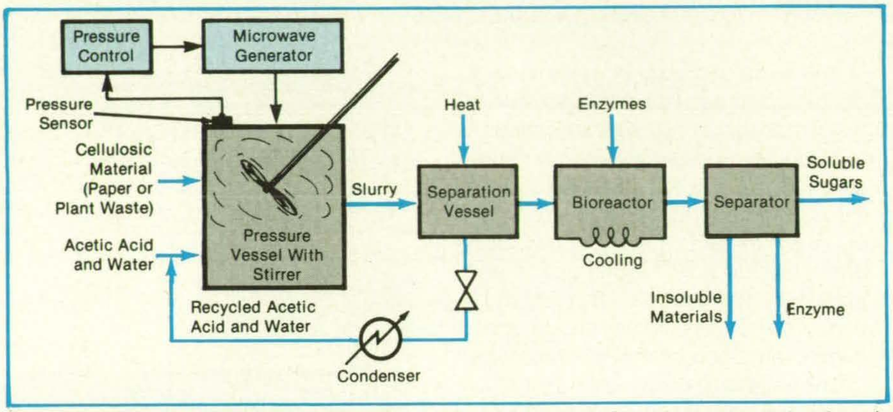

This **Apparatus Would Convert Cellulose to Sugars** by use of a microwave pretreatment followed by enzymatic hydrolysis.

The digested mass could be used as is or could first be passed through a separator to remove such insoluble materials as undigested cellulose and hemicellulose, lignin, crude protein, and ash. The separator could also separate the enzyme from the soluble sugars; the enzyme could be recycled to the bioreactor.

Where further processing is desired, the resulting sugars (soluble saccharides) could be fermented into alcohols by yeasts or other suitable microbes. The resulting alcohols, in turn, could be used for fuels or as starting materials for other organic chemicals including acids, esters, aldehydes, ketones, and hydrocarbons. The sugars could also be processed into carbohydrates and protein foodstuffs by culturing such other microbes as algae or fungi.

This work was done by Hatice S. Cullingford of **Johnson Space Center**, *Clifford E. George, and George R. Lightsey. For further information, Circle 6 on the TSP Request Card.*

This invention is owned by NASA, and a patent application has been filed. Inquiries concerning nonexclusive or exclusive license for its commercial development should be addressed to the Patent Counsel, Johnson Space Center [see page 24]. Refer to MSC-21936.

Flexible Sandwich Diaphragms Are Less Permeable

These diaphragms could be used in refrigerator compressors.

Lyndon B. Johnson Space Center, Houston, Texas

Diaphragms of a new type for use in refrigerator compressors are made as laminates of commercially available elastomers and metals. The new diaphragms are flexible, but are less permeable by chlorofluorocarbon refrigerant fluids than are diaphragms made of homogeneous mixtures of materials.

In the effort to make flexible compressor diaphragms relatively impermeable by chlorofluorocarbon refrigerants, specimen diaphragms were tested with Freon 502 (48.8 weight percent $CHClF_2$ + 52.2 weight percent C_2ClF_5), which has a strong tendency to permeate substances that might otherwise be useful in containing it. All specimens made of elastomeric (only) materials were found to be highly permeable by Freon 502. This finding led to the investigation of diaphragms in which impermeable layers were sandwiched between layers of structurally tough material.

Sandwich-type diaphragms made of elastomers with embedded impermeable thin sheets of metal and semirigid polymers were tested and found to have some utility. In the fabrication of these diaphragms, continuous metal films of gold and platinum/palladium 5 to 25 μm thick were vapor-deposited on the surfaces of thin sheets of uncured neoprene W and epichlorohydrin elastomers. Thin sheets of the uncured elastomers were then laid on the exposed surfaces of the metal coats to create the sandwich structures. Each elastomer/metal/elastomer sandwich was then placed in a mold, and the elastomer was cured under heat and pressure to produce a fully vulcanized product. The completed diaphragms were used in a conventional manner. In some specimens, semirigid polymer films were substituted for the thin deposited metal sheets, and sandwich diaphragms made with these materials were cured in the same way as were those that contained metals.

Still other diaphragms were produced in much the same way except that the metal films on the surfaces of the uncured elastomer were not continuous but were in regular grid patterns. The resulting diaphragms included many elastomer/elastomer connections at open spaces in the grid. These connections strengthened the overall diaphragm, providing greater resistance to wear by preventing delamination during long use. Diaphragms made in this configuration exhibited ¼ to ½ the permeability of homogeneous elastomer (only) diaphragms, and have been exercised in test compressors for more than 100 hours.

This work was done by John G. Michalovic and Franklin A. Vassallo of CALSPAN Corp. Advanced Technology Center for **Johnson Space Center**. *No further documentation is available.*

Title to this invention has been waived under the provisions of the National Aeronautics and Space Act [42 U.S.C. 2457(f)], to CALSPAN Corp. Inquiries concerning licenses for its commercial development should be addressed to

Roland Pilie
Chairperson of Patent Committee
CALSPAN Corp.
P.O. Box 400
Buffalo, NY 14225

Refer to MSC-21928, volume and number of this NASA Tech Briefs *issue, and the page number.*

Screening for Microcracking by Testing Unbalanced Laminates

Expensive, time-consuming thermal-cycling tests might be obviated.

Lewis Research Center, Cleveland, Ohio

An experimental study has demonstrated the feasibility of a relatively fast thermomechanical testing procedure for the screening and ranking of matrix/fiber composite materials with respect to resistance to microcracking. The procedure is intended to replace comprehensive thermal-cycling tests, which may ultimately be needed to characterize a candidate material that survives preliminary screening, but which consume too much energy, take too much time, and are too expensive for use in preliminary screening of many candidate materials.

The new procedure begins with the fabrication of a plate of unbalanced cross-ply (0°, 90° fiber orientations) matrix/fiber laminate. As used here, "unbalanced" means that with respect to the depths and orientations (0° or 90°) of the plies, the plate is not symmetrical about the plane

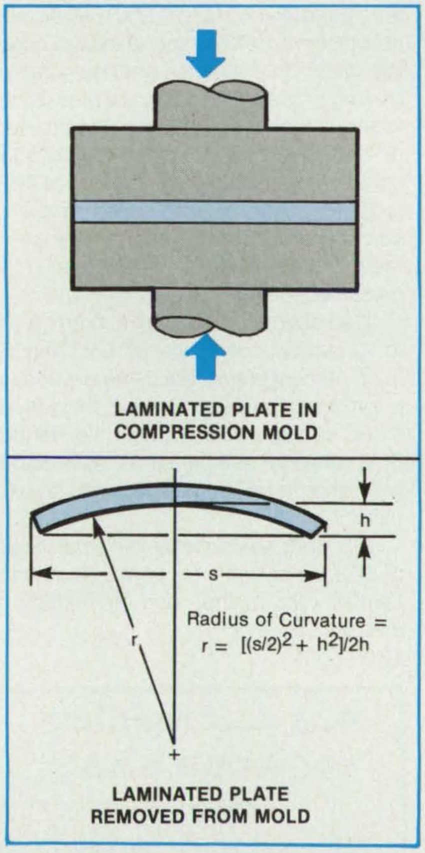

Residual Stress warps an unbalanced-laminate plate into a cylinder upon removal from a compression mold.

located halfway through its thickness. Because of the asymmetry, the anisotropy of each layer, and the difference between the coefficients of thermal expansion of the matrix and fiber materials, residual stresses are generated during fabrication and during the subsequent cooldown from the elevated curing temperature used in fabrication. These residual stresses give rise to strains, which can be measured. The basic idea underlying the new procedure is that these measured strains can be correlated with the intralaminar cracking that is observed in conventional thermal-cycling tests and that is presumably caused by similar stresses.

Immediately after fabrication, one component of the residual strain manifests itself visibly: upon removal from the mold, the plate acquires a cylindrical warp. The radius of curvature of the warp is easily measured (see figure) and used, along with pertinent data on the material and from the theory of laminates, to calculate the component of residual stress that causes the warp. It is also useful to determine that temperature (which is not necessarily the curing temperature) at which the cylindrical-warping residual stress decreases to zero. This is done by heating the plate and measuring its curvature as a function of temperature, the stress-free temperature being that temperature at which the plate becomes flat. Additional data on cracking can be obtained by use of the dye-penetrant inspection method to observe any surface damage resulting from excessive residual stresses.

In the experimental study, the new testing procedure was applied to specimens of eight different unbalanced laminates made with graphite fibers: six with matrices of PMR-15 polyimide, one with a matrix of PMR-II-50 polyimide, and one with a matrix of polyetheretherketone. The results of these experiments were compared with those of previous conventional thermal-cycling tests of balanced specimens. The combined results show that the surface conditions of the laminates affect the severity of cracking and the propagation of cracks, and both types of tests gave similar indications with respect to resistance to microcracking. Thus, it appears that the new test can be used for the qualitative screening of matrix/fiber combinations and surface treatments for resistance to microcracking.

This work was done by Kenneth J. Bowles of **Lewis Research Center** *and Demetrios S. Papadapoulos of Case Western Reserve University. Further information may be found in NASA TM-102517 [N90-21124], "Screening for Microcracking by Testing Unbalanced Laminates."*

Copies may be purchased [prepayment required] from the National Technical Information Service, Springfield, Virginia 22161, Telephone No. (703) 487-4650. Rush orders may be placed for an extra fee by calling (800) 336-4700.

LEW-15184

Safe Replacement for Asbestos in Nickel/Hydrogen Cells

Polyethylene fibers and potassium titanate particles perform as well as asbestos.

Lewis Research Center, Cleveland, Ohio

A new material for the separators of nickel-hydrogen electrochemical cells offers performance similar to that of the asbestos separator material used heretofore, but without the adverse health effects of asbestos. Because of these adverse effects, suppliers are no longer willing to continue producing asbestos separators in the long term.

In one version, a separator contains pure polyethylene fibers, and may or may not contain supplementary latices as bonding agents. In a standard wet-laying papermaking process, the fibers are pressed into a mat, then dried. The mat can be used as is or pressed further in a hot calender stack to soften and fuse the fibers at their crossing points. This treatment reduces porosity and increases the resistance of the mat to passage of air bubbles under pressure.

In an alternative version, a matrix of 20 to 40 percent polyethylene fibers and 60 to 80 percent potassium titanate particles is formed on a paper machine, then dried. It, too, can be treated by hot calendering. Both versions have performed satisfactorily in short-term tests in nickel/hydrogen cells.

This work was done by William E. Scott of Miami University for **Lewis Research Center**. *No further documentation is available.*

LEW-15051

Computer Programs

COSMIC: Transferring NASA Software

COSMIC, NASA'S Computer Software Management and Information Center, distributes software developed with NASA funding to industry, other government agencies and academia.

COSMIC's inventory is updated regularly; new programs are reported in *Tech Briefs*. For additional information on any of the programs described here, circle the appropriate TSP number.

If you don't find a program in this issue that meets your needs, call COSMIC directly for a free review of programs in your area of interest. You can also purchase the annual *COSMIC Software Catalog*, containing descriptions and ordering information for available software.

COSMIC is part of NASA's Technology Transfer Network.

COSMIC®—*John A. Gibson, Director,*
Phone (706) 542-3265; FAX (706) 542-4807
The University of Georgia, 382 East Broad Street,
Athens, Georgia 30602

Computer Programs

These programs may be obtained at a very reasonable cost from COSMIC, a facility sponsored by NASA to make computer programs available to the public. For information on program price, size, and availability, circle the reference number on the TSP and COSMIC Request Card in this issue.

Physical Sciences

Computing Thermodynamic and Transport Properties

CET89 computes compositions in chemical equilibrium and properties of mixtures.

Scientists and engineers need data on compositions for a chemical system in equilibrium as well as the resulting thermodynamic and transport mixture properties. This information is essential in the design and analysis of such equipment as compressors, turbines, nozzles, engines, shock tubes, heat exchangers, and chemical-processing equipment. The substantial amount of numerical computation required to obtain equilibrium compositions and transport properties for complex chemical systems led scientists at NASA's Lewis Research Center to develop CET89, a program designed to calculate the thermodynamic and transport properties of these systems.

CET89 calculates compositions in chemical equilibrium and the properties of mixtures for any chemical system for which thermodynamic data are available. Generally, mixtures may include condensed and gaseous products. CET89 provides the following options: it (1) obtains chemical-equilibrium compositions and corresponding thermodynamic mixture properties for assigned thermodynamic states, (2) calculates dilute-gas transport properties of complex chemical mixtures, (3) obtains Chapman–Jouguet detonation properties for gaseous mixtures, (4) calculates the properties of incident and reflected shocks in terms of assigned velocities, and (5) calculates theoretical performance of a rocket for both equilibrium and frozen compositions during expansion. The rocket performance may be based on the optional models of a finite or infinite area combustor.

CET89 accommodates problems that involve up to 24 reactants, 20 elements, and 600 products (400 of which may be condensed). The program includes a library of thermodynamic and transport properties in the form of least-squares coefficients for possible reaction products. It includes thermodynamic data for over 1,300 gaseous and condensed species for temperatures ranging from 300 to 5,000 K. Also provided are transport data for 151 gases.

This program was written by B. McBride of **Lewis Research Center** *and Sanford Gordon of Sanford Gordon & Associates. For further information, Circle 102 on the TSP Request Card.*
LEW-15113

Computing Properties of Pure and Mixed Fluids

Changes of phase and mixtures of phases are included.

Scientists at NASA's Lewis Research Center and across the United States working on the National Aero-Space Plane (NASP) Project required software to compute the physical properties of pure fluids, mixtures of fluids, and mixtures of phases. GASPLUS was created at Lewis as a two-part code: the first designed for use with pure fluids and the second designed for use with mixtures of fluids and phases. The first part of the code was created by coupling Lewis' existing pure fluid codes GASP, WASP, BT, and GASPAI to a user-friendly interface; the second part was created by writing a separate new code.

The pure-fluid side of GASPLUS is designed to calculate various physical properties for such fluids as hydrogen (ortho, normal, and para), oxygen, nitrogen, methane, carbon monoxide, carbon dioxide, water, argon, neon, helium, and ethylene glycol. It generates properties of fluids in the liquid phase (including saturated liquids and subcooled and compressed liquids), the vapor phase (including saturated vapors and superheated and supercritical fluids), the solid phase, and the vapor and liquid phases in equilibrium. This pure-fluid part of GASPLUS is a user-friendly code coupled with diagnostics designed to minimize errors in engineering uses.

The mixture side of the code provides properties of air [either National Institute of Standards and Technology (NIST) "standard" composition or with varying amounts of oxygen, nitrogen, argon, carbon dioxide, neon, and helium], wet air, hydrogen mixtures, and aqueous ethylene glycol. This part of GASPLUS predicts properties of saturated vapor/liquid phases, saturated solid/liquid phases (including slush hydrogen), and saturated vapor/liquid/solid phases of pure fluids and mixtures. GASPLUS cannot compute the properties of all combinations of phases of all mixtures of fluids, but it includes instructions and diagnostics to protect the user.

The entire code is available in interactive or "callable" form and comes complete with a user's manual, which details the separate parts of GASPLUS in different chapters and contains numerous examples of the use of the code. The code is available only with English units at present. GASPLUS is considered "engineering-grade" software, but it typically produces results to within 1 to 3 percent of current NIST data.

Both parts of GASPLUS are designed in modular form: given normal inputs of temperature and/or pressure (other inputs are occasionally allowed), individual subroutines calculate values of enthalpy, entropy, density, saturation pressure or temperature (or bubble-point pressure and dew-point pressure or bubble-point temperature and dew-point temperature in the case of a mixture of fluids), heat capacity, thermal conductivity, viscosity, speed of sound, quality, latent heat of vaporization, surface tension, critical pressure, critical temperature, freezing temperature, and derivative of pressure with respect to temperature within reasonable temperature and pressure conditions. While GASPLUS can compute properties at elevated temperatures and pressures, it is not intended for combustion calculations inasmuch as it does not predict properties of dissociated species or contain information on the kinetics of reactions at high temperatures.

Because it was intended as a precursor to a system-level analysis code, GASPLUS has an engineering orientation that is demonstrated by such capabilities as a unique isenthalpic, macroscopic-phase-determination or "flash" routine, which works as follows: A heat-transfer calculation typically involves the addition of a known quantity of enthalpy per unit mass to a fluid, the former conditions of pressure, enthalpy, and phase composition of which are known. This isenthalpic-flash routine accepts the final conditions of total enthalpy and pressure, it recognizes that masses of fluids have not changed, and it computes the correct temperature and fluid phase composition at the outlet. If multiple phases result, it computes the type and quantity (i.e., quality) of each phase. If the fluid is originally a mixture and the computed outlet conditions indicate a vapor and liquid phase in equilibrium, the routine apportions the fluid components to the two phases. If the fluid is a pure liquid initially and is cooled, the routine tells the user the correct outlet temperature and whether any solids (as with slush hydrogen) have formed. A similar routine that uses entropy is available.

GASPLUS offers routines for mathematical modeling of conditions of fluids in pumps, turbines, compressors and other machines. Other routines for calculating the performance of a para/ortho-hydrogen reactor and the heat of the para/normal-hydrogen reaction as well as a unique convergence routine further demonstrate the engineering flavor of GASPLUS.

GASPLUS was developed between 1986 and 1988. Future enhancements could easily expand the code to enable it to predict the properties of many other pure fluids and mixtures. Data for such calculations are readily available from NIST (DIPPR data package).

GASPLUS is written in FORTRAN 77 for DEC VAX-series computers and is known to run on VAX and IBM mainframe systems. Because of some non-ANSI-standard FORTRAN in the pure-fluid routines, GASPLUS cannot be compiled on CYBER computers. This program is available in DEC VAX BACKUP format on a 9-track, 1,600-bit/in. (630-bit/cm) magnetic tape (standard distribution) or on a TK50 tape cartridge. A PC version will soon be available.

DEC VAX and VMS are trademarks of Digital Equipment Corp. IBM and IBM PC are trademarks of International Business Machines Corp. CYBER is a trademark of Control Data Corp.

This program was written by J. R. Fowler of Sverdrup Technology, Inc., and Robert C Hendricks of **Lewis Research Center**. *For further information, Circle 20 on the TSP Request Card. LEW-15091*

Mechanics

Computing Pressure-vs.-Volume Properties of Bellows

SHELL computes displacements for use in other computer programs.

A majority of the liquid-fueled rockets developed in the past have been plagued by an instability known as POGO. The POGO phenomenon involves dynamics of the vehicle structure, dynamics of the propellant in the feedline, and the engine dynamic transfer function. Each of these three items must be accurately known to determine stability.

Metallic bellows are commonly used as segments of propellant feedlines for rocket-propelled vehicles to accommodate temperature-induced variations in length, manufacturing tolerances, and gimbaling of the engines. These bellows sections deform radially, and their volumes change, when internal pressures vary; the magnitudes of such deformations are much greater than those of the straight, cylindrical segments of the feedlines. Also, the greater flexibility of a bellows decreases the frequency of acoustic oscillations in the affected feedline.

The calculation of elastic stiffness is difficult because of the radial deformation of a bellows section. The SHELL computer program was developed specifically to calculate changes in volume of a bellows caused by changes in internal pressure. Input to the program consists of tables that describe the bellows material, the geometry of the convolutions, and loading. The output gives displacements and changes in volume that can be used for analysis of POGO or of water hammers.

SHELL is written in standard FORTRAN 77. This program was originally developed on a Univac 1100-series computer and has been successfully implemented on IBM 370-series computers running MVS and on DEC VAX-series computers running VMS. The main memory requirement for running SHELL under VMS is 116K. The program source code, IBM job-control language for compiling and running SHELL, and sample input are provided with the program. SHELL is available on a 9-track, 1,600-bit/

in. (630-bit/cm) ASCII CARD IMAGE magnetic tape. This program was developed in 1989.

IBM is a trademark of International Business Machines Corp. DEC, VAX, and VMS are registered trademarks of Digital Equipment Corp. Univac 1100 is a trademark of Unisys Corp.

This program was written by Larry Kiefling of **Marshall Space Flight Center**. *For further information, Circle 24 on the TSP Request Card.*
MFS-28436

Program Determines Minimum-State Approximations to Unsteady Aerodynamic Forces

MIST implements the minimum-state method for determining rational approximations of the matrix of aerodynamic force coefficients.

Various techniques for the analysis, design, and simulation of aeroservoelastic systems require the equations of motion to be cast in a linear, time-invariant state-space form. In order to account for unsteady aerodynamics by use of the first-order equations of the state-space formulation, rational-function approximations must be obtained. The MIST computer program determines minimum-state approximations of the matrix of the coefficients of the unsteady aerodynamics forces.

The minimum-state method facilitates the design of lower-order control systems, analysis of the performances of control systems, and near-real-time simulation of such aeroservoelastic phenomena as the outboard-wing acceleration response to gust velocity. Engineers who use the MIST program can calculate minimum-state rational approximations of the generalized unsteady aerodynamic forces. By use of the minimum-state formulation of the state-space equations, they can obtain state-space models with good open-loop characteristics while reducing the number of aerodynamic equations by an order of magnitude more than traditional approaches do. These low-order state-space mathematical models are good for design and simulation of aeroservoelastic systems.

The computer program, MIST, accepts complex tabular data representing the generalized unsteady aerodynamic forces over a set of reduced frequencies. It then determines approximations to these tabular data in the Laplace domain by use of rational functions. MIST provides the capability to select the coefficients of the denominator in the rational approximations, to constrain the approximation selectably without increasing the size of the problem, and to determine and emphasize critical frequency ranges in determining the approximations.

MIST provides two data-weighting options. The first weighting is a traditional normalization of the aerodynamic data to the maximum unit value of each aerodynamic coefficient. The second involves weighting the importance of different tabular values in determining the approximations based upon physical characteristics of the system. Specifically, the physical weighting capability is such that each tabulated aerodynamic coefficient, at each reduced-frequency value, is weighted according to the effect of an incremental error of this coefficient on aeroelastic characteristics of the system. In both cases, the resulting approximations yield a relatively low number of aerodynamic-lag states in the subsequent state-space model.

MIST is written in ANSI FORTRAN 77 for DEC VAX-series computers running VMS. It requires approximately 1 Mb of random-access memory for execution.

The standard distribution medium for this package is a 9-track, 1,600-bit/in. (630-bit/cm) magnetic tape in DEC VAX FILES-11 format. It is also available on a TK50 tape cartridge in DEC VAX BACKUP format. MIST was developed in 1991.

DEC VAX and VMS are trademarks of Digital Equipment Corp. FORTRAN 77 is a registered trademark of Lahey Computer Systems, Inc.

This program was written by Mordechay Karpel of National Research Council and Sherwood T. Hoadley of **Langley Research Center**. *For further information, Circle 72 on the TSP Request Card.*
LAR-14893

Space-Plane Spreadsheet Program

HYPERDATA provides data from three preliminary analyses of tentative design concepts.

In an effort to place payloads into orbit at the lowest possible costs, the use of air-breathing space planes, which reduces the need to carry the propulsion-system oxidizer, has been examined. Inasmuch as space planes would be required to fly at hypersonic speeds for times much greater than those required of rockets, many factors must be considered when analyzing the benefits of the space-plane approach. The Basic Hypersonic Data and Equations (HYPERDATA) spreadsheet computer program provides data gained from three analyses of the performance of a space plane. The equations used to perform the analyses are derived from Newton's second law of physics (i.e., force equals mass times acceleration); the derivation is included.

The first analysis is a parametric study of some basic factors that affect the ability of a space plane to reach orbit. Included in this step is a calculation of fraction, constituted by the fuel, of the total mass of the space plane at takeoff. The user can vary the altitude, the heating value of the fuel, the orbital gravitation, and the orbital velocity.

The second analysis includes a calculation of the thickness of a spherical fuel tank. For the purpose of this analysis, it is assumed that all of the mass of the vehicle (except that of fuel) is concentrated into the shell of the tank. This analysis provides a first-order estimate of how much material is required by a design in which the fuel represents a large portion of the total mass of the vehicle. In this step, the user can vary the values of gross weight, density of material (except fuel), and density of fuel.

The third analysis produces a ratio between the volume of fuel and the total mass for each of various aircraft. It shows that the volume of fuel per unit mass required for a liquid-hydrogen fuel is much larger than is the corresponding ratio for any other vehicle made.

HYPERDATA is intended for use on Macintosh-series computers running Microsoft Excel 3.0. The standard distribution medium for this package of software is a 3.5-in. (8.89-cm), 800K diskette in Macintosh format. Documentation is included in the price of the program.

Macintosh is a registered trademark of Apple Computer, Inc. Microsoft is a registered trademark of Microsot Corp.

This program was written by Dale Mackall of Dryden Flight Research Facility for **Ames Research Center**. *For further information, Circle 105 on the TSP Request Card.*
ARC-13185

Mathematics and Information Sciences

Interactive DIF Generator

This program serves as a specialized editing tool for directory interchange format files.

The Interactive DIF Generator (IDG) computer program serves as a utility to generate and manipulate directory interchange format (DIF) files. Its purpose as a specialized text editor is to create and update DIF files, which can be sent to NASA's Master Directory, also referred to as the International Global Change Directory at Goddard Space Flight Center. Many government and university data systems use the Master Directory to advertise the availability of research data.

The IDG interface consists of a set of four windows: (1) the IDG main window, (2) a text-editing window, (3) a text-formatting and -validation window, and (4) a file-viewing window. The IDG main window starts up the other windows and contains a list of valid keywords.

The keywords are loaded from a file designated by the user, and selected keywords can be copied into any active editing window. Once activated, the editing window designates the file to be edited. Upon switching from the editing window to the formatting-and-validation window, the user has options for making simple changes to one or more files; for example, inserting tabs, aligning fields, and indenting groups. The viewing window is a scrollable read-only window that enables fast viewing of any text file.

IDG is an interactive software tool and requires a mouse or a trackball to operate. IDG uses the X Window System to build and manage its interactive forms; it also uses the Motif widget set and runs under Sun UNIX.

IDG is written in C language for Sun computers running SunOS. This package requires the X Window System, Version 11 Revision 4, with OSF/Motif 1.1. IDG requires 1.8 Mb of hard-disk memory. The standard distribution medium for IDG is a 0.25-in. (6.35-mm) streaming-magnetic-tape cartridge in UNIX tar format. It is also available on a 3.5-in. (8.89-cm) diskette in UNIX tar format. The program was developed in 1991 and is a copyrighted work with all copyright vested in NASA.

SunOS is a trademark of Sun Microsystems, Inc. X Window System is a trademark of the Massachusetts Institute of Technology. OSF/Motif is a trademark of Open Software Foundation, Inc. UNIX is a trademark of Bell Laboratories.

This program was written by Larry E. Preheim, Laraine Amy, and Jimmie D. Young of Caltech for **NASA's Jet Propulsion Laboratory**. *For further information, Circle 34 on the TSP Request Card.*
NPO-18851

Mission-Clock-Display Software Tool

Displays that can include images of alarm clocks illustrate the temporal statuses of multiple events.

MCLK is a customizable clock-display computer program with a Motif user interface. The program can be used to keep track of such multiple "milestone" events as those that occur during countdowns in spacecraft launches, and can alert the user when an event time has been reached. In addition, the program can display time from several time zones. Real time is measured in Coordinated Universal Time.

All elements in the display window are completely movable. The software includes an object-oriented editor that enables a user to configure the display window interactively, with easy and fast on-screen editing capabilities. The program is unique in that it can be used to create such graphical objects as clocks and milestone alarm clocks that have specific, editable attributes. This program does not require computer expertise, and it is user-friendly.

MCLK is written in C language for computers of the Sun3 and Sun4 series. The MCLK source code requires X Windows Version 11 Revision 4 and the Motif 1.1 widget set to compile and run. The standard distribution medium for this program is a 0.25-in. (6.35-mm) streaming-magnetic-tape cartridge in UNIX tar format. It is also available on a 3.5-in. (8.89-cm) diskette in UNIX tar format. The program was developed in 1991 and is a copyrighted work with all copyright vested in NASA.

This program was written by Christine Aguilera, Susan C. Murphy, Kevin J. Miller, and Ana Maria P. Guerrero of Caltech for **NASA's Jet Propulsion Laboratory**. *For further information, Circle 71 in the TSP Request Card.*
NPO-18742

Software for Fault-Tree Diagnosis of a System

FTDS facilitates construction and use of fault trees.

When a system fails, it is necessary to determine the cause of the malfunction to restore the functional capacity of the system. The Fault Tree Diagnosis System (FTDS) computer program is an automated-diagnostic-system program that identifies the likely causes of a specified failure on the basis of information represented in system-reliability mathematical models known as fault trees. A fault tree is a graphical representation of the logical relationships among the components in a system. The structure of the tree describes how the system can reach an undesired state.

FTDS is a modified implementation of the failure-cause-identification phase of Narayanan's and Viswanadham's methodology for acquisition of knowledge and reasoning in analyzing failures of systems. The failure-cause-identification process outlined by Narayanan and Viswanadham is based on knowledge bases of if/then rules constructed directly from a fault-tree representation of the system to be diagnosed. In FTDS, the knowledge base of if/then rules has been replaced with an object-oriented fault-tree representation. This enhancement yields more-efficient identification of causes of failures and enables dynamic updating of the knowledge base.

FTDS can be run in several configurations: (1) the diagnosis software module in stand-alone mode, (2) the diagnosis module coupled with a graphical displayer, and (3) the graphical-display program running stand-alone. Software requirements vary according to which configuration is being used. When the diagnosis module is run in stand-alone mode, all input is entered via command lines, and results of the diagnosis are displayed in a list. In the second configuration, the command-line input is simplified since information about the system being diagnosed can be entered interactively via the displayer. In this mode, the forward and backward chaining processes and the results of the diagnosis can also be displayed graphically. In the third configuration, the diagnosis module has been run previously with the displayer to produce an output script, which is used as input to the graphical displayer. FTDS also includes the Tree Editor, which provides a graphical means of entering a fault tree and builds the input file to be used by FTDS automatically.

FTDS is written in C language, C++, and Common LISP for use on UNIX workstations. The diagnosis module itself requires Common LISP with Flavors extensions and foreign functions extensions. This module can be run on a variety of computers from a Mac II to a Sun SPARCstation, as long as the LISP programming environment is available. The two graphical utility programs that make the use of the diagnosis module much easier (Displayer and Tree Editor) require LEX, X11 release 4, Interviews 2.6, and Gnu C++ 1.37. A color monitor is recommended. The standard distribution medium for FTDS is a 0.25-in. (6.35-mm) streaming-magnetic-tape cartridge in UNIX tar format. It is also available on a 3.5-in. (8.89-cm) diskette in UNIX tar format. FTDS was developed in 1991.

UNIX is a registered trademark of AT&T Bell Laboratories. Sun and SPARCstation are trademarks of Sun Microsystems, Inc. X Windows System, Version 11 is a trademark of MIT.

This program was written by Dave Iverson and Ann Patterson-Hine of **Ames Research Center** *and Jack Liao of the University of California, Santa Cruz. For further information, Circle 42 on the TSP Request Card.*
ARC-13019

Mechanics

Conjugate-Gradient Algorithms for Dynamics of Manipulators

Fast serial and parallel algorithms are being developed.

NASA's Jet Propulsion Laboratory, Pasadena, California

Algorithms for serial and parallel computation of the forward dynamics of multiple-link robotic manipulators by the conjugate-gradient method are being developed. The parallel algorithms, especially, have potential for the speedup of computations on multiple linked, specialized processors that could be implemented in very-large-scale integrated circuits. Such processors would be used to simulate dynamics, possibly faster than in real time, for purposes of planning and control. For example, a human operator could view planned motions of a robot shortly before commanding the robot to execute them.

The forward-dynamics problem is to compute the joint accelerations, given the vectors of joint positions and velocities and the forces and torques applied to them. The conjugate-gradient method of solving this problem has been described in previous articles in *NASA Tech Briefs*. In summary, the conjugate-gradient method is an iterative-optimization method in which the solution is found by descent in an abstract n-dimensional space (where n is the number of degrees of freedom of the manipulator) along the gradient of an objective function, the minimum of which represents the global optimum and the solution.

The particular version of the conjugate-gradient method that is favored for the developmental algorithms is called the diagonal-scaling, preconditioned-conjugate-gradient (DS-PCG) method. Preconditioning is needed to reduce the number of iterations sufficiently to make the conjugate-gradient method competitive with or superior to other methods in parallel computation of forward dynamics. Preconditioning in general is effected via matrix multiplications. In the DS-PCG method, the preconditioning matrix is a positive definite diagonal matrix composed of the diagonal elements of the mass matrix.

The theoretical foundation of the DS-PCG method has been established and analyzed by use of a modified Newton–Euler formulation of the dynamics. This formulation incorporates the concept of an augmented body, which is a subchain of manipulator links treated as a composite rigid body for the purposes of some of the equations that appear in the dynamical algorithms. This formulation is highly efficient for both serial and parallel computation.

The theoretical analysis shows that DS-PCG algorithms offer an efficient alternative for the computation of the dynamics of multiple-rigid-link manipulators when implemented on a number (of the order of n) of processors. The table presents some of the results of the analysis, showing the number of computations required in DS-PCG and a few other algorithms. In addition, the architectural features (regarding interconnections and communications among processors) of computing systems needed to implement the DS-PCG algorithms were analyzed: The DS-PCG algorithms were found to involve simple requirements with respect to synchronization and communication (see figure), and thus to be particularly suitable for implementation in very-large-scale integrated circuitry.

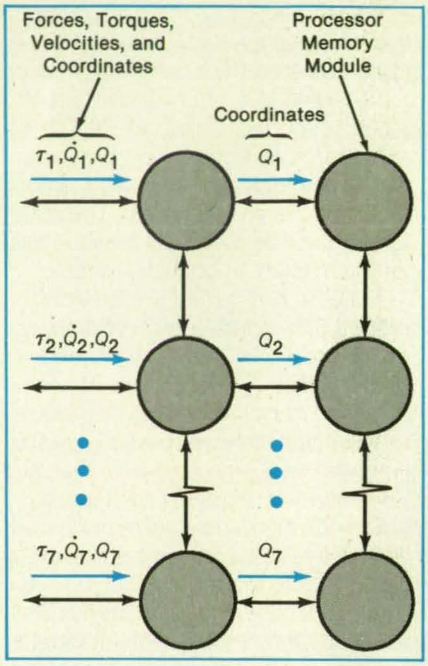

A **Simple Linear Array** of seven processors can implement a DS-PCG algorithm for parallel computation in the case $n = 7$.

This work was done by Amir Fijany and Robert E. Scheid of Caltech for **NASA's Jet Propulsion Laboratory**. *For further information, Circle 78 on the TSP Request Card. NPO-18567*

Algorithm		Cost of Computation: Number of Arithmetic Operations — In General	$n = 7$	Number of Processors	Speedup Factor
Serial	Prior Algorithm Without Explicit Computation and Inversion of Mass Matrix	$682n - 371$	4,403	1	—
	Prior Algorithm With Explicit Computtion and Inversion of Mass Matrix	$(1/3)n^3 + (43/2)n^2 + (2,149/6)n - 113$	3,562	1	—
	DS-PCG Algorithm	$77n^2 + 368n - 99$	6,390	1	—
Parallel	Prior Algorithm With Explicit Computtion and Inversion of Mass Matrix	$5n + 81\lceil \log_2 n \rceil + 409$	687	$n(n+1)/2$	6.4
	Classical (Not Preconditioned) Conjugate-Gradient Algorithm	$14n\lceil \log_2 n \rceil + 79n + 61\lceil \log_2 n \rceil + 211$	1,241	n	3.5
	DS-PCG Algorithm	$7n\lceil \log_2 n \rceil + 29n + 60\lceil \log_2 n \rceil + 301$	831	$2n$	5.3

The **Costs of Computation and Relative Speeds** of several algorithms were analyzed theoretically.

Flexure Test for Off-Axis Unidirectional Composites

Undesired torques are eliminated by use of rotatable mounts.

Langley Research Center, Hampton, Virginia

An improved flexure test yields data on the ply strength of an off-axis unidirectional composite material. "Ply Strength" denotes loosely the levels of multiaxial stresses that cause ply cracks: In a typical structure under load, ply cracks develop under the combination of a tensile stress perpendicular to the fibers and a shear stress parallel to the fibers. The improved flexure test helps to determine the combined effect of these two stresses. Ply-stength data provide a basis for predicting the onset of damage in composite structures and serve as a measure of the fiber-matrix adhesion.

Heretofore, little testing has been done to measure ply strengths under multiaxial stresses. Some older tests have used off-axis tension specimens that are limited by stress-concentration problems caused by end-grip restraint. Other tests have used expensive tubular specimens, which are also subject to grip-restraint problems. Attempts to test off-axis specimens under bending loads have been complicated by the bending-twist phenomenon. This phenomenon gives rise to twisting torques and eccentric loads that generate complicated nonuniform stresses, which are difficult to analyze and are unsuitable for characterization of ply strength.

The improved flexure test (see figure) is an updated version of the three-point bending test. Specimens are cut from a unidirectional composite laminate (the fibers in all plies lie along the same direction) with the fibers oriented at an angle, a, with respect to the longitudinal beam axis. Each specimen is loaded in three-point bending with a downward force, P, applied at its midlength and upward reaction forces of $P/2$ applied near its ends, at distances $L/2$ from the midlength.

A loading nose prevents rotation of the specimen about its longitudinal axis at midlength, but the end loads are applied via ball-bearing mounts that allow the ends to twist freely about the longitudinal beam axis. Thus, the end supports react to the bending load without introducing the undesired twist-resisting torques, and the spot where the specimen starts to crack (bottom surface at midlength) is subjected to stresses attributable to simple bending.

Under these conditions, the ply strength of the off-axis specimen can be computed by use of the measured failure load in the elementary beam-theory equation, followed by transformation of the stresses thus computed into tensile stress perpendicular and shear stress parallel to a plane that contains the fiber direction. By repeating the tests and computations for specimens with various fiber angles, α, one can obtain ply-strength data for a variety of stress states.

This work was done by John H. Crews, Jr., of **Langley Research Center** *and Rajiv A. Naik of Analytical Services and Materials, Inc. Further information may be found in NASA TM-107570 [N92-24880], "Measurement of Multiaxial Ply Strength by an Off-Axis Flexure Test."*

Copies may be purchased [prepayment required] from the National Technical Information Service, Springfield, Virginia 22161, Telephone No. (703) 487-4650. Rush orders may be placed for an extra fee by calling (800) 336-4700.
LAR-14770

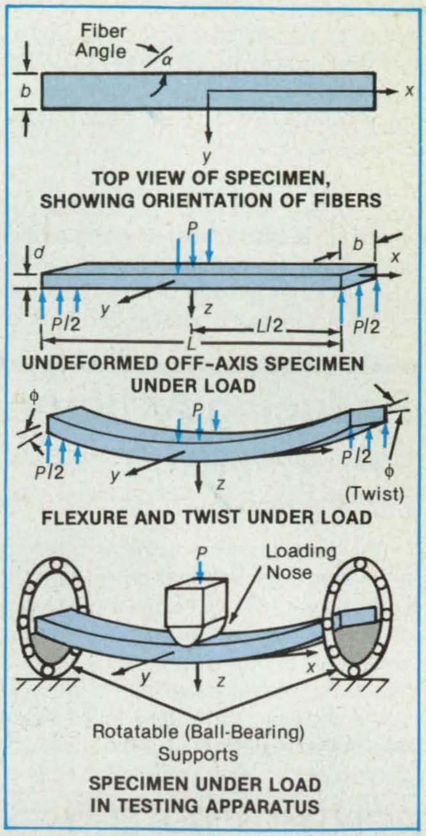

Rotatable End Supports allow the ends of the specimen to twist freely. Thus, the end supports apply only vertical loads, making this a simple three-point bending test.

Estimating Wear of Installed Ball Bearings

It is not necessary to remove bearings from machinery.

Marshall Space Flight Center, Alabama

A simple inspection and measurement technique makes it possible to estimate wear of balls in a ball bearing, without removing the bearing from the shaft on which it is installed. To perform the measurement, one observes the bearing cage (typically, through a borescope) while turning the shaft by hand to obtain an integral number of cage rotations and to measure, to the nearest 2°, the number (whole plus fractional) of shaft rotations that produced the cage rotations. The ratio between the numbers of cage and shaft rotations (the "turns" ratio) depends only on the internal geometry of the bearing and the applied load. Changes in the turns ratio reflect changes in the internal geometry of the bearing (for example, in the balls and raceway), provided that the measurements are made with similar bearing loads. By assuming that all wear occurs on the balls, one can compute an effective value for this wear from a change in the turns ratio.

To ensure accurate measurement of rotation of the cage, an index is marked on the cage at assembly and observed in alignment with a serial number, prominent surface scratch, or other distinguishing mark on an adjacent stationary surface: this approach enables the measurement of whole turns to an accuracy of several degrees. To ensure accurate measurement of fractional turns of the shaft, a sheet of polar graph paper is affixed to the stationary housing of the machine that contains the bearing, concentric with the shaft. The angle of rotation of the shaft is then measured against an index mark on the shaft or on a tool used to rotate the shaft.

The accuracy of the measurement is increased by increasing the number of turns of the cage for use in calculating the turns ratio. The measurement should also be checked by rotating the shaft in the opposite direction after an initial measurement and verifying that the cage and shaft return to their initial angular positions.

The turns ratio is given by the following equation, which is taken from *Rolling Bearing Analysis*, 3d edition, pages 205-211, by Tedric A. Harris:

$$\frac{N_c}{N_s} = ½\left[1 + \frac{d}{E}\cos(\beta)\right]$$

where N_c is the number of turns of the cage, N_s is the number of turns of the shaft, d is the diameter of a ball, E is the pitch diameter of the bearing, and β is the contact angle of the bearing under the applied load. The contact angle is an implicit function of the internal geometry of the bearing (internal clearance, curvature of the raceway, d, and E) and the applied load. This equation is used in the following way to compute ball wear from a change in the turns ratio:

1. The turns ratio is measured on a new installed, preloaded bearing.
2. The internal clearance of the new bearing is estimated by guessing and iteration: Whichever value of internal clearance, when used in the equation along with the known nominal values of the internal geometry of the bearing (d, E, and curvature of the raceway), gives the observed turns ratio is deemed to be the "as-installed" internal clearance.
3. The machine that contains the bearing is operated for the requisite time.
4. The turns ratio of the bearing is measured. If the turns ratio has changed, then a new internal clearance is calculated as in step 2 (because E and the curvature of the raceway are assumed to remain constant and all wear is assumed to manifest itself as a change in the effective value of d, with concomitant change in calculated internal clearance).

This work was done by John E. Keba and Scott E. McVey of Rockwell International Corp. for **Marshall Space Flight Center**. *No further documentation is available.*
MFS-29900

Reducing Airborne Debris in Wind Tunnels

Expendable adhesive material would trap airborne particles.

Langley Research Center, Hampton, Virginia

The wind in a wind tunnel is required to be free of debris that could damage such devices as hot-wire and hot-film anemometers. One way to determine the amount of debris is to install a strip of double-backed adhesive tape in the wind tunnel and examine the tape for collected debris after testing. Such debris can consist of dust, dirt, trash, paint flakes, oil droplets, and insulation. In the past, large tunnels have been cleaned manually with brushes and mops, but this practice can require elaborate equipment and labor and can detract significantly from the time available for operation of the wind tunnels.

In a proposed technique to trap the airborne particles during normal wind-tunnel testing, large sections of single-backed adhesive paper or cloth would be mounted with the adhesive side exposed to the flow (see figure). One suitable material of this type might be the material used to capture insects or small rodents. The adhesive material would be securely installed on the flow vanes, walls, or other surfaces of the wind tunnel in a manner that would facilitate replacement. The adhesive material could be installed or replaced anytime it was permissible to enter the tunnel.

This technique would provide a safe, inexpensive, rugged, passive, continuous, and otherwise inert cleansing action suitable for a wind tunnel of any size. As such,

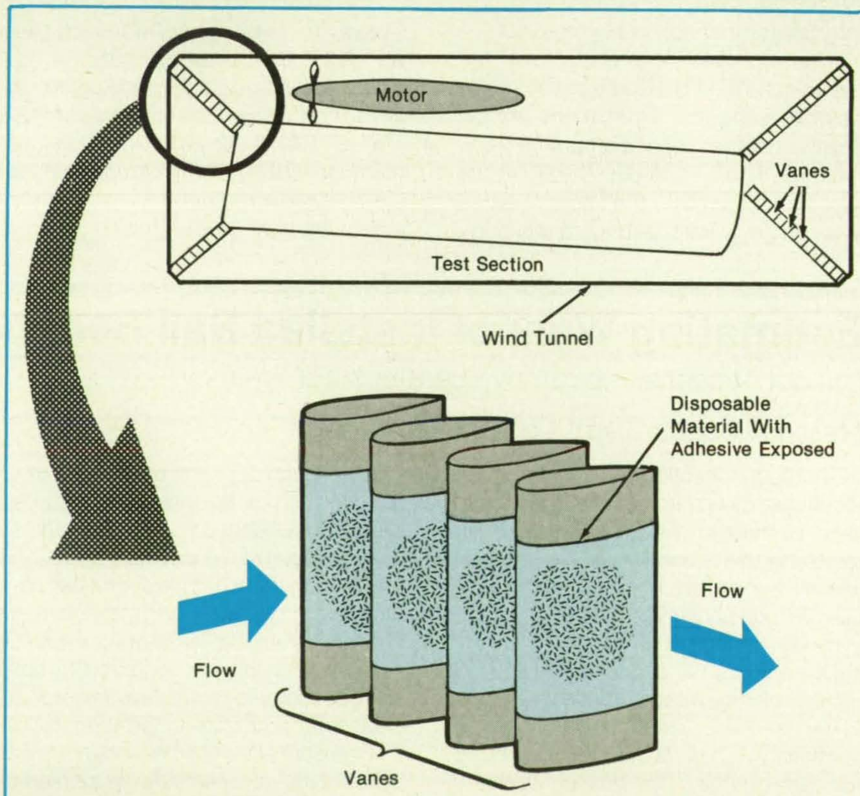

Disposable Adhesive Material would be attached to flow-turning vanes and other appropriate surfaces to collect airborne particles.

it would be a very simple solution to a very significant problem. In addition to its intended use in wind tunnels, this method could be applied to specialized clean-room environments and to air-conditioning systems in general.

This work was done by Robert K. Sleeper of Langley Research Center. No further documentation is available.

This invention is owned by NASA, and a patent application has been filed. Inquiries concerning nonexclusive or exclusive license for its commercial development should be addressed to the Patent Counsel, Langley Research Center [see page 24]. Refer to LAR-14358

Compensating for Shrinkage in a Cryogenic Seal

Part of the seal would expand while the rest contracted.

John F. Kennedy Space Center, Florida

A proposed design for seals in liquid-hydrogen plumbing may eliminate those leaks that are caused by contraction of the seals at the low operating temperature. Each seal would consist of a rubber, polytetrafluoroehtylene, or lead O-ring that included a hollow core filled with water. (see figure).

Water in its frozen state is one of the few materials that expands with decreasing temperature. Thus, at the temperature of liquid hydrogen, the anomalous expansion of water would keep the seal gland filled and leaktight despite the shrinkage of the surrounding O-ring material. This design could also be used in systems using cryogenic fluids other than liquid hydrogen.

This work was done by Arnold E. Hill of Lockhead Space Operations Co. for Kennedy Space Center. No further documentation is available.

Inquiries concerning rights for the commercial use of this invention should be addressed to the Patent Counsel, Kennedy Space Center [see page 24]. Refer to KSC-11555.

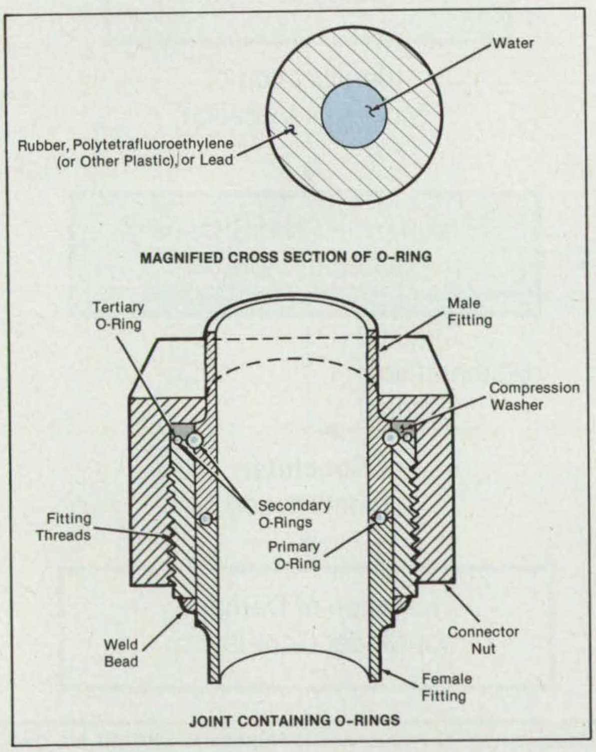

Hollow O-rings would contain distilled water. In this example, O-rings are positioned to provide three stages of protection against leakage.

Locating Damaged Truss Members From Responses to Vibrations

Experiments were performed on a scale-model truss structure to demonstrate this method.

Langley Research Center, Hampton, Virginia

Researchers involved in the development of structures to be placed in orbit are considering many issues, including on-orbit assessment of integrity. On-orbit assessment can be accomplished by use of information on dynamic responses through structural identification methods, which produce adjusted mathematical models, followed by model-correlation techniques, which locate any damage. In previous computer simulation studies of this method of locating damage in a structure, an optimal update o fhte mathematical model of the structure was formed by use of the response data then examined to locate damaged members.

The method of on-orbit assessment for location of damage is based on the use of capabilities of a vibration-control system to measure vibrations in the structure. In the present studies, an experiment was designed to demonstrate

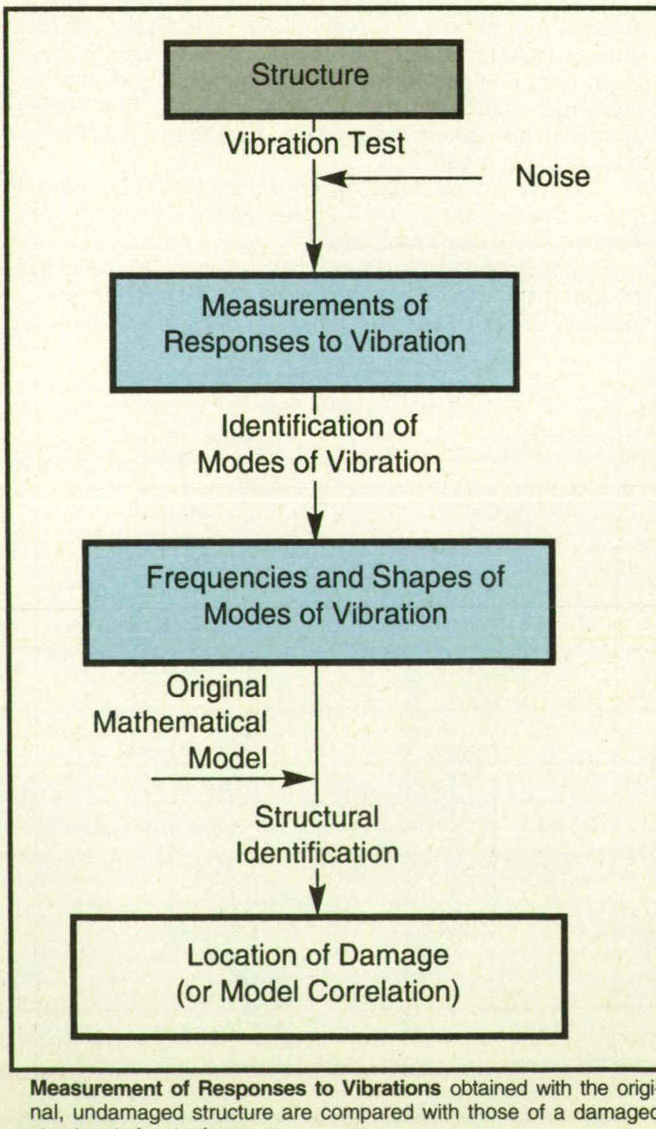

Measurement of Responses to Vibrations obtained with the original, undamaged structure are compared with those of a damaged structure to locate damage.

and verify this method. This experiment involved the use of a laboratory scale-model truss structure that exhibited expected characteristics of truss structures proposed for large spacecraft. This laboratory structure was one in a series designed for research into dynamic scale-model ground testing of space structures at NASA Langley Research Center.

The structure was 10 bays long, cantilevered, with a mass attached at its tip. Vibrations were excited in the truss, and measurements of the responses of this structure were used in a series of two identification algorithms to produce a mathematical model of the structure in its current condition, possibly containing damage. The model was compared with one obtained previously from the same structure in its undamaged condition to find regions of reduced stiffness, which indicate locations of damage. In the context of this study, a "damaged" structure was one from which a member was removed entirely. However, this method also applies to cases in which truss members become less stiff but remain intact.

The figure is a flow chart that illustrates the method. The key identification algorithm, labeled "Structural Identification," produces an optimally adjusted stiffness matrix for the structure by use of an original mathematical model and data on modes of vibration. Then the damage-location algorithm, which uses graph theory for matrices, finds any region(s) of reduced stiffness, thereby locating the damaged member(s).

Research on this method has been limited, thus far, to truss structures. The method is a new, valuable means for locating damage in a structure by examining vibrations. It could be applied generally, and similar methods are being considered for other significant endeavors such as examining buildings for damage by earthquakes.

This work was done by S. W. Smith of Virginia Polytechnic Institute & State University and P. E. McGowan of **Langley Research Center**. *Further information may be found in NASA TM-101595 [N89-23924], "Locating Damaged Members in a Truss Structure Using Modal Data: A Demonstration Experiment."*

Copies may be purchased [prepayment required] from the National Technical Information Service, Springfield, Virginia 22161, Telephone No. (703) 487-4650. Rush orders may be placed for an extra fee by calling (800) 336-4700.

LAR-14407

Characterizing Mode-I Fatigue Delamination of Laminates

The number of cycles to the onset of delamination is monitored.

Langley Research Center, Hampton, Virginia

The double-cantilever-beam (DCB) specimen (see figure) has been used previously to characterize fatigue delamination by relating the rate of growth of delamination, da/dN, with the applied cyclic strain-energy-release rate, G, by use of a power law. Because of both a high exponent in this power law and fiber bridging, this characterization technique has serious limitations.

An alternative method has been proposed for characterizing mode-I fatigue delamination by use of the DCB. In the new method, one monitors the number of cycles, N, to the onset of delamination from the end of a thin insert. Thus, fiber bridging is avoided. Results are presented easily in the form of a G-vs.-N plot.

One uses the threshold value of strain-energy-release rate, G_{th}. By testing several specimens at cyclic strain-energy-release rates above the threshold value, it is possible to obtain a complete G-vs.-N curve for the onset of delamination.

The method was demonstrated on specimens of two materials: a glass/epoxy and a graphite/epoxy, which are typically used in rotorcraft applications. The individual DCB specimens, cut from a panel of each material, had 24 plies, which were sufficient to prevent any geometric nonlinearities while testing. Prior to final curing during the preparation of each specimen, a Kapton® polyimide film sprayed liberally with a release agent (to prevent subsequent adhesion) was inserted at the midplane of the specimen. The load was applied through hinge tabs adhesively bonded to the surfaces of each specimen. The hinge tabs were cut from a stock aluminum piano hinge and were bonded by use of a commercially available adhesive.

The edges of the specimen in the vicinity of the insert end were coated in a thin layer of brittle white typewriter-correction fluid to ease observation of the onset of delamination. Because the end of the insert was difficult to locate in an unloaded specimen, the approximate location was marked on the edge of each specimen. The initial delamination length was approximated by measuring from the centerline of the hinge pin to the mark on the edge. A microscope with a magnification of approximately 60 was used to visually determine the onset of delamination.

Each specimen was installed in the test stand, and pertinent readings and settings were adjusted to zero. then, the mean load was applied, and the microscope was used to locate accurately the end of the insert. The fatigue test was then started. the onset of delamination was detected by visual examination and/or by monitoring the displacement. Upon detection of the onset of delamination, the number of elapsed cycles was noted, and the specimen was removed. After testing, the initial delamination length was remeasured. Between 15 and 20 specimens were tested to obtain a G-vs.-N plot, with the number of cycles to the onset of delamination ranging between 10^3 and 2×10^6.

Because there is a certain amount of scatter in the experimental data, one could predict a range of possible fatigue lives rather than a single value. To take a conservative approach to the prediction of the fatigue lives of components, one should use the lower curve derived from the data. then, for example, one could design a structure such that the individual modes of strain-energy-release rate calculated for an initial delamination in a component would never exceed its G_{th}.

This work was done by Roderick H. Martin of the National Research Council and T. Kevin O'Brien of the U.S. Army Aerostructures Directorate for ***Langley Research Center****. for further information,* Circle 60 *on the TSP Request Card. LAR-14414*

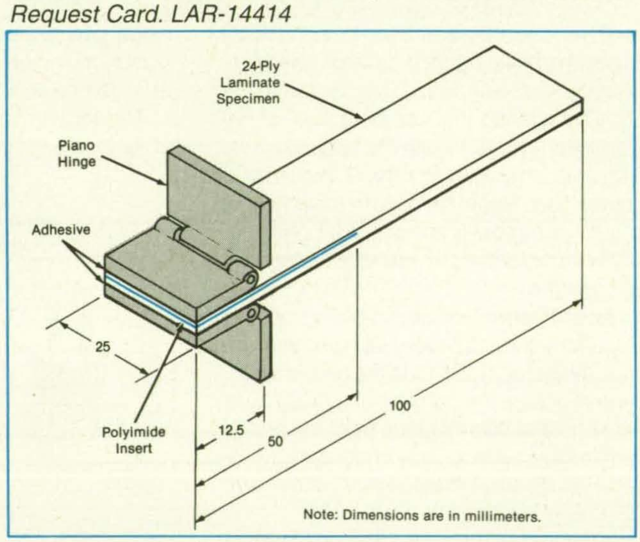

The Double-Cantilever-Beam Specimen, held in place with piano hinge, is monitored for onset of delamination.

Spiral Flow Separator

Separation would be effected at a high rate of continuous flow.

Marshall Space Flight Center, Alabama

A proposed liquid-separating device would rely on centrifugal force in a liquid/liquid or liquid/solid mixture in a spiral path. At present, centrifugal separation of such mixtures is done in small batches, which are spun in containers; consequently, rates of processing are low. In contrast, the proposed device would operate in continuous flow at relatively high rates.

The centrifugal force (in the reference frame moving with the liquid mixture) would push denser particles or liquids to

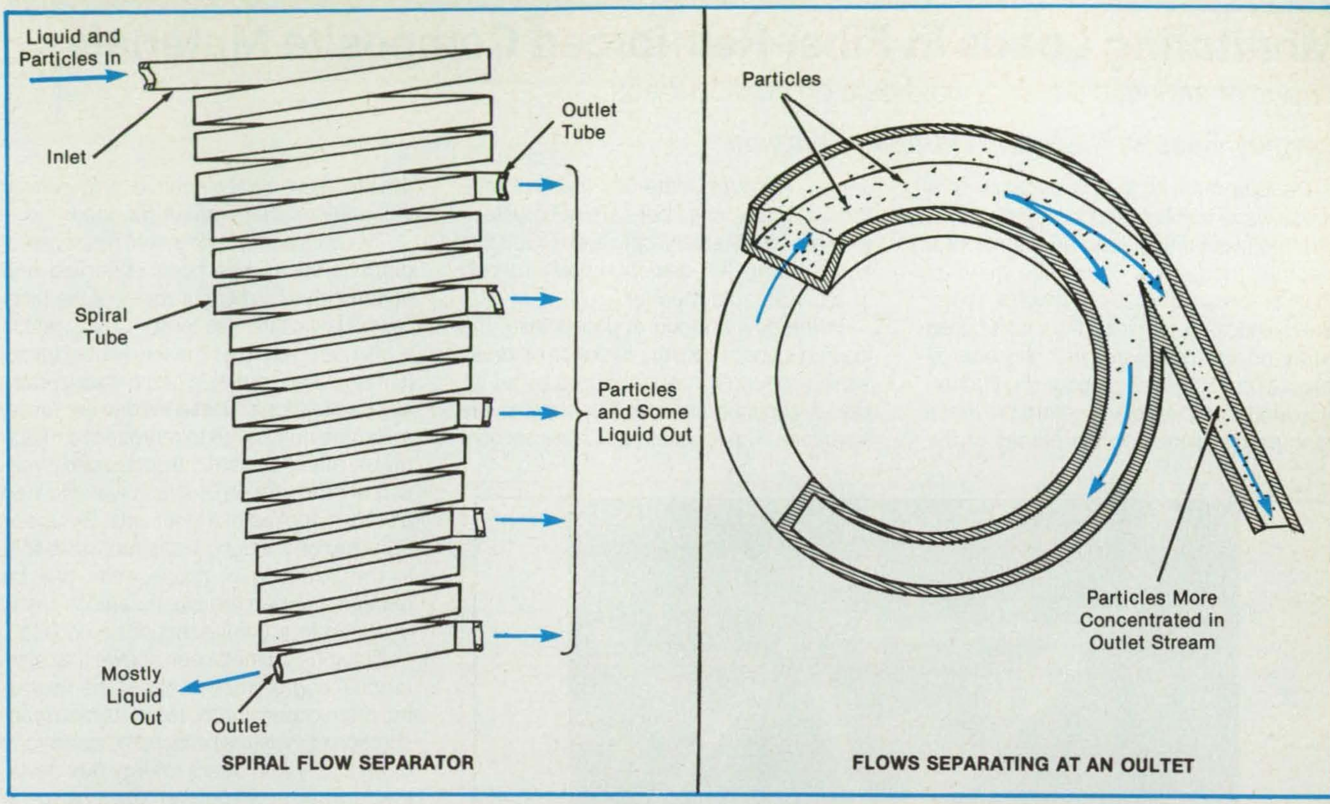

Spiral Tubes would be joined in sequence, with outlet tubes connected to the joints. The cross-sectional areas of successive spiral tubes would decrease by the cross-sectional areas of the outlet tubes.

the outer edge of the spiral, where they could be removed from the flow. This principle could be exploited to separate solids from wastewater, oil from fresh or salt water, or contaminants from salt water before evaporation, for example. It could also be used to extract such valuable materials as precious metals from slurries.

Several spiral tubes with progressively decreasing cross-sectional areas would be connected in series (see figure). At each junction between successive spirals, an outlet on the outer edge would divert the part of the flow that contained the denser particles and/or liquid(s). The flow remaining in the spiral would thus become progressively cleaner.

The diameters of the spirals would be decreased or increased to increase or decrease, respectively, the centripetal and centrifugal forces at a given flow speed to suit the mixtures of materials. The cross-sectional areas of the tubes would be selected to accommodate the expected rates of flow.

This work was done by Glen A. Robertson of **Marshall Space Flight Center**. *For further information, Circle 74 on the TSP Request Card.*

Inquiries concerning rights for the commercial use of this invention should be addressed to the Patent Counsel, Marshall Space Flight Center [see page 24]. Refer to MFS-28658.

Monitoring Loads in Fiber-Reinforced Composite Materials

Arrays of acoustic sensors yield data on applied loads.

Langley Research Center, Hampton, Virginia

Measurement of the propagation of a stress wave can be used to determine, in situ, the mechanical load on a structural member made of a composite material such as epoxy reinforced by graphite fibers. The method of determining the load is based partly on the discovery that the energy fluxes of stress waves propagating through anisotropic crystals deviate from the directions perpendicular to the planes of the waves. Although materials that are reinforced by graphite fibers are not crystals, they are highly anisotropic and exhibit this same energy-flux-deviation phenomenon in a predictable manner.

In the new method of determining the load on a specimen, the direction of stress wave propagation is measured by an array of acoustic sensors attached to the specimen. The responses of these sensors are then analyzed by strain-energy-density calculations to calculate the load.

The nonlinear mechanical response of graphite/epoxy has been observed and documented by measurement of the sixth-order elastic stiffness tensor C_{ijklmn}, which is also referred to as the third-order terms (strain-cubed terms) in strain-energy-density calculations. These third-order terms are sufficiently large to represent a measurable effect on both the speed and direction of propagation of stress waves when a load is applied along an axis. By use of an array of acoustic transducers, a shift in the direction of propagation can be measured when the elastic anisotropy is changed in a unidirectional composite.

Previously, it had been shown that preferential degradation of either the fiber or the matrix constituents (such as matrix absorption of moisture) affects the anisotropy of elasticity and alters energy flux deviation. In the new method, the change in anisotropy of elasticity is caused by an applied load and a corresponding induced strain. Therefore, the method is a means to monitor an applied load that corresponds to a measurable shift in the direction of propagation of a stress wave.

Such graphite-fiber-reinforced composites as graphite/epoxy, graphite/magnesium, and graphite/aluminum, exhibit very high stiffness-to-weight and strength-to-weight ratios. They are excellent materials for lightweight aerospace structures. Because the main purpose of these materials is to carry loads, the new method can be particularly useful for in situ monitoring of the loads applied to them. Indeed, a monitoring device based on this method can be made an integral part of an airframe in which a unidirectional section of the structure, such as a spar cap or longeron, carries a primary load.

This work was done by William H. Prosser of **Langley Research Center** *and Ronald D. Kriz and Dale W. Fitting of the National Institute of Standards and Technology. For further information, Circle 23 on the TSP Request Card.*

This invention is owned by NASA, and a patent application has been filed. Inquiries concerning nonexclusive or exclusive license for its commercial development should be addressed to the Patent Counsel, Langley Research Center [see page 24]. Refer to LAR-14399.

Stirling Engine With Radial Flow Heat Exchangers

A conflict between thermodynamical and structural requirements is resolved.

Lewis Research Center, Cleveland, Ohio

In a Stirling engine of a new cylindrical configuration, the flow of heat is predominantly radial rather than predominantly axial as in prior Stirling engines with cylindrical configurations. The new radial-flow configuration resolves an engineering conflict between thermodynamical and structural requirements that arises when attempting to scale up an axial-heat-flow engine to higher power: thermodynamics requires a short, wide regenerator (one of several heat-exchange units), while structural considerations require a long, narrow regenerator.

In the new configuration (see figure), the regenerator and the acceptor and rejector heat exchangers channel the flow of the working gas in the radial direction. As a consequence, the isotherms in the regenerator are ideally concentric cylinders (rather than axially spaced disks), and the gradient of temperature across the regenerator is radial rather than axial. The acceptor and rejector heat exchangers are located radially inward and outward of the regenerator, respectively.

The radial configuration makes it possible to increase the heat-exchange area of the regenerator by increasing the axial length of the regenerator rather than by increasing its diameter. This enables a substantial increase in the power of the engine without a corresponding increase in the diameter of its pressure vessel. For example, in one case, the radial-flow configuration made it possible to design a high-frequency free-piston Stirling engine (70 Hz, helium working gas) capable of an output power of 150 kW — about three times the power of an annular, axial-flow-regenerator Stirling engine designed under similar constraints.

As shown in the lower part of the figure, the acceptor heat exchanger consists of axially oriented heat pipes arranged in concentric rows. The heat pipes enter the pressure vessel of the engine at the "front" of the engine close to the centerline. This is the only part of the pressure vessel that must be hot. As a consequence, in the new configuration, the amount of hot material in the pressure vessel is limited, and the hot material is located close to the center-

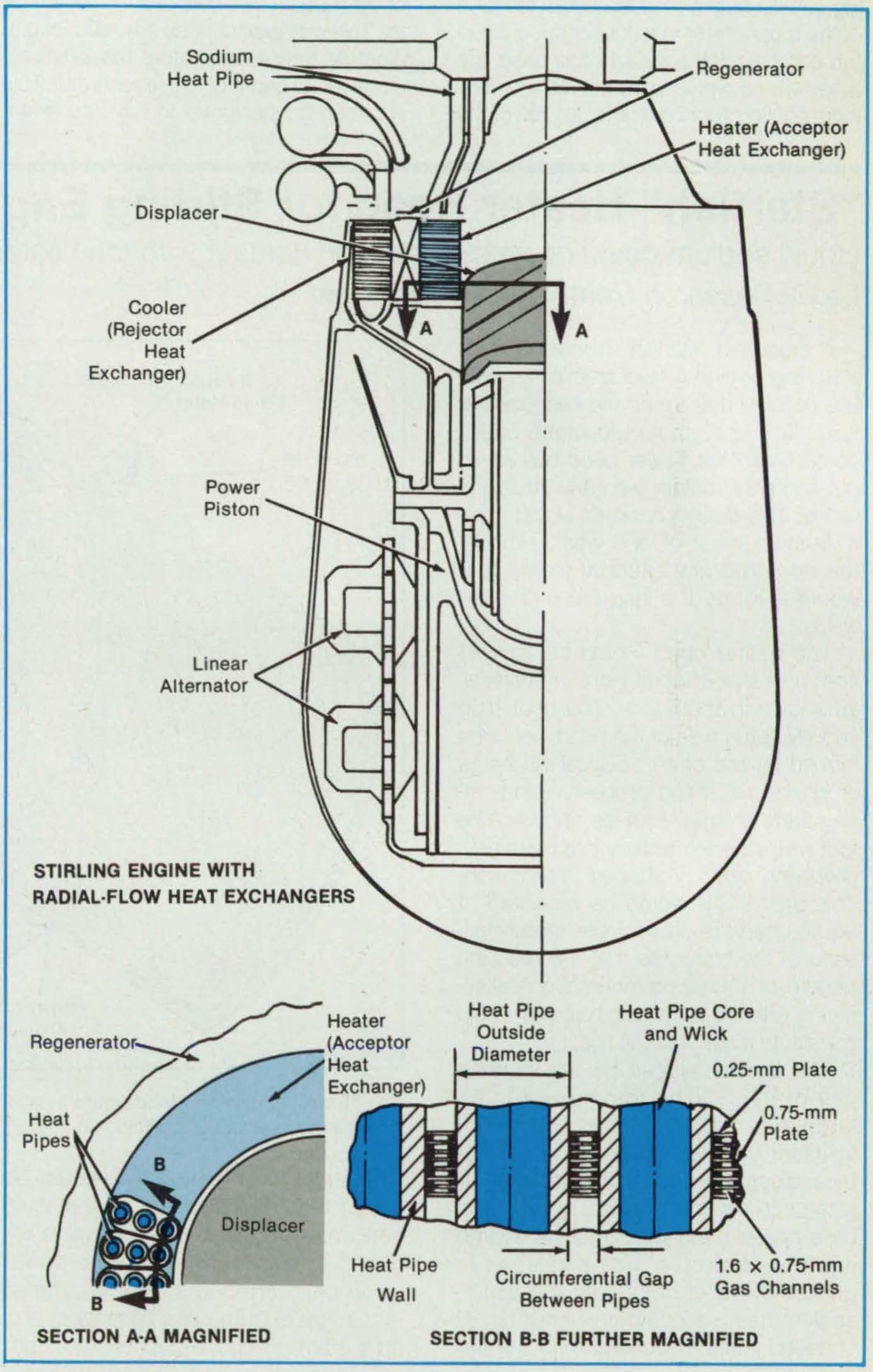

A **Stirling Engine With Radial-Flow Heat Exchangers** is more readily scalable to higher power.

line, where the stresses induced by pressure are lowest. This enables a reduction in the overall weight of the engine and in the amount of expensive high-creep-strength alloy required in the pressure vessel. The outside surface of each heat pipe is in contact with the working fluid and is finned to reduce the drop in temperature and increase the transfer of heat between the heat pipe and the working fluid.

The rejector heat exchanger can be a set of tubes oriented radially, with the working gas flowing in the tubes from the face of the regenerator to a duct connecting to the compression space. In this case, the tubes would typically be cooled by passing a cooling liquid over the outside of the tubes by means of a suitable cooling jacket surrounding the bundle of tubes and separating this coolant from the working gas. Alternately, the coolant could be made to flow in axially oriented tubes. In this case, the outside of the tubes would typically be finned to increase the transfer of heat between the working fluid and the coolant tubes so as to reduce the drop in temperature between the working gas and the surfaces of the tubes.

One important consideration is the wall of the module that contains the regenerator. This wall experiences a significant gradient of temperature over the relatively small radial depth of the regenerator. This wall can be designed to have sufficient flexibility to accommodate the consequent thermal growths, and sufficient strength to support the stresses induced by the periodic variation of the pressure of the working gas. The wall consists of a number of concentric cylindrical shells welded together at alternating ends in the radial direction. Finite-element stress analysis of the resultant structure indicates that it can accommodate both the oscillating pressure stress and the thermal stresses.

This work was done by N. Vitale and George Yarr of Mechanical Technology, Inc., for **Lewis Research Center**. *For further information, Circle 9 on the TSP Request Card.*
LEW-15112

"Starfish" Heater Head for Stirling Engine

Liquid sodium could be safely placed in contact with the heater head.

Lewis Research Center, Cleveland, Ohio

A proposed "starfish" heater head for a Stirling engine would enable the safe use of liquid sodium as the heat-transfer fluid. The sodium would make direct contact with the heater head but would not come in contact with any structural welds. This design concept would minimize the number of, and would simplify, the nonstructural thermal welds and would facilitate the inspection of such welds.

The heater head would be formed from a washer-shaped blank of material, as shown in the figure. The heat-pipe (radially outer) side of the head would be formed by use of an electrical-discharge or similar machining process, with a triangularly shaped tool as shown. The tool would be fed radially into the blank, hollowing out a V-shaped indentation. This procedure would be repeated at equal intervals around the circumference of the blank, so that the resulting pattern of V-shaped indentations alternating with the remaining material would constitute a set of radial fins.

The flow passages for the working gas of the Stirling engine would be formed by STEM (shaped tube electro-chemical machining) drilling or electrical discharge-machining holes axially through the fins. The final result would be a heater head that contains a large number of circular gas passages in good thermal contact with the liquid-sodium heat source but without highly stressed joints in contact with the liquid sodium.

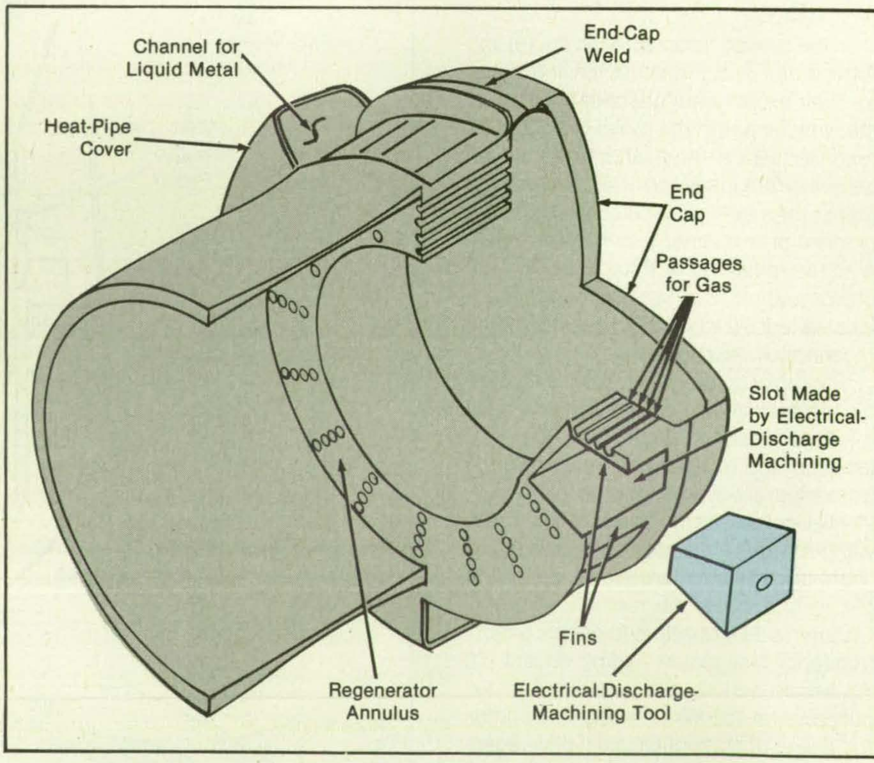

The **"Starfish" Heater Head** would enable the use of sodium as the heat-transfer fluid in a heat pipe connected to a Stirling engine.

An outer heat-pipe cover would be added to form a passage for the liquid sodium. An annular Stirling-engine regenerator and a Stirling-engine cooler could be inserted to the left (as shown in the figure) of the gas passages, and an expansion-space cap or an identical opposed-piston engine could be welded on the right end.

This work was done by N. Vitale of Mechanical Technology Inc. for **Lewis Research Center**. *For further information, Circle 3 on the TSP Request Card.*
LEW-15064

Portable Lifting Seat

This briefcase-size unit is easy to operate.

Marshall Space Flight Center, Alabama

A portable lifting machine assists a user in rising from a seated position to a standing position, or in sitting down. It is small and light enough to be easily carried like a briefcase. It can be used on a variety of chairs and benches.

The machine contains a battery-powered dc motor, which drives a gear-train-and-crank assembly. The gears and cranks are designed to effect motion along a path that closely approximates that of natural standing and sitting. This path is higher than that of an older spring-powered lifting seat. The machine is also easier to refold after standing: the user simply reverses the motor to return the mechanism to its compact stowed configuration. In contrast, a spring-driven unit is held open by the spring until someone closes it by sitting on it. This arrangement is inconvenient for the user, who may have to call upon an assistant to close the unit. Moreover, a spring-driven lift is largely uncontrolled when released, while the motion of the motor-driven unit can be controlled by turning the motor on and off.

The motor-driven lift includes two main bodies: an upholstered seat and a base that contains the electromechanical components (see figure). The gear-train-and-crank assembly includes inner and outer shaft-and-arm subassemblies with integral spur gears that mesh with each other. The motor drives a worm gear, which drives a lead screw, which drives a slider, which drives a pair of crank arms, which rotate the outer shaft-and-arm subassembly. Because of the meshing of the gears between the two subassemblies, the rotation of the outer arms is accompanied by opposite rotation of the inner arms.

The outer ends of the outer arms ride along tracks on the underside of the seat. The inner arms are hinged to the underside of the seat. The resulting motion of the seat is a combination of translation and rotation away from or toward the base along the desired path. The user operates the motor with a three-position switch (raise, stop, and lower).

This work was done by Bruce Weddendorf of **Marshall Space Flight Center**. *For further information, Circle 44 on the TSP Request Card.*

Inquiries concerning rights for the commercial use of this invention should be addressed to the Patent Counsel, Marshall Space Flight Center [see page 24]. Refer to MFS-28610.

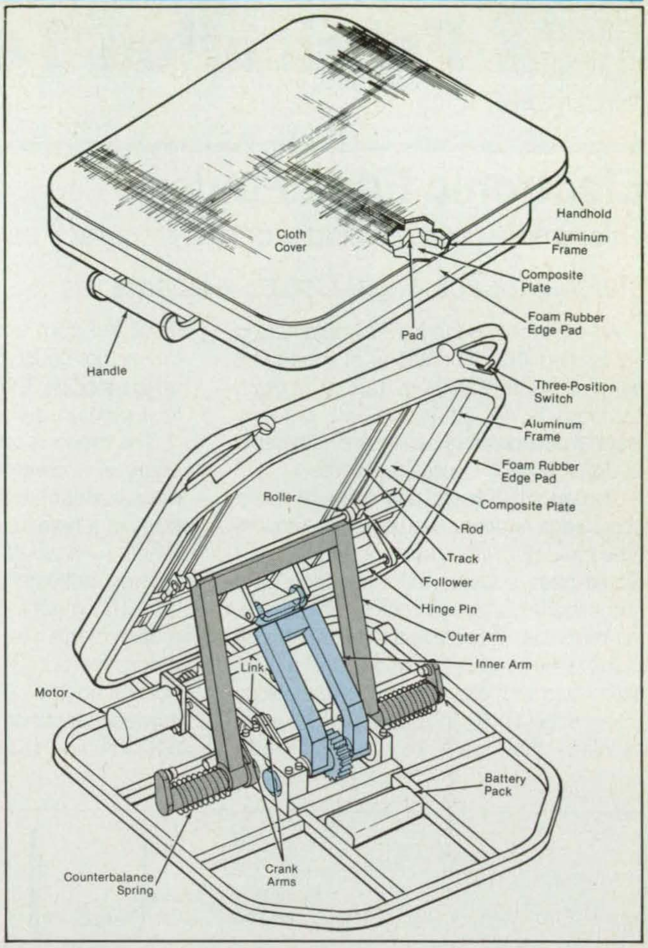

An **Upholstered Aluminum Box** houses the mechanism of the lifting seat. Springs on the outer shaft-and-arm subassembly counterbalance part of the user's weight to assist the motor.

Electronic Edge Finder

This simple device would reduce inaccuracy caused by deflection.

Marshall Space Flight Center, Alabama

An electronic edge finder would help in measuring the dimensions of machined parts to within 0.0001 in. (2.5 μm). Such accuracy is not attainable with ordinary touch-type indicators, which are vulnerable to deflections by contact forces.

A machinist could use the new electronic edge finder instead of another touch-type indicator, with assurance that a part would pass subsequent inspection by a numerically controlled coordinate-measuring machine. This should eliminate much of the unnecessary rejections and rework associated with other touch-type indicators.

The edge finder includes a probe — a stainless-steel tube — mounted in a chuck insulated from the jig borer or other machine tool used as the coordinate-measuring machine. The tip of the probe is flared to a precise diameter (see figure).

The probe is connected to sensing circuitry in a control box. When the probe made contact with the workpiece — the edge of a hole in a bolt hole circle, for example — it would complete a circuit and thereby activate a buzzer in the control box. The machinist would then stop the motion of the machine tool and probe and record the coordinates of the machine at point of contact. By stopping the machine immediately upon contact, the machinist could avoid the inaccuracy of overtravel and deflection. The electronic edge finder should be especially helpful when the machinist cannot directly observe the probe — for example, in blind holes.

This work was done by Richard K. Burley of Rockwell International Corp. for **Marshall Space Flight Center**. *For further information, Circle 30 on the TSP Request Card.*

Inquiries concerning rights for the commercial use of this invention should be addressed to the Patent Counsel, Marshall Space Flight Center [see page 24]. Refer to MFS-29854.

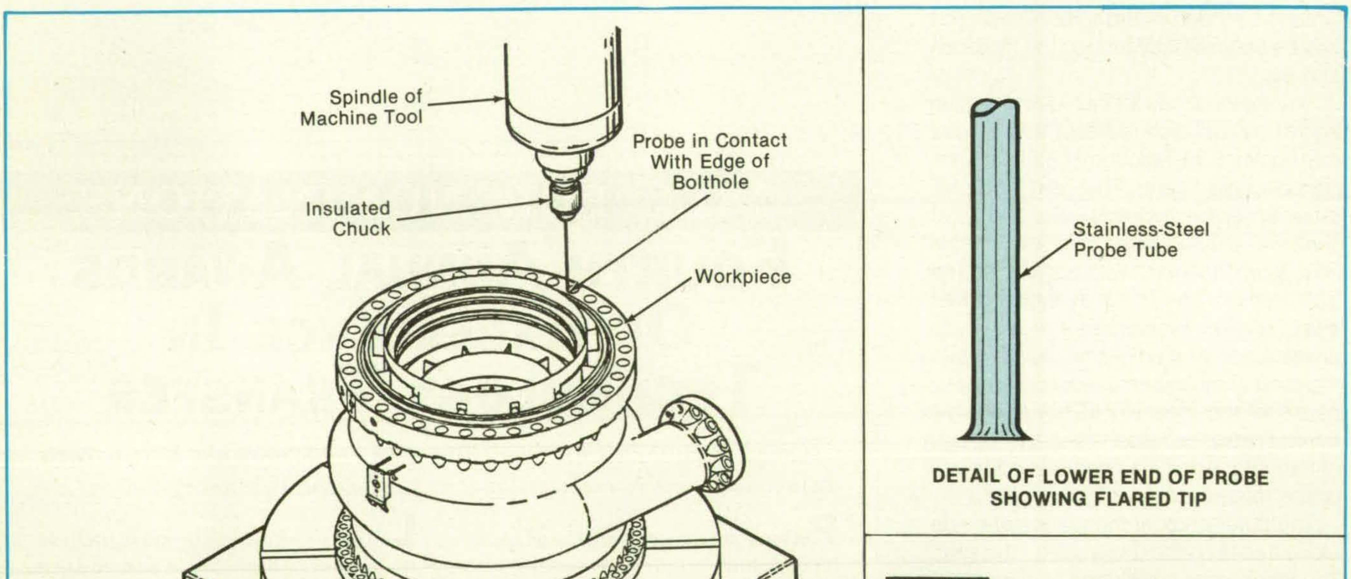

The **Tubular Probe** could be used to measure the accuracy of placement of holes in a bolthole circle. The control box would contain circuitry that would activate a buzzer to indicate electrical contact between the probe and the workpiece.

Adjustable Powder Injector for Vacuum Plasma Sprayer

Position and orientation of external injection can be varied.

Marshall Space Flight Center, Alabama

An attachment for a plasma spray gun (see figure) provides four degrees of freedom for adjustment of the position and orientation at which powder is injected externally into the plasma flame. This adjustment is desirable because it can help to optimize deposition in the specific plasma process. Previous external injectors have been fixed or have been adjustable in only two degrees of freedom.

A collar on the injector is slipped onto the protruding cylindrical portion of the plasma gun and is positioned repeatably on the gun by three setscrews, spaced 120° apart, that rest in shallow holes on the gun. Three approximately semicircular recesses in one edge of the collar provide clearance to enable the internal injection of powder (injection of powder from within the gun into the plasma flame).

An extension bar holds the injection tube and a manipulator (which is essentially an adjustable clamp). The bar slides and rotates in a bracket, so that the axial position and the yaw angle of the injection tube can be adjusted. Scribed lines on the collar and extension bar indicate the yaw angle.

The manipulator provides for adjustment of the pitch angle of the injection tube: It can be set to inject powder at any angle ranging from perpendicular to parallel to the cylindrical axis. Scribed lines on the extension bar and manipulator indicate the pitch angle of the extension tube.

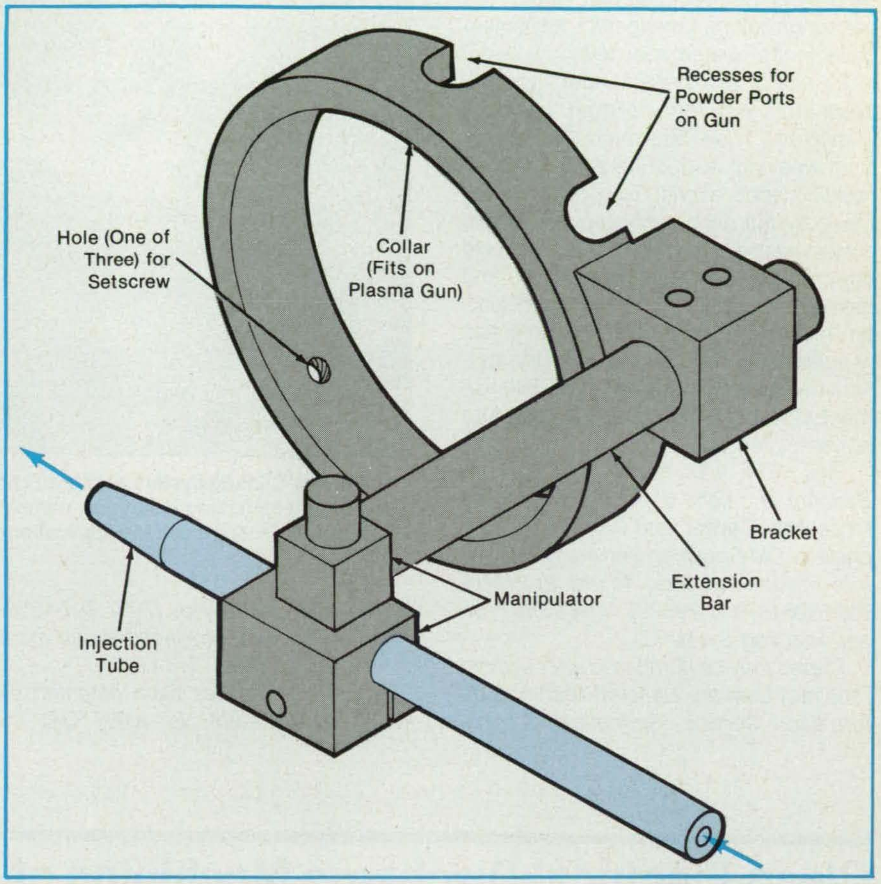

The **Adjustable Powder Injector** is mounted on a plasma gun. The collar can be changed to adapt the injector to a different gun.

With the exception of the collar, the components of the injector can be used with a plasma gun of any size and type. (The collar must be changed to fit a gun of different diameter or design.) Therefore, vacuum plasma spraying that requires different guns in sequence can be done with only one external powder injector.

This work was done by D. H. Burns of **Marshall Space Flight Center** *and W. H. Woodford, T. N. McKechnie, D. C. McFerrin, W. M. Davis, and G. P. Beason, Jr., of Rockwell International Corp. For further information, Circle 19 on the TSP Request Card.*
MFS-28684

System Applies Polymer Powder to Filament Tow

Polymer powder is applied uniformly and in a continuous manner.

Langley Research Center, Hampton, Virginia

The general disadvantage of most current methods for producing composite prepreg materials is the nonuniform distribution of the polymer materials throughout the filamentary materials. In a system developed at NASA Langley Research Center, polymer powder particles are evenly distributed to filamentary materials in a continuous manner.

The powder-coating system, shown in the figure, consists of five functional stations: filament-supply rolls, filament-spreading chamber, powder-coating chamber, fusion furnace, and takeup rolls. The rolls are mounted on internally pressurized air bearings to minimize friction and thereby enhance precise control of tension in the filament tow. A specially designed bulk-carbon-faced brake provides accurate control of the tension on the feed spool during processing.

The filament-spreading chamber provides a unique method for uniformly spreading the filament bundle to preselected widths prior to entry into the powder-coating chamber. The tow bundle is fed into a slot tunnel composed of upper and lower plates separated by divergent bars that have holes perpendicular to the fiber-tow-feed direction. Suction is applied to a plenum chamber that surrounds the slot tunnel. This suction, in turn, is drawn through the holes in the bars on both sides of the slot tunnel. The flow of air lateral to the filament-feed direction uniformly spreads the fiber tow bundle into an even band. The spread of the tow is controlled by the level of suction in the slot tunnel and the tow tension applied at the supply-roll station.

The spread carbon tow is directed into the powder-coating chamber, in which a cloud of airborne powder particles is recirculated. The polymer powder material is uniformly applied to the traveling spread tow bundle. Additional powder material is added to the chamber as the powder is deposited on the filament tow.

The fusion furnace is a standard laboratory horizontal tube furnace. The powder-coated tow travels through this furnace, where it is heated to fuse the powder material onto the fiber material. Finally, the traveling/rotating takeup-roll mechanism collects the coated fiber tow.

By use of this system, fiber tows impregnated with dry polymer powders ("towpregs") have been produced for preform-weaving and composite-material-molding applications. Towpreg material made by the dry-powder process in this system has been formed into unidirectional fiber moldings and has been woven and molded into preform material of good quality. This system and process are potentially valuable to the prepreg industry, particularly for the production of flexible filament-windable tows and high-temperature polymer prepregs.

This work was done by Robert M. Baucom and John J. Snoha of **Langley Research Center** *and Joseph M. Marchello of Old Dominion University. Further information may be found in NASA TM-102648 [N92-22639], "LaRC Dry Powder Towpreg System."*

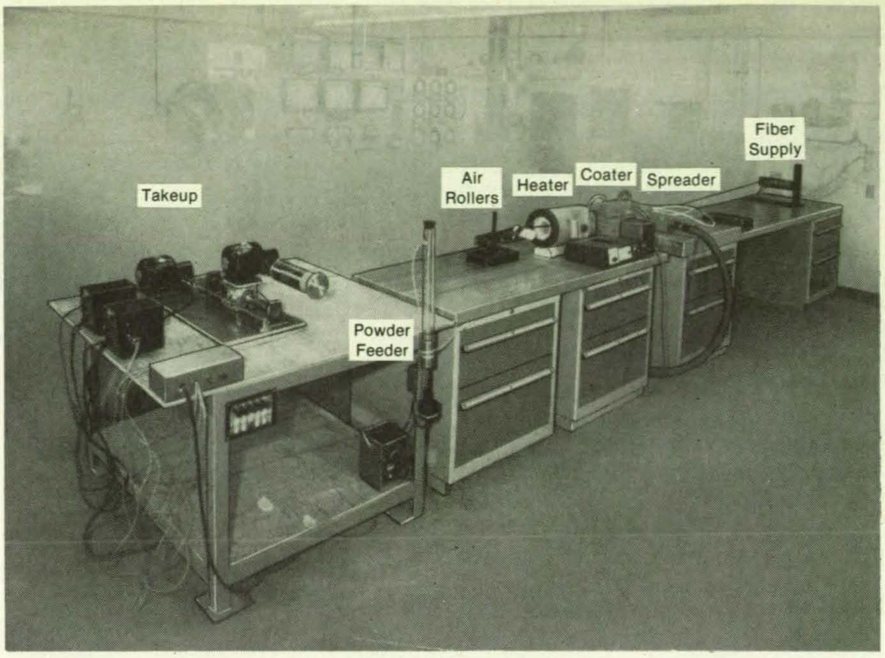

This **Powder-Coating System** applies dry polymer powder to a continuous fiber tow. The unique filament-spreading technique, combined with precise control of tension on the fibers in this system, ensures uniform application of polymer powder to the web of spread filaments.

Copies may be purchased [prepayment required] from the National Technical Information Service, Springfield, Virginia 22161, Telephone No. (703) 487-4650. Rush orders may be placed for an extra fee by calling (800) 336-4700.

This invention has been patented by NASA (U.S. Patent No. 5,057,338). Inquiries concerning nonexclusive or exclusive license for its commercial development should be addressed to the Patent Counsel, Langley Research Center [see page 24]. Refer to LAR-14231.

Clean Electrical-Discharge Machining of Delicate Honeycomb

Special tooling is used, and the recesses are bored with the workpiece in nonstandard alignment.

Goddard Space Flight Center, Greenbelt, Maryland

Precise recesses in fragile metal honeycomb blocks can be formed in a special electrical-discharge machining process. In the original application for which the process was devised (making honeycomb collimator modules for a scientific instrument), there was a requirement to do the machining in an environment free of oil and other contamination. Heretofore, to assure the proper functioning of the only electrical-discharge machine capable of forming holes in plunge-type operation (in which the cutting electrode advances depthwise into the workpiece), it was necessary to immerse the workpieces and cutting electrodes in oil.

In the special process, one uses a newer traveling-wire electrical-discharge machine, which is capable of motion in two perpendicular directions (*x* and *y*) but is not capable of motion in the third perpendicular direction (*z*), in which it would ordinarily have to move in plunge-type operation. This machine is designed for operation with deionized water instead of oil. It features computer control of cutting-electrode current and feed rates, which can be ad-

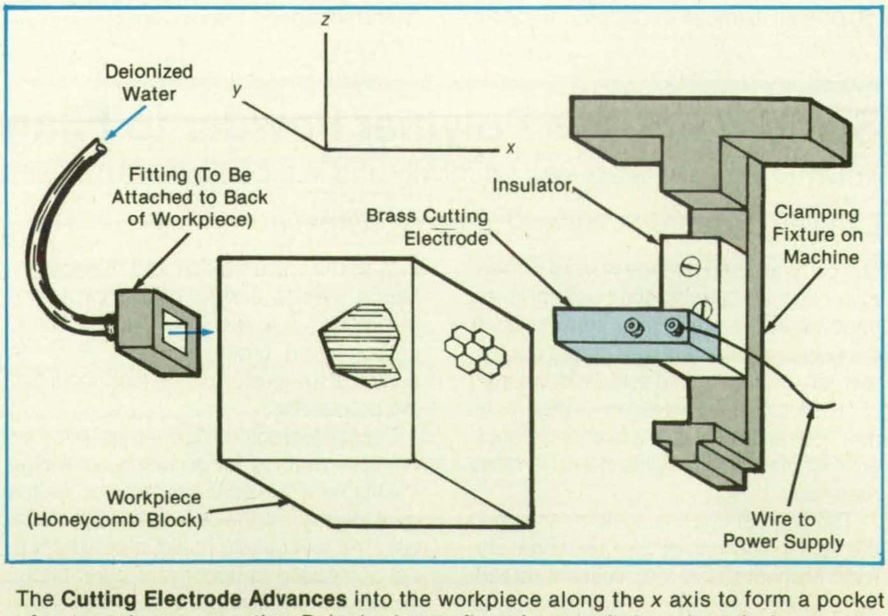

The **Cutting Electrode Advances** into the workpiece along the *x* axis to form a pocket of rectangular cross section. Deionized water flows from the fitting, along the honeycomb tubes of the workpiece, to the electrode/workpiece interface.

justed to suit the delicate honeycomb material.

Obviously, the way to effect plunge-type operation with the newer machine is to orient the cutting electrode and workpiece so that the *x* or *y* axis is the depthwise axis of motion and so that the workpiece and cutting electrode are mounted in the required relative *z* position. In the original application, this meant that the tubes of the honeycomb structure were parallel to the axis of motion — a fortuitous condition because the water could be fed toward the cutting electrode along the honeycomb tubes. For the latter purpose, a water-supply fitting was attached to the back of the workpiece (see figure).

This work was done by Clarence S. Johnson of **Goddard Space Flight Center**. *For further information, Circle 67 on the TSP Request Card.*
GSC-13526

Recessed-Contact Cleaner

A tool cleans receptacles for circuit-card connectors.

John F. Kennedy Space Center, Florida

A tool cleans receptacles for electronic-circuit-card connectors. It applies a commercial cleaner and/or lubricant liquid to the receptacles, which are located in deeply recessed slots and are difficult to reach. The tool thus helps to ensure reliable connections between the circuit cards and the receptacles, even in a dirty field environment.

The tool (see figure) is shaped somewhat like a circuit card and holds a lint-free cloth around one of its edges, which corresponds to the connector edge of the circuit card. A cleaning solution is applied to the cloth, then the tool is inserted in a receptacle. The cloth rubs the receptacle contacts, thereby cleaning them. The cloth can be advanced to expose a fresh area on each insertion.

The tool is made primarily of aluminum alloy sheet, cut to the same dimensions as those of the circuit card to be fitted into the slot. The cleaning edge is made of epoxy/fiberglass. The tip of the cleaning edge is machined precisely to 0.04 in. (1 mm) so that it applies adequate but not excessive pressure to the contacts.

A sliding wedge plate and two wedge bars hold the cloth in position. The wedge plate is pulled back to release the grip on the cloth, and the cloth can then be advanced. When the wedge plate is returned to its forward position, the fresh cloth is pulled tight and held in place by a shaped aluminum rail handle.

This work was done by Roger J. Juenemann of Grumman Technical Services, Inc., for **Kennedy Space Center**. *For further information, Circle 85 on the TSP Request Card.*

Inquiries concerning rights for the commercial use of this invention should be addressed to the Patent Counsel, Kennedy Space Center [see page 24]. Refer to KSC-11560.

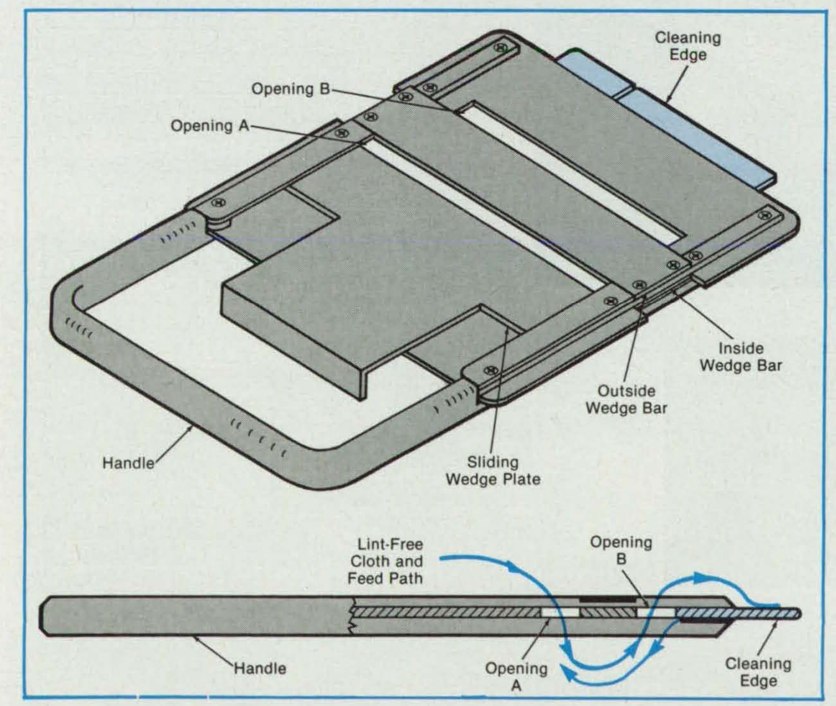

The **Strip of Lint-Free Cloth** is held taut on the cleaning edge by the sliding wedge plate and two wedge bars.

Computer Program for Generation of Surface Grids

S3D is efficient and easy to use.

Ames Research Center, Moffett Field, California

S3D is a useful computer program for the generation of grids on the surfaces of bodies that have complicated shapes. These surface grids are prerequisite to the generation of volume grids for use in computing flows bounded by the surfaces; heretofore, the generation of surface grids has proved to be one of the most time-consuming parts of the preprocessing that must be done prior to computations of flows. S3D is a product of the integration of a robust (in the computational sense) and widely applicable interpolation technique with the latest in computer-workstation technology. Incorporating highly efficient and easy-to-use graphical-interface software, S3D enables real-time and interactive analyses of surface-geometry data and facilitates the construction of surface grids.

The central feature of S3D is its approach to the use of interpolation in the analysis of curves and surfaces. A complicated surface is first decomposed into a network of simple patches, in a manner compatible with the global topology of a multiple-block grid. Surface points are generated in the patches by use of piecewise Hermite cubic-spline interpolation, with extrapolation at ends of curves and on boundary surfaces for use in computing derivatives.

Grid points are distributed along curves by use of a globally composite chord-length parameterization that incorporates two-sided stretching functions based on hyperbolic functions. To highlight such dominant geometrical features as discontinuities in slopes and sharp curves, different (usually, finer) point spacings can be set between specified break points in the vicinities of those features.

Points are distributed across surfaces in quasi-rectangular arrays, in two steps. First, the distributions along the four edges are defined (break points can be included). The next step is the iterative process of calculation of the points of intersection of cubically blended curves between corresponding points on opposite edges. This process is equivalent, in a sense, to generating a grid on a unit square while satisfying orthogonality and the specification of points on the edges. The process is fast, even for grids with as many as 100×100 points.

The distributions of points described above are in terms of global parameteriza-

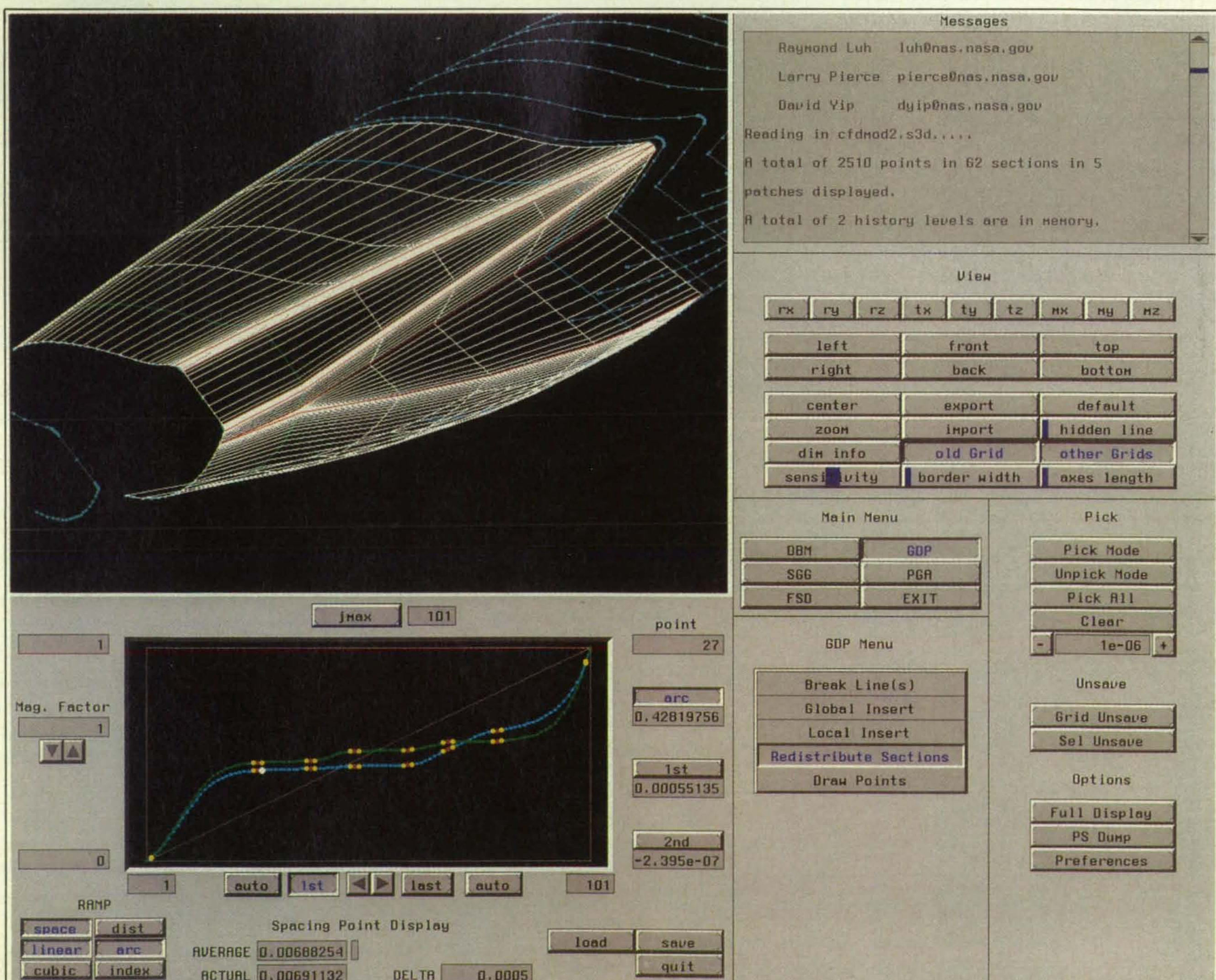

This **Display Is Generated** by the GDP portion of S3D to assist the user in redistributing grids on cross sections.

Multiple Pages Intentionally Left Blank

tion. Interpolation requires transformations to local parameterizations of the piecewise-cubic curve or bicubic surface constructs. Transformations based on cubic or bicubic interpolation of the global parameters have been shown to produce smoothly redistributed curves or surfaces, respectively.

The five major parts of the S3D software are Data Base Manager (DBM), Geometry Data Processor (GDP), Surface Grid Generator (SGG), Patch Grid Assembler (PGA), and Free-Form Surface Designer (FSD). DBM handles input, output, and other data-management functions, interacting with the user via menu displays. GDP works like a section-data editor, enabling primitive point data to be processed into the definition of a surface. Along the way, it enables domain decomposition (in the case of a multiple-block grid) to be carried out on the surface. The key function under GDP is the redistribution of sections, the workstation display of which is shown in the figure.

The output of GDP is a set of surface patches that clearly define the surface geometry and are ready for the generation of surface grids. As redistribution in GDP is confined to the individual sectional curves, the bidirectional redistribution of these patches becomes the central task in SGG.

PGA satisfies the variety of needs that arise in the generation of grids or as a consequence of the specification of a particular geometry. The graphical interactive approach of PGA provides an easy and efficient way to accomplish the simple cutting-and-pasting tasks.

FSD provides for the design of grids on free-form or otherwise unconstrained surfaces, in addition to simple analytic surfaces like planes and conics. FSD is used to design curves and surfaces based on transfinite interpolation. With GDP and FSD, it is possible to feed the definition of a surface of any type to SGG quickly.

This work was done by Raymond Ching of MCAT Institute and Lawrence Pierce of Sterling Zero One for **Ames Research Center**. *Further information may be found in AIAA paper A91-21621, "Interactive Surface Grid Generation."*

Copies may be purchased [prepayment required] from AIAA Technical Information Services Library, 555 West 57th Street, New York 10019, Telephone No. (212) 247-6500.
ARC-13162

Digital Low-Pass Filter Without Phase Shift

The signal is convolved with a causal exponential: first forward, then backward, in time.

John F. Kennedy Space Center, Florida

A relatively simple low-pass-filtering algorithm suppresses high-frequency noise in a digitally sampled signal. The algorithm is derived from the convolution of the signal with a causal exponential, but unlike prior causal filters, the filter implemented by this algorithm does not introduce a phase shift. This is because the algorithm applies a forward convolution in time followed by a backward convolution in time, and the phase shift in the second convolution cancels the phase shift in the first convolution.

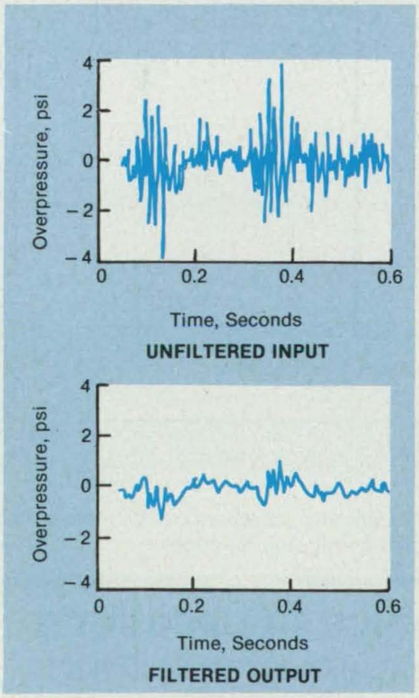

The **Unfiltered Input Signal** (in this case, a fluctuating pressure) was characterized by a Nyquist frequency of 200 Hz. This signal was processed by one pass of the low-pass filter algorithm with a corner frequency of 40 Hz.

The signal is considered to have been observed for all time up to the present time, t, and the first convolution is given by

$$g(t) = \frac{1}{\tau}\int_{-\infty}^{t} f(u)e^{(u-t)/\tau}du$$

where $f(u)$ represents the unfiltered input signal at time u and τ is the time constant of the exponential filter memory. The second convolution is given by

$$h(t) = -\frac{1}{\tau}\int_{-t}^{-\infty} g(u)e^{(u-t)/\tau}du$$

The zero-phase-shift and low-pass-filtering properties of $h(t)$ are demonstrated easily by applying it to the sinusoidal signal $f(t) = \sin(\omega t)$. The result is

$$h(t) = \frac{\sin(\omega t)}{1+(\omega\tau)^2}$$

The filter can be applied N times in succession to obtain sharper low-pass filtering of the sinusoid; namely,

$$h_N(t) = \frac{\sin(\omega t)}{[1+(\omega\tau)^2]^N}$$

The time constant can be chosen to obtain a desired half-power corner angular frequency, ω_c, via the equation

$$\tau = \frac{[2^{1/2 N}-1]^{1/2}}{\omega_c}$$

If the signal is sampled at regular intervals of Δt, then the low-pass-filtered signal at the time of the $i+1$st sampling time is given (for $N = 1$) by

$$g_{i+1} = \left(e^{-\Delta t/\tau}\right)g_i + \left[1-\left(1+\tfrac{\Delta t}{\tau}\right)\left(e^{-\Delta t/\tau}\right)\right]f_i + \left(\tfrac{\Delta t}{\tau}e^{-\Delta t/\tau}\right)f_{i+1}$$

where g_i and f_i denote the filtered and unfiltered signals, respectively, at the ith sampling time and f_{i+1} denotes the unfiltered signal at the $i+1$st sampling time. The figure shows the result of application of this equation to a noisy signal. In most practical cases, $\Delta t/\tau \ll 1$, and the simpler equation can be used:

$$g_{i+1} = \left(1-\tfrac{\Delta t}{\tau}\right)g_i + \left(\tfrac{\Delta t}{\tau}\right)f_{i+1}$$

This work was done by Wayne E. Simon of Martin Marietta Corp. for **Kennedy Space Center**. *For further information, Circle 51 on the TSP Request Card.*
KSC-11471

Rounded Approximate Step Functions for Interpolation

Local abrupt changes in tabulated data can be interpolated with minimal computation.

Marshall Space Flight Center, Alabama

Rounded approximate step functions of the form $x^m/(x^n+1)$ and $1/(x^n+1)$ have been found to be useful in interpolating between local steep slopes or abrupt changes in tabulated data that vary more smoothly elsewhere (see figure). These functions can be used instead of polynomial curve fits, which, under some conditions, can be inadequate to represent steep slopes or can introduce spurious oscillations at steps. Interpolation formulas based on these functions can be implemented quickly and easily on computers; for example, they can be used in real-time control computations to interpolate between tabulated data that govern control responses.

The approximate rounded step functions have been nicknamed "creation" and "destruction" functions (not to be confused with quantum-mechanical creation and destruction operators, which represent the creation and destruction of quanta, and some of which include functions). Provided that m and n are real, positive, and ≥ 1, the creation function $x^m/(x^n+1)$ starts from 0 at $x = 0$, rises to ½ at $x = 1$, and increases asymptotically in the following way: If $m = n$, the value of the function approaches 1. If $m \neq n$, then the function approaches x^{m-n} at large values of x followed by a line that has a chosen slope at $x \geq 1$. The corners are quite round at m and n near 1 but become sharper as m and n increase. Thus, by choosing m and n conveniently large, one can make the creation function approximate a unit step function at $x = 1$.

Whereas a creation function represents an abrupt increase, one can use a destruction function to represent an abrupt decrease. A destruction function could be obtained, for example, by subtracting a creation function from 1 to obtain $\frac{x^n+1-x^m}{x^n+1}$ [which amounts to $1/(x^n+1)$ if $m = n$].

The creation or destruction function is scaled to the size of the step by multiplying it by a suitable constant. If a set of tabulated data represents a curve that includes several steps, then one can choose m, n, and the multiplicative constant to fit a unique creation or destruction function to each step, each time scaling the independent variable x so that when the step occurs.

This work was done by Arthur C. Nunes, Jr., of **Marshall Space Flight Center**. *For further information, Circle 35 on the TSP Request Card.*

Inquiries concerning rights for the commercial use of this invention should be addressed to the Patent Counsel, Marshall Space Flight Center [see page 24]. Refer to MFS-28630.

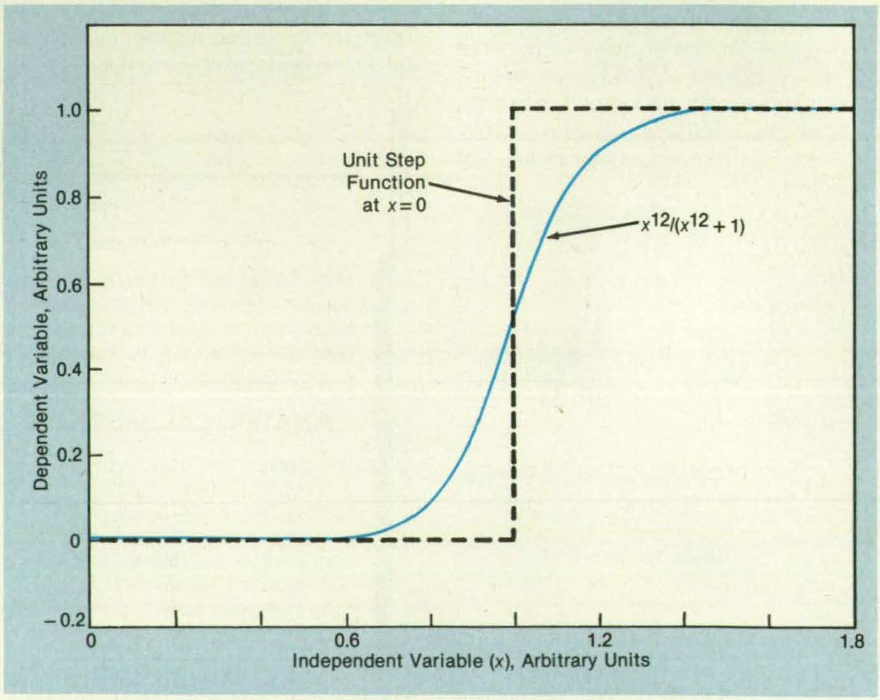

A **Local Step** in tabulated data that vary more smoothly elsewhere can be represented by an interpolating function that approximates a unit step function.

Programming Language Software for Graphics Applications

A new approach reduces repetitive development of features common to different applications.

NASA's Jet Propulsion Laboratory, Pasadena, California

A high-level programming language and interactive environment with access to graphical hardware and software has been created by adding graphical commands and other constructs to a standardized, general-purpose programming language, "Scheme." This augmented version of Scheme is designed for use in developing other software that incorporates interactive computer-graphics capabilities into application programs. It provides an alternative to programming entire applications in C or FORTRAN, specifically ameliorating the design and implementation of the complex control and data structures that typify applications with interactive graphics. It enables experimental programming and the rapid development of prototype software, and yields high-level programs that can serve as executable versions of software-design documentation.

Heretofore, the developers of graphical software have had two basic alternatives: (1) graphical code could be locked in compiled code along with other parts of an application program that have nothing to do with graphics, or (2) a new interpreter for graphical commands could be constructed and embedded in the application program to unlock the graphical code from the other parts of the application. Systematically taking the second alternative results in a "little language" strategy that has been documented in the computer science literature.

It has been found that every little language can be divided into a part that provides ordinary, well-understood programming features (variable binding, loops, conditionals, and the like) and a part that implements the unique, application-specific functionality for which the language was designed. The ordinary programming part is necessary infrastructure that is, at least functionally, common to all little languages. It is proposed that this infrastructure be encapsulated in a reusable "extension language" or "meta-shell" so that it need not be designed and implemented anew every time a little language is needed (see figure).

It is shown, by example, that Scheme is a good choice for this infrastructure extension language. It is demonstrated that a little language for the development of interactive graphics applications can be built by extending an implementation of Scheme with graphics functions implemented in C. The Scheme interpreter can then be viewed as a very high-level programmable command interpreter for driving a large library

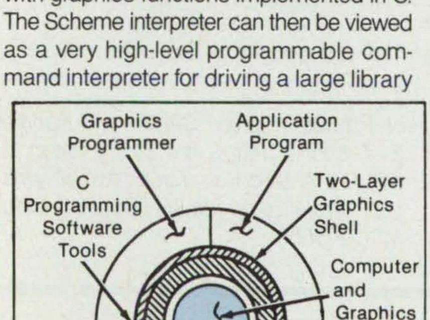

Graphical Capabilities are provided by a two-layer software shell.

of C functions. The same approach could link Scheme to a communications library, an operating system, or any library of functions. The extension language approach allows a programmer immediate, interactive access to a library, gives the programmer an experimental programming and prototyping capability, and frees the programmer from having to reinvent syntax and semantics for all the ordinary programming features of a little language.

Some further justifications for the choice of Scheme as the extension language are as follows:

1. Scheme is a small, simple, elegant language (the reference manual is 43 pages long);
2. Scheme has been standardized by the IEEE (standard P-1178); and
3. Extendable, robust implementations of Scheme in C are available copyrighted or in the public domain.

Basing a software system on an existing language like Scheme enables the programmer to take full advantage of interactive programming while avoiding the distractions of language design, implementation, and maintenance.

This work was done by Brian C. Beckman of Caltech for **NASA's Jet Propulsion Laboratory**. *For further information, Circle 45 on the TSP Request Card.* *NPO-18461*

High-Performance Water-Iodinating Cartridge

Water is iodinated to near saturation in a single pass.

Lyndon B. Johnson Space Center, Houston, Texas

A high-performance cartridge that contains a bed of crystalline iodine can iodinate water to near saturation in a single pass. The resulting concentration of iodine is biocidal; it can suppress the growth of microbes in stored water or disinfect contaminated equipment. The cartridge resists corrosion and can be stored wet. Furthermore, it can be reused several times before it is necessary to refill it with fresh iodine crystals.

The limited solubility of iodine in water (saturation level, 290 mg/L at 20 °C) and the unfavorable kinetics of dissolution are the primary obstacles that must be overcome in producing significant concentrations of iodine in water. In previous efforts to iodinate water by the direct dissolution of iodine, water was recirculated several times through the iodine bed until the desired concentrations of iodine were obtained. This proved too time consuming to be practical. In another approach, one first dissolves iodine in ethanol to form a tincture, which is then added to the water system; the iodine/ethanol disperses readily in water. In yet another, analogous approach, the solubility of molecular iodine (I_2) can be increased by codissolution with potassium iodide (KI) in the appropriate stoichiometric ratio. This combination produces the highly soluble triiodide ion (I_3^-), which provides a "reservoir" of the biocidal form, I_2, under equilibrium conditions. However, the disadvantage of both the tincture and the iodide methods is that they require the addition of substances other than iodine to the water.

As shown in the figure, the cartridge includes a stainless-steel housing equipped with an inlet and outlet for water. The bed of iodine crystals is divided into layers by polytetrafluoroethylene baffles. Holes are made in the baffles and are positioned to maximize the length of the flow path through the layers of iodine crystals. In a single pass through this cartridge, water is iodinated to concentrations of up to 280 mg/L (nearly saturation level) at rates of flow up to 400 mL/min.

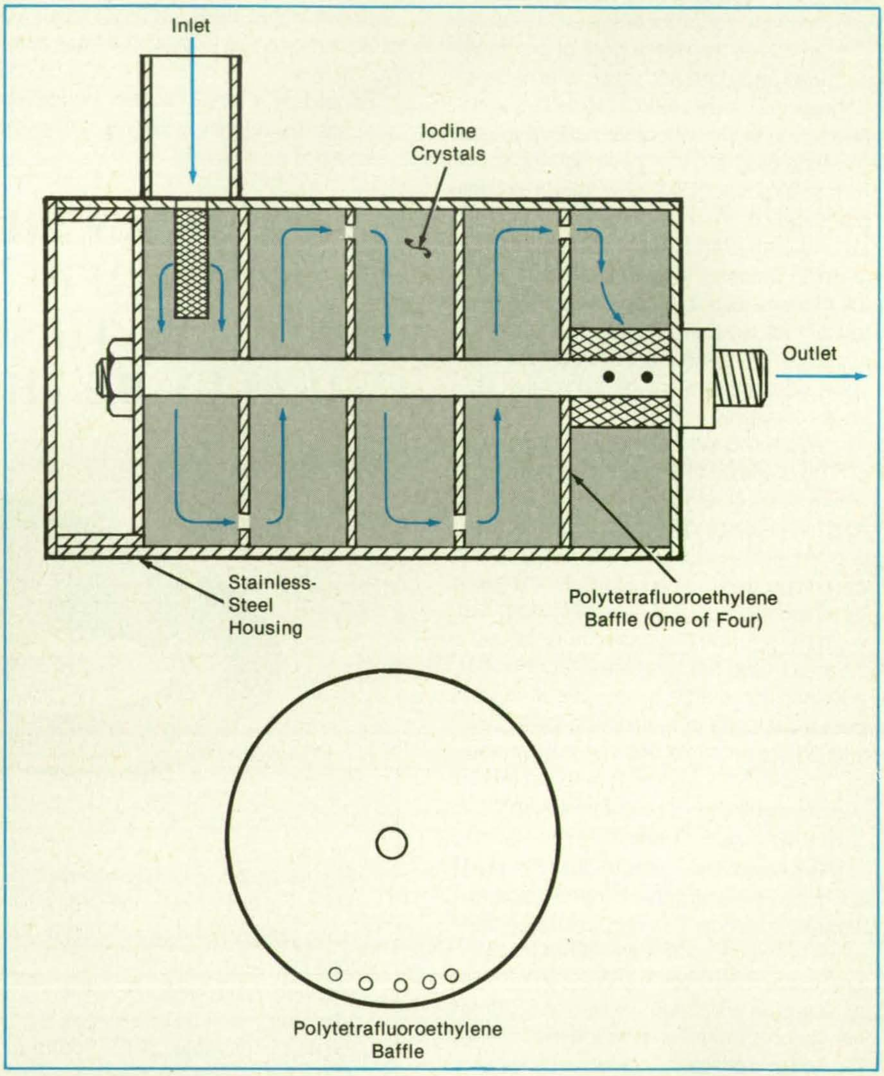

The **High-Performance Iodination Cartridge** iodinates water to near saturation in a single pass.

This work was done by Richard Sauer of **Johnson Space Center** *and Randall E. Gibbons and David T. Flanagan of KRUG Life Sciences. For further information, Circle 26 on the TSP Request Card. MSC-21855*

Kinetic Tetrazolium Microtiter Assay

The production of a metabolite can be monitored without killing the cells.

Lyndon B. Johnson Space Center, Houston, Texas

A kinetic tetrazolium microtiter assay (KTMA) involves the use of tetrazolium salts and Triton X-100 (or equivalent), which is a newly discovered, nontoxic, in vitro color developer that solubilizes the colored metabolite formazan without injuring or killing the metabolizing cells. This assay provides for the continuous measurement of metabolism and thereby makes it possible to determine the rate of action of an antimicrobial agent in real time as well as to determine effective inhibitory concentrations. It can also be used to monitor growth after addition of stimulatory compounds. This assay is done in 96-well microplates, providing multiple specimens that enable statistical evaluation of the results. Furthermore, the primary calculations are of rates determined from multiple plots of formazan produced over time; such calculations are more nearly reproducible than are the calculations that are performed in conjunction with assays by prior methods.

In an older end-point method, organic solvents are added to solubilize the formazan, which is solid, and which is produced by the cleavage of tetrazolium salts by microbial dehydrogenase. The organic solvents kill the cells. Because the new assay does not kill the cells, it provides for kinetic determination of the efficacy of a biocide, thereby greatly increasing the reliability and precision of the results. Furthermore, this assay can also be used to determine the relative effectiveness of an antimicrobial agent as a function of time.

Both of these factors are important in using this assay; for example, to select a biocide appropriate for treatment of potable water or to measure physiological changes that may have occurred in a microbial isolate. This assay can also be easily automated and used as a general-purpose antimicrobial-susceptibility assay. The capability of generating results on the day of the test is extremely important in treatment of water, treatment of waste, and disinfection of hospital rooms, and in the pharmaceutical, agricultural, and food-processing industries. This assay can also be used in many aspects of cell biology; for example, to evaluate mammalian growth factors or cytotoxicity levels, or to measure rates of invasion of bacteria (infection) into mammalian cells.

The procedure of the assay can be summarized as follows:

1. Grow cultures of microbes (target cells) overnight on an appropriate medium.
2. Dilute the microbial stock to the appropriate concentration.
3. Dilute the test chemical stock to the appropriate concentration.
4. Prepare microtiter plates as follows:
   (a) Add test chemicals (or effector cells) to wells.
   (b) Add suspensions of target cells to wells.
   (c) Shake plates for 30 s.
   (d) Incubate at the appropriate temperature for the appropriate time.
   (e) Add antimicrobial neutralizer (or cell-growth stimulator or inhibitor) if required.
   (f) Shake plates for 30 s.
   (g) Add microbial-metabolism medium.
   (h) Add tetrazolium salt solution.
   (i) Add phenazine methosulfate.
   (j) Add Triton X-100 (or equivalent).
   (k) Shake plates for 30 s.
   (l) Incubate plates at the appropriate temperature in a kinetic plate reader for the appropriate time (typically 20 min to 2 h). (The kinetic plate reader is a controlled-temperature, dual-wavelength spectrophotometer that measures the colors and, thereby, the concentration, of formazan in the wells.)
   (m) The concentration of cells and tetrazolium salt can be changed to obtain maximum results.

This work was done by Duane L. Pierson of **Johnson Space Center** *and Raymond Stowe and David Koenig of Krug Life Sciences, Inc. For further information, Circle 70 on the TSP Request Card.*

This invention is owned by NASA, and a patent application has been filed. Inquiries concerning nonexclusive or exclusive license for its commercial development should be addressed to the Patent Counsel, Johnson Space Center [see page 24]. Refer to MSC-21979.

Books & Reports

These reports, studies and handbooks are available from NASA as Technical Support Packages (TSP's) when a Request Card number is cited; otherwise they are available from the National Technical Information Service.

Physical Sciences

Analysis of Transfers of Cryogens in Low Gravity

A report discusses calculations of the thermodynamic aspects of refilling tanks with cryogenic liquids in low or zero gravity. Such calculations are required to design a prototype system that will resupply cryogenic propellant liquids to re-usable spacecraft that do not return to Earth. The equations and computer programs developed for the thermodynamic analysis will be used to extrapolate important design information from orbiting small-scale versions of the system.

This work was done by David M. DeFelice and John C. Aydelott of **Lewis Research Center**. *Further information may be found in NASA TM-89921 [N87-22949/NSP], "Thermodynamic Analysis and Sub-scale Modeling of Space-Based Orbit Transfer Vehicle Cryogenic Propellant Resupply."*

Copies may be purchased [prepayment required] from the National Technical Information Service, Springfield, Virginia 22161, Telephone No. (703) 487-4650. Rush orders may be placed for an extra fee by calling (800) 336-4700.
LEW-14715

Study of Bubble-Count Measurement of Surface Tension

A report presents a study of the bubble-count method of measurement of surface or interfacial tension of liquids. In the bubble-count method, a gas (in the case of surface tension) or a liquid (in the case of interfacial tension) is pumped at a known rate along a capillary tube. One end of the tube is open and immersed in a liquid that wets the tube. The pumped gas or liquid forms bubbles, which then detach themselves from the immersed open end of the tube, and one measures the average period, Π, for the formation and detachment of bubbles.

This work was done by Gary M. Nishioka and James I. Berg of H & N Instruments, Inc., for **Marshall Space Flight Center**. *To obtain a copy of the report, "A New Method for the Measurement of Surface Tension," Circle 104 on the TSP Request Card.*
MFS-27275

Materials

Synthesis, Properties, and Applications of Boron Nitride

A report comprises mostly the title page, introduction, and chapter-opening pages (including abstracts of chapters) of a two-volume book, published in 1990, that describes the synthesis, properties, and applications of boron nitride — especially in the thin-film form. The book contains 19 invited chapters written by leading researchers throughout the world.

Boron nitride films may become useful as masks in x-ray lithography; as layers for the passivation of high-speed microelectronic circuits; as insulating films; as hard, wear-resistant, protective films for optical components; as lubricants; and as radiation detectors. In addition, the present status of single-crystal growth of boron nitride indicates that it is a promising candidate for use in high-temperature semiconductor electronics.

The report was written and the book edited by John J. Pouch and Samuel A. Alterovitz of **Lewis Research Center**. *To obtain a copy of the report, "Synthesis and Properties of Boron Nitride," Circle 17 on the TSP Request Card.*
LEW-15299

Amorphous-Carbon Films

A report comprises mostly the title page, introduction, and chapter-opening pages (including abstracts of chapters) of a two-volume book, published in 1990, that describes the structure, preparation, characterization, and applications of films of amorphous-carbon (also known as diamondlike carbon). The book contains 29 invited chapters written by leading researchers throughout the world. Amorphous-carbon films are potentially useful as masks in x-ray lithography, as layers for the passivation of high-speed microelectronic circuits, as hard films to protect magnetic recording media and optical components from degradation by chemical etching or wear, and as radiation detectors.

The report was written and the book was edited by John J. Pouch and Samuel A. Alterovitz of **Lewis Research Center**.
LEW-15298

Structural Efficiencies of Fluted-Core Graphite/Epoxy Panels

Because laminated composite materials have densities that are low and stiffnesses that are high in comparison with those of aluminum, such materials offer the potential for the construction of aircraft components that have structural efficiencies better than those of the corresponding components made from metals. A report discusses one concept that may provide a practical alternative to some aluminum structural components of wings: fluted core panels made of graphite/epoxy material. The report includes a description of a structural-efficiency study of fluted-core sandwich panels of two different configurations. The results of this study were compared with the results of a similar study of conventional aluminum panels and blade-stiffened graphite/epoxy panels.

This work was done by Dawn C. Jegley of **Langley Research Center**. *Further information may be found in NASA TM-101681 [N90-18070], "A Study of the Structural Efficiency of Fluted Core Graphite-Epoxy Panels."*

Copies may be purchased (prepayment required) from the National Technical Information Service, Springfield, Virginia 22161, Telephone No. (703) 487-4650. Rush orders may be placed for an extra fee by calling (800) 336-4700.

Inquiries concerning rights for the commercial use of this invention should be addressed to the Patent Counsel, Langley Research Center [see page 24]. Refer to LAR-14539

Chemical-Vapor Deposition of Silicon Carbide

A report describes experiments in the chemical-vapor deposition of silicon carbide (SiC) by pyrolysis of dimethyldichlorosilane [$(CH_3)_2SiCl_2$] in hydrogen and argon carrier gases. The experiments were directed toward understanding the chemical-kinetic and mass-transport phenomena that can affect the infiltration of the reactants into, and the deposition of SiC upon, fabrics. This and related studies are parts of a continuing effort to develop a method of efficient and more nearly uniform deposition of silicon carbide matrix throughout fabric plies to make improved fabric/SiC-matrix composite materials.

This work was done by D. E. Cagliostro and S. R. Riccitiello of **Ames Research Center**, *J. Ren of DeAnza College, and F.*

Zaghi of San Jose State University. To obtain a copy of the report, "A Comparison of the Pyrolysis Products of Dimethyldichlorosilane in the Chemical Vapor Deposition of Silicon Carbide in Hydrogen or Argon," Circle 69 on the TSP Request Card.
ARC-13067

Growth of Fatigue Cracks in an Aluminum Alloy

The closure of cracks as they propagate may be caused by residual plastic deformations, roughness of crack surfaces, and corrosion or oxide products remaining in the wake of advancing cracks. However, in many structural applications, plasticity-induced closure is probably the dominant closure mechanism. The report discusses the application of a mathematical crack-closure model to study the growth of cracks under various load histories. The model was based on a crack-tip-plasticity concept, which was modified to leave plastically deformed material in the wake of the advancing crack tip. The effect of the thickness of the material on plasticity was accounted for by using a "constraint" factor in connection with tensile yielding at the crack tip.

This work was done by J. C. Newman, Jr., of **Langley Research Center** *and D. S. Dawicke of Purdue University. Further information may be found in NASA TM-101544 [N89-22135], "Prediction of Fatigue-Crack Growth in a High-Strength Aluminum Alloy Under Variable-Amplitude Loading."*

Copies may be purchased (prepayment required) from the National Technical Information Service, Springfield, Virginia 22161, Telephone No. (703) 487-4650. Rush orders may be placed for an extra fee by calling (800) 336-4700.

Inquiries concerning rights for the commercial use of this invention should be addressed to the Patent Counsel, Langley Research Center [see page 24]. Refer to LAR-14439

Tubing for Sampling Hydrazine Vapor

A report evaluates flexible tubing used for transporting such hypergolic vapors as those of hydrazines for quantitative analysis. For accurate measurement, a tube should allow free passage of the highly chemically active vapor without absorbing or reacting with the vapor.

The report describes experiments in which a variety of tubing materials, chosen for their known (or assumed) compatibility with hydrazine, their flexibility, and their resistance to heat.

This work was done by Josh Travis of **Kennedy Space Center**, *Patricia S. Taffe of Geo-Centers, Inc., and Susan L. Rose-Pehrsson and Jeffrey R. Wyatt of the Naval Research Laboratory. To obtain a copy of the report, "Inert Sample Transport Tubing," Circle 18 on the TSP Request Card.*
KSC-11458

Mechanics

Deriving Indicial Response From Navier-Stokes Equations

A report discusses research directed toward recasting the indicial-response approach into a form appropriate to the study of vortex-induced oscillations and related aerodynamic and aeroelastic phenomena. This is one in a continuing series of papers on the mathematical modeling of these phenomena, and as such, it serves two purposes: (1) to show how the deficiency of a prior mathematical model (which does not predict the self-sustained oscillations that are observed in experiments) can be overcome to include the effects of memory (that is, of prior flow conditions), which are necessary for modeling of an oscillatory but otherwise equilibrium state; and (2) using the method thus developed to analyze the particular case of flow past a cylinder that is in periodic forced transverse motion.

This work was done by K. V. Truong and M. Tobak of **Ames Research Center**. *Further information may be found in NASA TM-102856 [N91-13408], "Indicial Response Approach Derived From Navier–Stokes Equations Part I — Time-Invariant Equilibrium State."*

Copies may be purchased [prepayment required] from the National Technical Information Service, Springfield, Virginia 22161, Telephone No. (703) 487-4650. Rush orders may be placed for an extra fee by calling (800) 336-4700.

ARC-13091

Computations of Flows in Flapper Valves

Three reports describe computational studies of the flows of liquid oxygen and liquid hydrogen in the flapper valves that are located at the quick-disconnect interface between the main propellant feedlines of the Space Shuttle orbiter and the Space Shuttle external tank. Each flapper can be oriented at various positions and angles of attack with respect to the affected flow, by use of a pneumatic actuator on the orbiter side. One of the main design requirements, and the major concern in these studies, is that the flappers remain stable in a valve-open position and orientation; that is, that neither valve closes during flow.

This work was done by Mastanaiah Kandula and Dan Pearce of Lockheed Engineering & Sciences Co. for **Johnson Space Center**. *To obtain copies of the reports, "Computational Fluid Dynamics Analysis of Space Shuttle Main Propulsion Feed Line 17-Inch Disconnect Valves," "Flow Analysis of Space Shuttle Feed Line 17-Inch Disconnect Valve," and "Three-Dimensional Navier–Stokes Simulation of Space Shuttle Main Propulsion 17-Inch Disconnect Valves," Circle 62 on the TSP Request Card.*

MSC-21993

Experiments in Characterizing Vibrations of a Structure

A report discusses experiments that were conducted to test methods of identification of vibrational and coupled rotational/vibrational modes of a flexible structure. The report is one in a series that chronicle the development of an integrated system of methods, sensors, actuators, analog and digital signal-processing equipment, and algorithms to suppress vibrations in a large, flexible structure even when the dynamics of the structure are partly unknown and/or changing. The two most recent prior *NASA Tech Briefs* articles that describe aspects of this continuing research are "Autonomous Frequency-Domain Identification" (NPO-18099), Vol. 16, No. 3 (March 1992), page 70, and "Automated Characterization of Vibrations of a Structure" (NPO-18141), Vol. 16, No. 5 (May 1992), page 79.

This work was done by Yeung Yam, Fred Y. Hadaegh, and David S. Bayard of Caltech for **NASA's Jet Propulsion Laboratory**. *To obtain a copy of the report, "Experiments in On-Orbit Identification for Control of Space Structures," Circle 4 on the TSP Request Card.*

NPO-18279

New on the Market

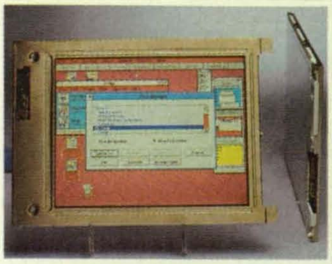

A passive **liquid crystal display** (LCD) developed by Sharp Electronics Corp., Camas, WA, mirrors the image quality, color saturation, and brightness of thin-film transistor displays costing much more. The new LM64C08P features split screen/dual scan multiplexing, high-speed drivers for a 1:240 duty cycle, and improved color filters.

For More Information Circle No. 567

A **wireless data logger** introduced by John Fluke Mfg. Co. Inc., Everett, WA, enables immediate data collection and transmission from locations previously considered too remote, inaccessible, or environmentally hostile for real-time monitoring. The portable, 21-channel 2625A/RF Hydra Wireless Logger uses spread-spectrum RF technology to transmit data to a PC up to 800 feet away. Hydra measures a range of input types without external signal conditioners or danger of damage from ground loop, common voltage, or voltage spikes.

For More Information Circle No. 572

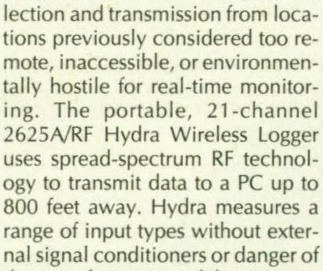

Lucas Schaevitz, Pennsauken, NJ, has announced the Linear Ball Bearing series of **LVDT-type gauging probes** for on-line dimensional measurement in a variety of quality control and metrology applications. The probes utilize linear ball bearing assemblies to minimize radial play and friction for ultra-precise measurement. Precision fitting of probe and bearings to the plunger tube provides exceptional gauge head repeatability (0.000004 in.).

For More Information Circle No. 571

A 64-bit **microprocessor** developed by NEC Corp. and MIPS Technologies Inc., Mountain View, CA, enables notebook computer users to run application programs easily under Windows NT™ and other advanced operating systems. The first member of the MIPS® low-power processor family, the R4200 achieves an 80 MHz internal clock speed doubled from a 40 MHz external clock source and delivers 55 SPECint92 and 30 SPECfb92.

For More Information Circle No. 563

BBN Software Products, Cambridge, MA, has released BBN/Cornerstone™, **data analysis software** for client/server computing that integrates data access, visualization, statistical analysis, and presentation. Integrating object-oriented technology, the GUI-based package comprises a base module providing a data analysis framework, broad data access capability, dynamic graphics, and an innovative worksession capture mechanism.

For More Information Circle No. 569

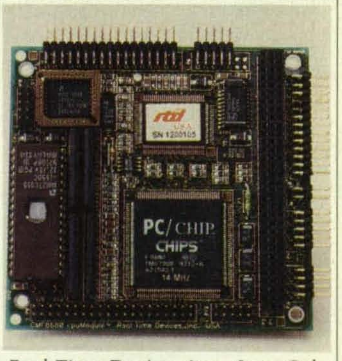

Real Time Devices Inc., State College, PA, has unveiled the CMF8680 cpuModule™, a **personal computer** measuring 3.8" x 3.6" and weighing just 3 ounces. It includes a CGA graphics and LCD interface, 16-bit IDE hard drive controller, high-density floppy controller, PCMCIA interface, AT-enhanced bidirectional parallel port, two RS-232 ports, and an RS-485 series port.

For More Information Circle No. 560

The ACUITY™ gm865x1 Image Resizing Engine announced by Genesis Microchip Inc., Markham, Ontario, is a patented **image/video resizing IC** designed for high-quality multimedia, video conferencing, and desktop publishing systems. Containing more than 500,000 transistors and executing billions of operations per second, it is the first device capable of providing both image shrink and zoom while maintaining the maximum image quality possible with a single IC, according to the manufacturer.

For More Information Circle No. 564

New Literature

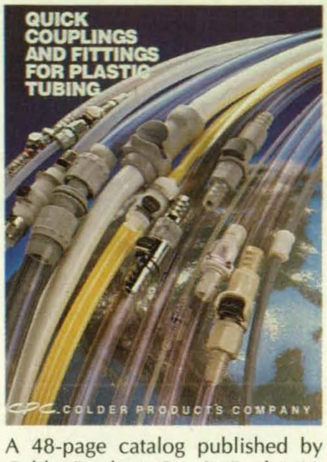

A 48-page catalog published by Colder Products Co., St. Paul, MN, describes more than 700 standard sizes and configurations of **quick couplings for plastic tubing**, including panel mount, in-line, and elbows to fit 1/16" to 1/2" tubing. Pipe thread, hose barb, or ferruleless polytube fittings are built in. High flow valve options include straight-through flow and single- or double-sided shutoff.

For More Information Circle No. 586

A full-color brochure from American Poly-Therm Company Inc., Lincoln, CA, describes its design, fabrication, and production of **advanced composite components**. The company offers presses ranging from 20 to 2500 ton capacity, filament winding of structures up to 120 inches in diameter, and autoclaves up to 8 feet in diameter, as well as layup, tube winding, rubber molding, and precision foam molding.

For More Information Circle No. 583

A free brochure from Anorad Corp., Hauppauge, NY, focuses on its **precision motion control** products and capabilities. Showcased products include linear, rotary, and multi-axis stages; single- and multi-axis electronic motion controllers; vision and process equipment; linear motors; and a variety of structural materials.

For More Information Circle No. 587

Literature from Metal Powder Industries Federation, Princeton, NJ, outlines **powder metallurgy** (P/M) capabilities. The 20-page brochure explains the benefits of P/M, secondary operation, materials properties, design guidelines, near-fully dense products, applications, and how to specify parts.

For More Information Circle No. 581

Microfocus **noncontacting measurement systems**, showcased in a brochure from UBM Corp., Rosell, NJ, feature autofocusing, laser scanning microscopy, triangulation, focus error measurement, and inductive sensors. The systems conduct macro and micro surface profilometry, recognize defects, and measure surface structure and roughness. They can be applied to metals, coatings, micromechanics, glass, lenses, paper, and solder paste.

For More Information Circle No. 584

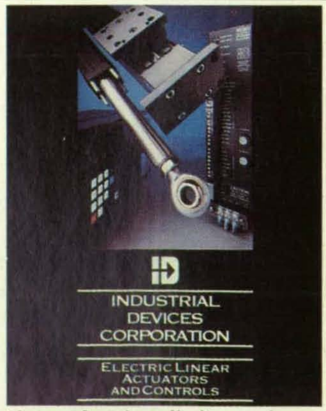

Linear electric cylinders and controls are highlighted in a 200-page product catalog and engineering guide from Industrial Devices Corp., Novato, CA. It includes specifications, speed versus thrust performance charts, options, and accessories for rod-type and rodless electric cylinders and positioning controls. New products include the NS series rod-type cylinders for automated linear motion applications requiring high load and duty cycle.

For More Information Circle No. 585

Lockheed's Aerospace Ceramic Systems, Sunnyvale, CA, has released a brochure featuring HTP fused-fiber **ceramics**, which offer thermal, cryogenic, and load-bearing insulation; high tensile and compressive strength; moisture resistance; light weight; and long life. Available vacuum-formed, cast, or machined, the materials can be tailored to provide specific characteristics for use in antenna radomes, microwave components, frequency-selective surfaces, artificial dielectric lenses, and laser-hardened systems.

For More Information Circle No. 582

MARKETPLACE To Advertise—Call (212) 490-3999

ADVERTISERS INDEX

For More Information Circle No. 468

The Technology Connection

To Advertise Call (800) 944-NASA

Meetings/Workshops

Databases/ Information Searches

Professional Services

Technologies for Transfer

NASA Tech Briefs, ISSN 0145-319X, USPS 750-070, copyright© 1993 in U.S., is published monthly by Associated Business Publications Co., Ltd., 41 E. 42nd St., New York, NY 10017-5391. The copywrited information does not include the (U.S. rights to)individual tech briefs which are supplied by NASA. Editorial, sales, production and circulation offices at 41 East 42nd Street, New York, NY 10017-5391. Subscription for non-qualified subscribers in the U.S., Panama Canal Zone, and Puerto Rico, $75.00 for 1 year $125.00 for 2 years; $200.00 for 3 years. Single copies $10.00. Foreign subscriptions one-year U.S. Funds $150.00. Remit by check, draft, postal, express orders or VISA, MasterCard, or American Express. Other remittances at sender's risk. Address all communications for subscriptions or circulation to NASA Tech Briefs, 41 East 42nd Street, New York, NY 10017-5391. Second Class postage paid at New York, NY and additional mailing offices.

POSTMASTER: please send changes to NASA Tech Briefs, 41 E. 42nd Street, Suite 921, New York, NY 10017-5391.